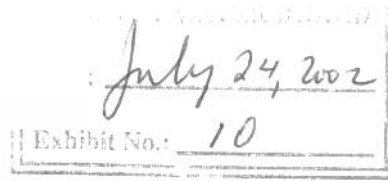


INSTITUTE OF GEOGRAPHY  
University of Copenhagen



Copenhagen, June 21, 2002

R. Halim, P.Eng., P.E.  
Acres International Limited,  
6th Floor, 500 Portage Avenue,  
Winnipeg, Manitoba R3C 3Y8 Canada

Dear R. Halim:

Thanks for your mail and interest. I have performed a research project aiming to quantify ARD effects in Nanisivik the last 5 years. Please see: <http://www.geogr.ku.dk/arctic-env/> for an introduction to project activities.

Results have been published and sent to day to your address. References are listed at the end of this letter.

Quick answers to your questions:

- does the depth of water play significant role in slowing down the oxidation process?  
Yes, it is important to which extent wind may introduce redistribution at the bottom. I suggest thin layers of inert material on top of saturated tailings and a thin water cover.
- The colder the water, the higher the oxygen solubility in the water. Will this result in more harmful effect than in warmer water?  
No, the net effect of an increasing oxygen solubility and slower diffusion is that colder water is better than warmer water (see Elberling and Damgaard, 2001). However, it is a concern if the system is not diffusion controlled.
- To ensure that the tailings under a pond will not create acid problem at Nanisivik, what would be the minimum acceptable depth of water to be kept in the pond?

Please see above, if an inert cover of sand is applied (0.5), the minimum acceptable depth of water should be based on estimates of the fluctuating water balance (during summer months) which seem to be very important to maintain a water cover.

- Were your research studies at Nanisivik published in journal papers or Symposium proceedings?

Please see list below

I am willing to go further into these aspects (recommendation and reviews) but expect a more directly involvement in the activities. Work on contract is possible through our University Company: GRAS (see: <http://www.gras.ku.dk/>).

Best regards,

  
Bo Elberling

- Elberling, B. (2001) Control strategies for acid mine drainage in Arctic regions. In: *Mining in the Arctic* (eds. Olsen H.K., Lorentzen, L. & Rendal, O.) A.A. Balkema Publishers, The Netherlands, 37-48.
- Elberling, B. & Damgaard, L.R. (2001) Microscale measurements of oxygen diffusion and consumption in subaqueous sulfide tailings. *Geochimica et Cosmochimica Acta* 65, 1897-1905.
- Kyhn, C. & Elberling, B. (2001) Frozen cover strategies for preventing acid mine drainage from sulfidic tailings deposited on land in Arctic Canada. *Cold Regions Science and Technology* 32, 133-142.
- Elberling, B. (2001) Environmental controls of the seasonal variations in oxygen uptake in sulfidic tailings deposited in a permafrost-affected area. *Water Resources Research* 37, 99-107.
- Elberling, B., Schippers, A. & Sand, W. (2000) Bacterial and chemical oxidation of pyritic mine tailings at low temperatures. *Journal of Contaminant Hydrology* 41, 225-238.

# Control strategies for acid mine drainage in Arctic regions

B. Elberling

*Institute of Geography, University of Copenhagen, Copenhagen, Denmark*

**ABSTRACT:** Mining in permafrost-affected areas raises unique issues that need to be addressed to minimize the environmental impact of mining. The exploitation and disposal of sulfidic tailings can lead to acid mine drainage (AMD) including acidification and leaching of heavy metals. Permafrost features that influence the deposition of sulfidic waste include processes within the active layer that produce pathways for reactant and contaminant transport, barriers such as snow and ice covers, and low temperatures that slow most chemical and biological processes. Primary issues for disposal of sulfidic mine tailings are summarized and strategies for controlling the oxidation of sulfide minerals at sub-zero temperatures are discussed. Results from a case study in Canada illustrate the possibilities of keeping tailings permanently water-saturated or frozen, thereby controlling AMD. Future research should focus on AMD generation rates at sub-zero temperatures and solute migration in frozen media.

## 1 INTRODUCTION

The main environmental concern facing the mining industry today is the occurrence of dissolved heavy metal contaminants and acidic effluents caused by sulfide oxidation (Paktunc 1999), generally referred to as acid mine drainage (AMD). There are numerous abandoned, operating and proposed base metal mines in permafrost-affected regions, and the disposal of sulfidic mine waste and AMD are problems known at several mine sites in the Arctic. Mine tailings which result from the processing of ore are usually transported to nearby disposal areas and acidic drainage will in most cases cause metals to spread to watershed stream systems and the marine environment.

Pyrite ( $\text{FeS}_2$ ) is by far the most common sulfide mineral giving rise to AMD. The oxidation of pyrite is a complex biogeochemical process involving several redox reactions, hydrolysis, complex ion formation, solubility control and microbial catalysis. Although several aspects of this process are not fully understood, the following equation of reaction is commonly given to describe the complete oxidation of the iron and sulfur moieties of pyrite:



In the reaction, ferric iron and sulfuric acid are formed and heat is released. Recent reviews on the process and

controls are available (e.g., Evangelou 1995). It is well known that aerobic sulfide-oxidizing bacteria can catalyse the oxidation of sulfide minerals and numerous studies describe the catalysing effects of chemolithotrophic bacteria such as *Thiobacillus ferrooxidans* (Evangelou 1995, Nordstrom & Southam 1997). These bacteria are in particular known to be able to catalyse the oxidation of sulfide minerals (Eq. 1) under highly acidic conditions, thereby increasing the overall oxidation rate by orders of magnitude as compared to abiotic reactions (Nordstrom & Southam 1997). As well as the degree and type of microbial activity, the following factors are generally thought to influence AMD generation: position of the sulfide body within the hydrological regime, types and abundances of sulfides and neutralizing gangue minerals, grain size distribution (specific surface area), climate, internal tailing temperatures and oxygen availability.

The first part of this review (sections 2 and 3) will discuss the influence of bacteria, temperature and oxygen on AMD generation as these factors play a unique role in permafrost regions. In addition, freezing-point depression, unfrozen water content and solute redistribution will be considered, since these factors influence the environmental impact of AMD. The last part of the review (sections 4 and 5) will focus on literature reporting observed AMD in permafrost-affected areas and discuss the current knowledge on strategies for controlling AMD.

## 2 BIOTIC SULFIDE OXIDATION AT SUB-ZERO TEMPERATURES

In the permafrost region, temperatures are low for most of the year and temperature fluctuations can be extreme over short periods of time. Temperature is an important control on the physical and chemical reactions that are the basis for all biogeochemical processes. Therefore, subsurface temperature is considered one of the most important parameters regulating the activity of bacteria within the soil environment. Bacteria that have adapted to live in cold conditions and to survive periods of extreme low temperatures have been known for more than 100 years (Forster 1887). Since then, several surveys have documented the presence of viable bacteria in permafrost environments (e.g., Morita 1975). Cold-adapted microbes have been classified as either psychrophiles (cold-loving, optimal temperatures for growth below 15°C, active to below zero) or psychrotrophs (cold-tolerant, optimal temperatures for growth above 15°C, active to below zero). One of the key conditions for the presence of viable microbes at freezing temperatures is the presence of liquid water. In frozen soil, thin intergranular water films allow chemical processes to continue even in winter and may represent survival niches for microbial life. The winter survival strategies for bacteria in the Arctic are not well understood, but bacteria are able to survive extremely low temperatures and viable microorganisms occur in permafrost to depths of at least 18 m and in material older than 70,000 years (Boyd & Boyd 1964, Kjeller & Ødum 1971).

### 2.1 The presence of sulfide-oxidizing bacteria in permafrost regions

The number of studies addressing the presence and potential activity of psychrophilic or psychrotrophic sulfide oxidizing bacteria in High Arctic environments is limited. Kalin (1987) reported the presence of psychrophilic thiobacilli at the Nanisivik Mine, Baffin Island, Arctic Canada. Psychrotrophic iron- and sulfide oxidizing bacteria, e.g., *Thiobacillus ferrooxidans*, have been detected in alkaline tailings at Nanisivik Mine (Elberling et al. 2000). In the latter study, microcalorimetric measurements revealed that as much as 35% of the overall oxidation of tailings (measured as heat production) was due to the presence of the bacteria. Langdahl (1999) isolated a psychrotrophic acidophilic sulfide-oxidizing microbial population (dominated by *T. ferrooxidans*) from naturally exposed sulfide ore material in North Greenland (83°N).

The presence of the well known sulfide-oxidizing bacteria *T. ferrooxidans* in High Arctic environments indicates that these bacteria populations are likely to be found at any location in the permafrost zone where

reactive sulfide minerals are or have been present.

### 2.2 Temperature-dependent biotic and abiotic sulphide oxidation

Most biogeochemical reaction rates decrease with decreasing temperatures and are described well by the Arrhenius equation:

$$\ln(k_1/k_2) = E_a(T_1 - T_2) / RT_1T_2 \quad (2)$$

where  $k_1$  and  $k_2$  are reaction rates at temperatures  $T_1$  and  $T_2$ ,  $E_a$  is the activation energy of the reaction and  $R$  is the gas constant. Values of  $E_a$  for pyrite oxidation reported in the literature range from 39 to 88 kJ/mol under a variety of experimental conditions (Nicholson et al. 1988). Although the effects of temperature on sulfide oxidation rates can be complex, particularly under field conditions, several studies confirm that the simple relationship given by the Arrhenius equation is a valid approximation of chemical and of microbial reaction rates (Dawson & Morin 1996). However, the Arrhenius equation considers only a single activation energy that is not temperature-dependent, whereas complex biological systems are presumed to have several temperature-dependent forms.

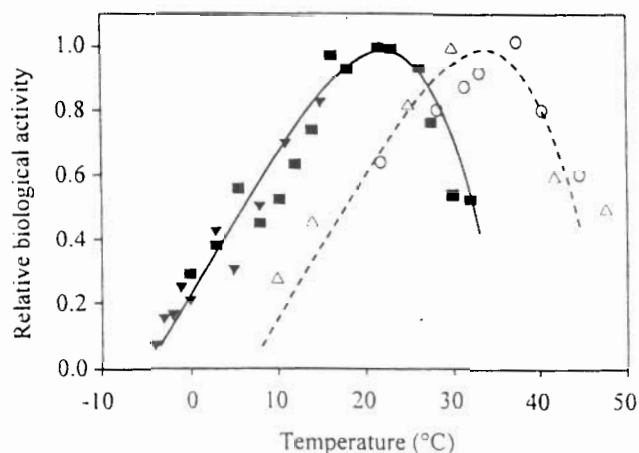


Figure 1. Relative changes in biological oxidation rates of pyrite collected from temperate latitudes (open marks) and arctic latitudes (filled marks). Changes in oxidation are given relative to the maximum oxidation observed. Open marks represent data from Jaynes et al. (1984), filled squares are from Langdahl & Ingvorsen (1997), and filled triangles are from Elberling (2000).

Figure 1 shows the temperature-dependent biotic activity of sulfide-oxidizing bacteria collected from arctic and temperate regions. The dashed line represents an equation fit (Jaynes et al. 1984) to relative activity measurements ( $X_r$ ) of bacteria collected at temperate latitudes and considered valid for the temperature range 4° to 55°C (T):



$$X_t = -1.2 \times 10^{-5} T^3 - 4.4 \times 10^{-4} T^2 + 0.066T - 0.25 \quad (3)$$

The solid line represents a fit to bacteria collected in the Arctic. An overall difference in temperature optimum of 7-8°C is observed and indicates an important biological adaption to cold climate.

It is evident that metabolic processes are active at temperatures as low as -10°C (Gilichinsky et al. 1992). However, limited information is available on the growth of specific sulfide-oxidizing bacteria at sub-zero temperatures. Langdahl & Ingvorsen (1997) studied the production rate of dissolved  $\text{Fe}^{2+}$  and  $\text{Fe}^{3+}$  of an enriched *T. ferrooxidans* culture from naturally exposed sulfide ore material in North Greenland. After laboratory investigations it was concluded that the overall rate of microbial activity at 0°C constituted as much as 30% of the maximum activity at 21°C.

Oxygen uptake rates as a result of sulfide oxidation have been observed at temperatures as low as -4°C. These rates are based on the difference in oxygen uptake in ambient and sterilized tailing samples from Nanisivik Mine (Elberling 2000). Results from that study reveal a uniform decline in biotic and abiotic oxygen uptake rates in pyritic tailings with decreasing temperatures (Fig. 2). The temperature-dependent oxygen uptake rate was consistent with the Arrhenius relation in the temperature range above 0°C.

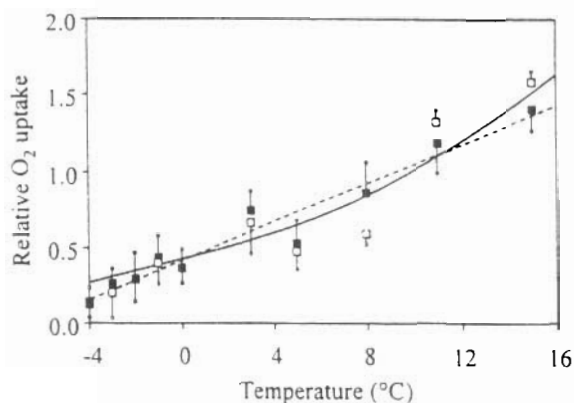


Figure 2. Relative oxygen uptake in pyritic tailings from Nanisivik Mine versus temperature. Biotic rates are shown as solid squares and chemical rates as open squares (Elberling 2000). The solid line is generated from the Arrhenius equation and the dashed line from a linear regression equation.

Below 0°C an increasing deviation is observed and the linear correlation provides the best fit for the entire temperature interval studied. Significant variations between the dependency of biological and chemical oxidation on temperature were not observed, indicating that the influence of temperature on the overall AMD

is not sensitive to the degree of biological oxidation. Meldrum et al. (1999) studied the oxygen uptake in tailings from Rankin Inlet in Arctic Canada, in freezer experiments at temperatures as low as -10°C. The authors conclude that oxygen consumption and heat generation due to oxidation are negligible at -10°C. The few studies mentioned above indicate that bacteria in natural systems may to a large extent be adapted to activity at sub-zero temperatures. Although the observed bacteria activity reviewed above indicates a significant reduction at 0°C compared to maximum activity, the results suggest that biological sulfide oxidation may take place at temperatures as low as -4°C, and that the activity becomes negligible as temperatures approach -10°C. Although the kinetics of sulfide oxidation show significant potential AMD at sub-zero temperatures, sulfide oxidation will only occur if oxygen and liquid water are present. The next section deals therefore with the potential transport and redistribution of oxygen and water in frozen tailings.

### 3 TRANSPORT IN FROZEN GROUND

Frozen sediments consist of several phases including solid particles, ice, unfrozen water, and gas. Within the frozen sediment, ions may be transported as a result of a concentration gradient (diffusion) or by a pressure gradient (advection). Extreme differences in the diffusivity within the various phases play a major role in the control of the overall AMD generation and spreading of contaminants. Ion diffusion in pure monocrystalline ice is considered to be insignificant as ion diffusion coefficients are about five orders of magnitude lower than in water (Barnall & Slotfeld-Ellington 1983). For components present in the gas phase, e.g., oxygen, the diffusion coefficients are about four orders of magnitude higher in the gas phase than in the water phase. Consequently, atmospheric oxygen will reach the depth where sulfide oxidation takes place primarily as a result of diffusion through the partially gas-filled pores (e.g., Pantelis & Ritchie 1992, Elberling et al. 1993, 1994). Only for waste material stored under near-saturated or fully-saturated conditions the lower oxygen diffusion in the water phase becomes important.

#### 3.1 Transport of oxygen

As pyrite oxidizes in tailings, atmospheric oxygen is consumed and the change in concentration with depth results in a concentration gradient, which is the driving force for the diffusive transport of oxygen. In tailing systems, one-dimensional molecular diffusion of oxygen gas can be described by Fick's First Law:

$$F_D = -D_e \frac{dC}{dz} \quad (4)$$

where  $F_D$  is the flux of  $O_2$ ,  $D_e$  is the effective diffusion coefficient, and  $dC/dz$  is the vertical concentration gradient for oxygen.  $D_e$  is a function of the diffusion coefficient for oxygen in air and a factor that depends on the percentage of gas-filled pores (relative to the volumetric moisture content) and the tortuosity (Troeh et al. 1982). Several models are available for estimating  $D_e$  but few are based on tailing material. Assuming that water-filled and air-filled pathways represent parallel resistance to diffusion in tailing material, Elberling & Nicholson (1996) showed that the effective diffusion coefficient ( $D_e$ ) in tailings can be accurately approximated as the weighted sum of the diffusion coefficients in air and water (see dashed line in Fig. 3).

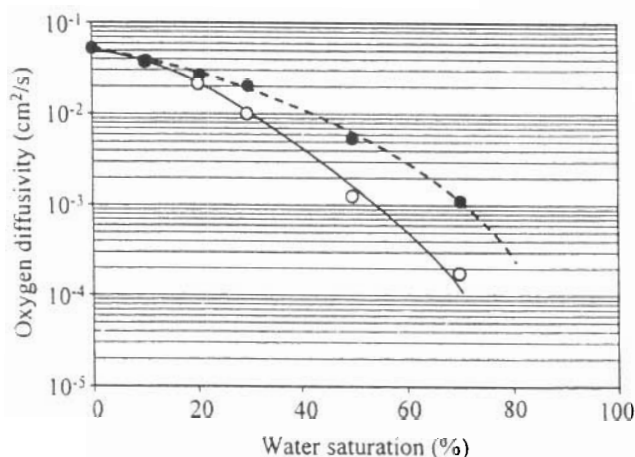


Figure 3. The effective diffusion coefficient in non-frozen tailings (filled circles and dashed line) and frozen tailings (open circles and solid line) at water saturations up to 70%. The dashed line is an empirical equation for estimating  $D_e$  based on saturation values (Elberling & Nicholson 1996) while the solid line is a free-drawn line representing the observed effect of freezing for comparison (Elberling 1998).

In frozen media, diffusion estimates require oxygen diffusion coefficients for super-cooled water as well as estimates on the overall change in gas pore volume fraction and connectivity during freezing. Such data are currently not available from the literature, and diffusion coefficients for oxygen gas in unfrozen and frozen tailings with variable water saturation are only known from experimental designs. Diffusion measurements on unfrozen and frozen tailings from Nanisivik Mine have shown that freezing has no significant effect on  $D_e$  in tailings with a water saturation less than 30% (Elberling, 1998). Above 30% saturation, freezing lowers  $D_e$ , reaching a reduction factor of about 10 at 70% water saturation. It was concluded that freezing well-drained tailings deposited on land is not expected to decrease the overall availability of

oxygen in tailings. The study points out that changes in the degree of saturation may be as important as freezing in permafrost areas and that a combination of saturation and freezing seems ideal for controlling oxygen availability in tailings deposited in the Arctic.

### 3.2 Unfrozen water

The amount of liquid water present in "partly" frozen soil and waste materials is critical for controlling microbial activity and oxygen diffusion. It also affects water and solute movement in frozen soils, which in turn influences soil strength, frost heaving and contaminant transport.

Solutes lower the freezing point of water during freezing and the relationship is given by the Van't Hoff equation. The freezing-point depression in dilute solutions can be calculated by using the following simplified equation (Marion 1995):

$$\Delta T \approx -1.86 \nu m_b \quad (5)$$

where  $\Delta T$  is the freezing-point depression,  $\nu$  is the number of aqueous species resulting from the dissolution of the solutes, and  $m_b$  is molarity of the solute. For pore water extracted from approximately 7-year-old pyritic tailings in Nanisivik (unpublished data) concentrations of magnesium and sulfate alone result in a freezing-point depression of more than 1°C compared to the corresponding freezing-point of pure water. However, deviations from Equation 5 are apparent for high concentrations, and particularly for electrolytes that dissociate into ions of higher valence.

A nearly pure ice phase will form when temperatures drop below the freezing-point, concentrating solutes in the remaining unfrozen solution and thereby further decreasing the freezing point. If equilibrium is maintained between the solution and ice phases during freezing the concentrations of various ions in solution will follow the ice-solution equilibrium line, increasing in concentration as the temperature decreases towards the eutectic composition. In a pure NaCl-H<sub>2</sub>O system with an initial NaCl molality greater than 5.17 mol/kg, the solution will not freeze until it reaches the eutectic temperature of -21.2°C. Below this temperature the solution will solidify as a mixture of ice and salt (Marion 1995).

The chemical equilibrium and the unfrozen water content during freezing can be modelled by FREZCHEM (Mironenko et al. 1997) as this model includes the coefficients for the Pitzer equations as well as solute redistribution during freezing. However, under natural conditions, and particularly for tailing water, site-specific characteristics will influence the ion exclusion and thereby the unfrozen water content. These characteristics include texture, specific surface area, charged surfaces, freezing rate and the initial

distribution of salts (Marion 1995), and are not included in the model. Within these limitations, FREZCHEM has been used to simulate the observed unfrozen water content measured in columns filled with mine tailings from Nanisivik (Elberling 2000). Unfrozen water content was measured by time domain reflectometry (TDR) and the tailings were samples from the upper reactive zone and partly oxidized zone (20 cm) as well as the lower reduced zone near the permafrost (80 cm). The chemical composition of the pore water from the same site and depths was used as input to FREZCHEM to predict the amount of unfrozen water content versus temperature (Fig. 4).

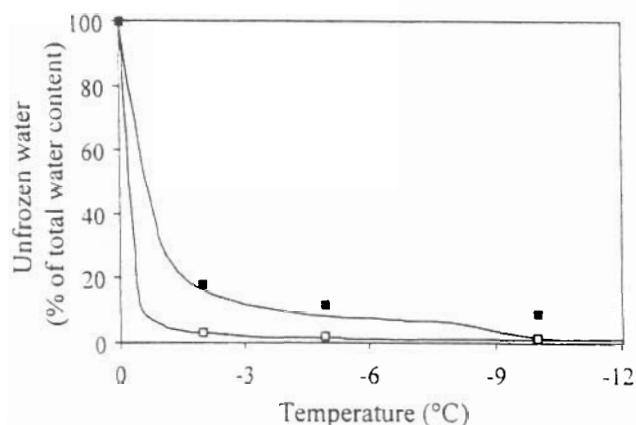


Figure 4. Unfrozen water content (% of total water content) in mine tailings collected at 20 cm within the oxidized zone (filled squares) and at 80 cm in the reduced zone (open squares) versus temperature. Observations are compared to FREZCHEM simulations (Elberling 2000).

The significant amount of unfrozen water, in particular in the reaction zone, suggests that liquid water is available for biological activity and contaminant transport well below 0°C.

### 3.3 Water movement in frozen soil

A potential environmental effect of the presence of unfrozen water is the diffusion of pollutants in the water phase and water movement within tailing profiles. The water movement is caused by the liquid films on particles which provide a route for water and solutes in frozen tailings (Godwaldt et al. 1999). In general, water in frozen sediments moves from warm to cold regions, from regions with low concentration to regions with higher concentrations and along water tension gradients (Marion 1995). As tailings in permafrost areas freeze from the top downward and from the permafrost table upward, the thermal gradients will induce a water flow towards the freezing fronts. The comparative importance of these two freezing fronts is determined during the freezing

process by environmental factors such as water content, temperature and snow cover.

As solutes are largely excluded in the freezing process, maximum solute concentrations are generally found close to the freezing front. The solute concentration in front of the freezing front may rise to 80 times the original concentration if no solutes are included in the frozen zone, and thus cause the freezing front to leap over solute pockets (Hallet 1978). These solute pockets may ultimately freeze, resulting in alternating bands of high and low ion concentrations in frozen tailings. This ion exclusion in freezing sediment has received much attention and is shown to be controlled by temperature gradient (freezing rate), pore water composition, water content, mixing and sediment type (e.g., Konrad & McCammon 1990). The extent of ion exclusion increases with decreasing freezing rate (Marion 1995). For freezing rates smaller than 0.1°C/day, corresponding to most field freezing conditions, more than 90% of the solutes have been observed to be rejected from the pore ice formed (Konrad & McCammon 1990).

The ion exclusion may result in an increased environmental impact from AMD during springtime when thawing starts from above and causes highly variable ion concentrations in the meltwater. Ion pulses (meltwater with very high ion concentrations) are known from most arctic areas (Melak & Sickman 1995, Rasch et al. 2000). Such pulses will have a maximum impact on living organisms sensitive to toxic levels of for example, heavy metals as well as on the overall flux of contaminants from tailing areas.

Water flow in frozen soils containing pore ice can be described by Darcy's Law in which the gradient in liquid pressure is the driving force and the hydraulic conductivity the transport characteristic. Although this Darcy flow is coupled to water flow induced by gradients in electrical potential and solute concentrations, values of apparent hydraulic conductivity for frozen soil have been derived (summarized by Kay & Perfect 1988). Generally, the apparent hydraulic conductivity decreases by orders of magnitudes as a result of freezing. However, this conclusion is based solely on laboratory observations of porous media with low or moderate concentrations of ions and has not been verified for partly weathered tailings with extreme concentrations of weathering products. The extent to which a general understanding of transport properties in frozen ground can be used to predict the potential movement of contaminants in frozen tailings is therefore unclear.

### 3.4 Soil strength

Frost heaving occurs as a result of the formation of segregated ice, e.g., lenses and needles, as well as the

volumetric expansion of water during freezing. Models are available to simulate and predict the mechanisms responsible for frost heaving (e.g., Chamberlain 1981, Black & Hardenberg 1991). Marion (1995) summarized the most important factors for the degree of frost heaving, including soil texture, pore size, freezing rate, temperature gradients, moisture and overburden stress. Frost heaving in tailings is considered a disadvantage as it produces cracks and preferential pathways that allow the infiltration of oxygen gas and oxygenated water. However, frost heaving is seldom observed in tailing areas, probably due to high ion concentrations that tend to reduce frost heaving. As pointed out by Sheeran & Yong (1975), this is to be expected because high ion concentrations increase the unfrozen water content and reduce the water available for forming segregated ice in tailings. Frost heaving may be important in cover materials provided as protection on top of tailings, and grain size and porosity should be considered in order to minimize frost heaving.

#### 4 AMD IN PERMAFROST REGIONS

Temperature fluctuations in continuous permafrost regions cause the surface layer to thaw annually. The thaw depth, defined as the active layer, varies typically between <0.5 m under thick organics to several metres under mineral soil. Pyrite oxidation is known to occur naturally in the active layer in permafrost areas where mining activity has never taken place. Cameron (1977) studied the oxidation of a massive sulphide body named the Agricola Lake prospect located northeast of Yellowknife, Canada. Apparently, intensive sulfide oxidation was occurring in the active layer both near the surface and at depth, and the lack of carbonate minerals in the area had resulted in natural acidic drainage (pH ~3-4) and metal leaching. Cameron (1979) observed the same phenomena in a massive sulfide deposit on Melville Peninsula in Northwest Territories, Canada. However, the presence of calcareous outcrops neutralized the acidic drainage and surface water. Active oxidation in permafrost areas in Canada has been confirmed by more recent observations in Yukon, Canada (Kwong 1995).

Another example of naturally exposed sulfide body is at Citronen Fjord in North Greenland where the mean air temperature varies between -15 and -20°C and temperatures above zero are only recorded during a very short summer period. During this period, the *in-situ* oxygen uptake was measured directly in well-drained and ochre-coloured sediment below the exposed sulfide outcrops in order to estimate the sulfide oxidation rate (Elberling & Langdahl 1998). Oxygen uptake rates in the order of 0.2-0.4 moles/m<sup>2</sup> per day were observed during September 1996. As

organic carbon was absent, the amount of oxygen consumed was assumed to represent the overall rate of sulfide oxidation. The high oxygen uptake rates observed were consistent with high concentrations of dissolved zinc and sulfate in pore water and surface drainage from the area.

The examples above illustrate that high sulfide oxidation rates occur naturally in continuous permafrost areas, at least during the short summer. Thus, weathering of naturally exposed sulfidic material may be important in relation to evaluating background concentrations of metals prior to mining activity.

##### 4.1 Oxidation of mine tailings deposited in continuous permafrost areas

Various waste materials are produced during the mining process. Mine waste consists of large chunks of rocks or overburden which are transported by trucks or dragline to waste dumps. The ore material is transported to the mill where processing consists of grinding followed by the extraction of the metals such as Zn, Pb, and Cu. Mine tailings, the waste product of metal extraction, consist of fine-grained sulfidic ore material with a reduced content of heavy metals. Mine tailings and waste rocks have very different hydrogeological, geochemical, and geotechnical characteristics and must therefore be considered separately in relation to AMD. The following section only evaluates the disposal of mine tailings; a more thorough discussion of the disposal of waste rocks in permafrost areas is provided by Dawson & Morin (1996).

Mine tailings consist of ore material finer than 0.2 mm and comprises a high proportion of sulfide grains with a large, fresh surface area. The results of ongoing investigations of oxygen uptake and heavy metal release in pyritic mine tailings deposited on land near Nanisivik Mine on Baffin Island (NWT) in northern Canada (73°N) are used in the following to illustrate the controlling parameters for AMD generation in well-drained tailings deposited in the continuous permafrost region (Elberling 2000).

In Nanisivik, the annual mean temperature (1994-1998) is -15.6°C and the annual precipitation is approximately 125 mm. Since 1976 mine tailings have been deposited under water in a tailings impoundment. As the available subaqueous storage capacity was exhausted in 1991 disposal of tailings began on land. A test plot within this area was selected and *in-situ* oxygen uptake rates were estimated by changes in oxygen concentrations in closed gas chambers placed on top of the tailings (Elberling & Nicholson 1996). Measurements were made periodically throughout the year and were accompanied by climatic measurements. Figure 5 shows that by the end of the summer the active layer extended to a depth of approximately 2 m and that this zone freeze during autumn.



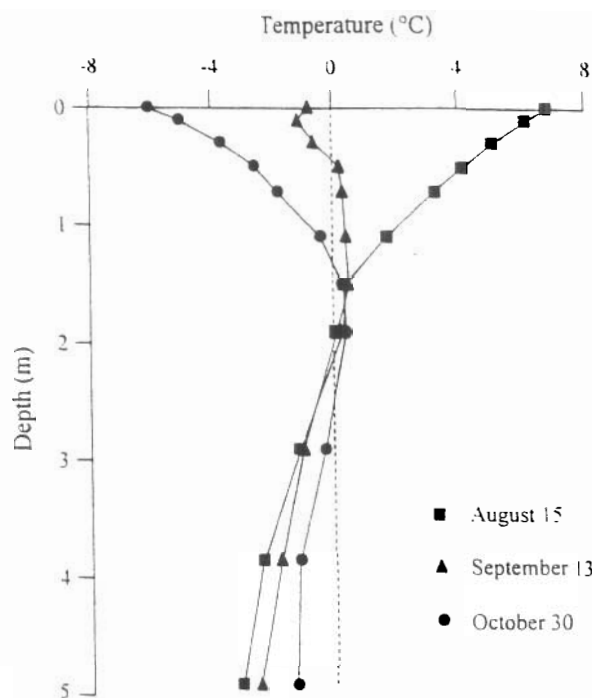


Figure 5. Soil temperature profile of an uncovered site at the tailings impoundment in Nanisivik. The tailings froze during a period of three months in 1997 (Elberling 1998).

However, the freezing of the active layer varies significantly between years depending on water content and snow accumulation that insulates the ground from low air temperatures.

During summer months, oxygen uptake rates in 6-year-old well-drained tailings were 0.2 to 0.5 moles  $O_2/m^2$  per day (Elberling 2000), similar to rates observed in temperate climates (Elberling et al. 1996). During the following 2-months period, the air temperature dropped below  $0^\circ C$ , resulting in significant effects on soil temperatures and the observed oxygen uptake (Fig. 6). Soil temperatures were used to model temporal variation in the reaction constant  $k$  (Eq. 2), and subsequently the expected variation in oxygen uptake over time, assuming that the diffusion coefficient within the reaction zone remained constant (Fig. 6). The model failed to predict the oxygen uptake during the first days following a major precipitation event on Julian day 216 (11 mm over less than 10 hours). However, a site covered with plates to prevent rain water infiltration but allowing free oxygen diffusion made it possible to differentiate between the effects of temperature and increasing water content on the overall oxygen uptake. Figure 6 shows that the model can predict the effect of temperature but not the effect of decreasing oxygen diffusion. The observations reveal the importance of soil temperature and water content on AMD.

Measurements during winter revealed that temperatures in the upper part of the snow-covered

tailings were in the range of  $-1$  to  $-3^\circ C$  and the oxygen consumption was about  $0.12 \pm 0.02$  moles of  $O_2/m^2$  per day or approximately 20-25% of the rates observed during summer. During early spring, temperatures the upper part of tailings were below  $-10^\circ C$  and oxygen uptake was not detectable. The first oxygen uptake during spring was observed as the soil temperature rose to  $-4^\circ C$ . These detailed measurements of oxygen uptake throughout the year indicate that AMD generation is highly sensitive to changes in temperature and that the effect of maintaining tailings below  $0^\circ C$  is predictable (Fig. 2).

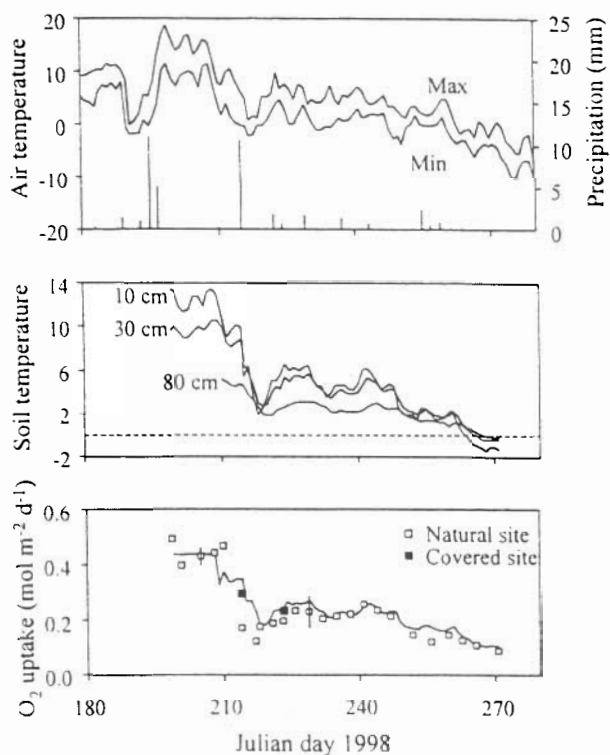


Figure 6. Air and soil temperatures (curves), precipitation (bars), and *in-situ* oxygen consumption rates at a natural site (open squares) and a covered site (solid squares) in well-drained tailings measured in 1998. Bars through squares represent the SD of replicates ( $n=6$ ). The simulated oxygen consumption is shown as a solid line (Elberling 2000).

## 5 AMD CONTROL STRATEGIES

AMD control strategies are based on control of AMD generation, control of contaminant migration, or collection and treatment of contaminated effluent. Although collection and treatment of contaminated effluent is a proven and demonstrated control strategy, maintaining such a facility at remote northern mine-

sites, following closure, is costly and logistically difficult (Dawson & Morin 1996). AMD generation and contaminant migration will be discussed in the following in relation to different control strategies, as these strategies aim to limit both AMD generation and contaminant migration.

### 5.1 Frozen covers

Permafrost regions offer a unique possibility for controlling AMD that is not naturally available in warm climates: the freezing of mine tailings by covering the tailings with an inert material and thereby forcing the frost table to move up and maintain the tailings at sub-zero temperatures all year round. The application of frozen covers has been tested in few places in continuous permafrost areas. At Lupin Mine, located 400 km NE of Yellowknife, Canada (65°N), sulfidic tailings (containing pyrrhotite, FeS) have been covered with 60 cm of gravel sand. Temperatures below the cover were above 0°C for more than 4 months each year and tailing temperatures as high as 20°C were observed during the summer (Dawson & Morin 1996). At Nanisivik Mine, results indicated that a 2-m cover consisting of natural cover materials (shales, till and sand) without any sulfide minerals will adequately induce the permafrost table to move up, thereby maintaining reactive tailings below 0°C on an annual basis (Fig. 7). However, as the test pads in Nanisivik during the test period were almost snow-free, additional snow in larger covered areas may result in increased insulation during autumn and higher early winter temperatures, but later thaw onset in spring. The impact of snow on ground temperatures and AMD generation in general is discussed in greater detail in section 5.3.

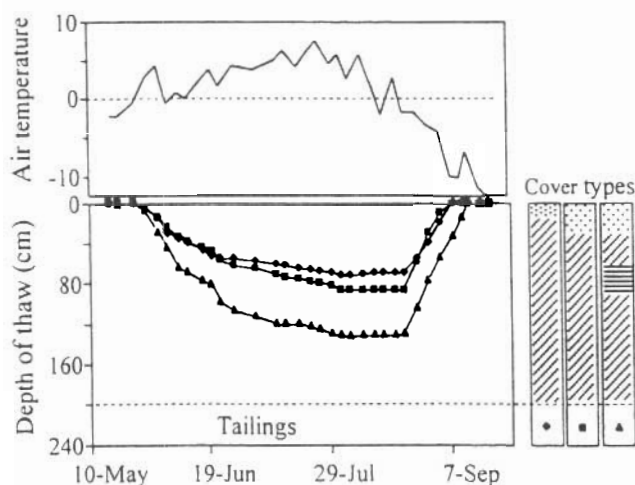


Figure 7. Active layer depths in tailings 1997 covered by two metres of inert covers near Nanisivik Mine, Canada (unpublished data from Nanisivik Mine). Covers consist of sand and gravel (dots), till (horizontal lines), and shale (hatched lines).

As shown in Figure 2, temperatures slightly below zero will not guarantee negligible sulfide oxidation or completely frozen tailing conditions. Therefore, the temperature at the tailing-cover interface becomes an important environmental parameter controlling AMD generation. Temperature readings below various cover schemes in Nanisivik reveal that temperatures typically vary between -15 to few degrees below zero. Thus, the recommended thickness of covers must be based on predictions of the sub-zero temperatures below the cover and the acceptance of the corresponding AMD generation. Several models are available for such predictions. Kyhn & Elberling (2001) calibrated the WinSoil model (Jansson 1998) to observed field conditions in Nanisivik and simulated the temperature below different cover schemes. Figure 8A shows an example of the importance of cover thickness on the temperatures at the tailing-cover interface. In this case snow was not considered.

Although freezing is considered a method to control AMD generation in permafrost areas, several factors complicate the application of ground temperature as a fine-tuned control method for AMD generation. As pyrite oxidation leads to a heat generation of approximately 12,000 kJ per kg pyrite (Dawson & Morin 1996) the oxidation process may influence the rate of ground freezing and result in higher temperatures near sulfide minerals than the temperature measured in bulk material. Assuming an annual average uptake of about 38 moles  $O_2/m^2$  as observed in Nanisivik 1998/99 (Elberling 2000) more than 1 kg pyrite per  $m^2$  oxidizes annually, generating about 32 kJ/ $m^2$  per day. Compared to 334 kJ required to melt 1 kg of ice (Godwaldt et al. 1999) the rate of heat loss from oxidizing tailings to the surroundings may be enough to maintain elevated temperatures and AMD generation for some time after bulk freezing.

Further laboratory studies of bacterial adaptation and temperature feedback mechanisms on sulfide oxidation in the temperature range 0 to -10°C seem crucial in order to provide reasonable long-term estimates for AMD generation at sub-zero temperatures.

### 5.2 Engineered dry and partly-saturated covers

Engineered layered soil covers have been used to achieve an effective reduction of oxygen and water movement within tailings. Typically, cover systems are constructed from natural sediments and consist of layers with different hydraulic properties. The upper layers aim to prevent erosion and evaporation, the middle layers aim to retain water and act as a barrier for oxygen, while the lower layers aim to prevent drainage from overlying layers. Using numerical simulation, Akindunni et al. (1991) showed that such barrier systems are possible when taking into account



the air-entry value of the middle layer and the pressure head at which the lower layer approaches residual saturation. However, in permafrost areas cracking caused by seasonal freezing and reduced moisture caused by evaporation may alter the transport properties and even enhance oxygen and water migration due to preferential flow in crack systems.

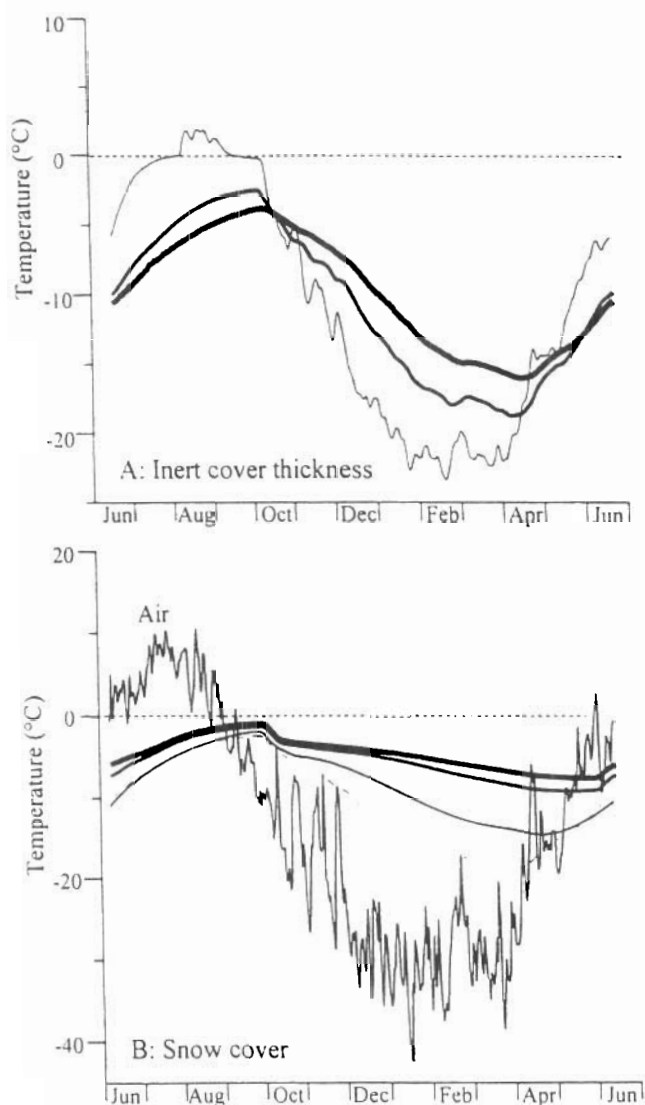


Figure 8. Simulated temperatures at the tailing-cover interface below covers. A: temperatures below 1 (thin line), 2 (solid line), and 3 (thick solid line) m of inert cover material represents characteristics of shale used in Nanisivik. B: temperatures below a 2-m metre cover in addition to no snow (dashed line), 5 cm (thin solid line), 25 cm (thick solid line) and 50 cm (very thick solid line) of snow. Meteorological variables are based on 1995/96 observations in Nanisivik.

### 5.3 Snow fences and snow covers

In the Arctic, most precipitation falls as snow during

winter. Snow covers are known to prevent wind erosion and redistribution of mine tailings during storms. Consequently, snow fences have been built, resulting in additional snow accumulation in tailing areas. The snow cover may also limit oxygen diffusion during winter and delay thawing in spring, thereby limiting the period of active layer development. However, decades of field observation in Alaska and Canada have shown that snow has a crucial influence on ground temperatures because its insulating effects that reduce winter heat loss (e.g., Nicholson & Granberg 1973). This insulation effect again depends on the thickness and density of the snow layer and it has been concluded that ground temperature variations from year to year are closely related to annual variations in snow accumulation (Nicholson & Granberg 1973). Results presented by Brooks et al. (1997, 1998) confirm that snow covers insulate frozen ground from the low winter air temperatures resulting in surprisingly high subnival levels of bacterial activity under seasonal snow cover. In a study by Brooks et al. (1997) fluxes of  $\text{CO}_2$  and  $\text{N}_2\text{O}$  as well as active microbial biomass were measured when soil temperatures under a snow cover ranged from  $-5^\circ\text{C}$  to  $0^\circ\text{C}$ . These observations led the authors to suggest that subnival bacteria activity may be a significant component of the annual C and N cycling in these environments. Elberling (2000) and Kyhn & Elberling (2001) have suggested that similar conditions exist in sulfidic tailings deposited in permafrost regions. The study by Kyhn & Elberling (2001) presented simulations based on WinSoil to verify the potential insulation effect of a snow cover (Fig. 8B). Further investigations are needed to quantify the effect of snow as a barrier for oxygen gas compared to snow as a barrier for heat controlling ground temperatures.

Although global changes in air temperatures have received much attention, global and local changes in snow covering (winter precipitation and wind regimes) may prove to be the most critical parameter for long-term AMD generation. This is probably particularly important for facilities constructed for permanent frozen disposal of well-drained tailings whereas facilities for permanent subaqueous disposal will be more sensitive to global changes that affect the water balance, such as summer evaporation rates and annual precipitation.

### 5.4 Subaqueous tailing disposal

Mine tailings have been placed under water in tailing impoundments in many locations worldwide, primarily to minimize oxygen diffusion into the tailing materials (Fig. 3). This disposal strategy has also been used in permafrost areas and may be attractive in areas where mine tailings can be placed in natural water bodies in a controlled fashion as is the case at Polaris Mine, a

lead-zinc mine on Little Cornwallis Island, Canada. Here, mine tailings have been discharged 26 m below the lake surface (Dawson & Morin 1996).

In permafrost areas without a suitable natural water body, construction of dams may be an alternative. The effect on AMD of covering tailings with water in permafrost areas has not received much attention although the potential effect is well known and can be easily illustrated. Considering the maximum oxygen diffusion in tailings covered with 30 cm saturated sand again covered by a thin cover of oxygen-saturated water. The maximum amount of oxygen which at steady state can diffuse through the 30 cm saturated cover at 5°C will be approximately  $1.5 \times 10^{-4}$  mol/m<sup>2</sup> per day (Eq. 4) or about 10,000 times less than the oxygen uptake observed in dry tailings at 5°C in Nanisivik (assuming instantaneous oxygen uptake at the tailing surface). The above predictions are consistent with laboratory tests on the reactivity of tailings under water (Mugo et al. 1999, Elberling & Damgaard 2001), indicating that the storage of reactive tailings under water is effective in attenuating long-term fluxes of contaminants to the overlying water column.

The local hydrology and water balance are important factors to consider when designing a water-covered tailing impoundment. After mine closure, the water balance will be based on the precipitation, melt water input and evaporation of the catchment area. Strategies can be designed to maintain an equilibrium state, such as snow fences to increase snow accumulation and meltwater and construction of channels to regulate water input and output to the pond area. Difficulties include sufficient storage capacity for extreme precipitation and the potential stability of dyke constructions in permafrost-affected areas.

Increasing oxygen solubility in cold water has been suggested as a concern when designing water covers (Dawson & Morin 1996, Davé & Blanchette 1999). The amount of oxygen in the water increases by a factor of 1.4 as the temperature decreases from 15 to 0°C, whereas the oxygen diffusivity decreases by a factor of 1.6 (Ramsing & Gundersen 1994) which is seldom taken into account. Comparisons of a saturated system at two different temperatures, using the above example with 30 cm saturated sand, the combined effect of increasing oxygen solubility and decreasing diffusivity will result in a reduction of the potential flux of oxygen at 2°C to approximately 90% compared to the flux at 15°C. The results of such simple calculations are consistent with measurements of micro-scale oxygen gradients and diffusivity in saturated tailings investigated at various temperatures (Elberling & Damgaard 2001). It can be concluded that subaqueous tailings disposal is probably a more effective remediation action in cold regions than elsewhere.

## 6 CONCLUSIONS AND FUTURE RESEARCH

There is currently great interest in understanding the chemical and physical processes occurring in frozen sediments in both natural and engineered systems. Concern about contamination in the Arctic is growing and frozen barriers have recently been considered as an option for preventing AMD generation. This review shows that AMD is not eliminated nor reduced to negligible levels at sub-zero temperatures, although it is reduced significantly. Very low temperatures for most of the year in the continuous permafrost zone can be shown to inhibit AMD generation. The effect of using ground temperature and freezing as the major control on tailing oxidation and release of pollutants in permafrost areas is only partly understood. Reduction of AMD may also be achieved by limiting the availability of oxygen to the tailings to maintain the reactive material nearly or fully water-saturated. In the latter case, natural freezing and the permafrost provide additional protection against AMD generation and reduce contaminant movement.

Several key issues need to be better understood for accurate prediction of acid mine drainage in cold regions and the overall limiting effects of freezing. These issues include environmental controls on oxidation processes below 0°C, the lower temperature limit for sulfide oxidation and the behaviour of contaminants migration in aqueous solutions in unsaturated and saturated frozen soils.

## ACKNOWLEDGEMENTS

Funding for this review was provided by the Danish Environmental Protection Agency, Ministry of Environment and Energy, Denmark, as part of the MIKA project "Chemical fluxes in frozen soil". MIKA is now known as DANCEA (Danish Cooperation for Environment in the Arctic). The author is solely responsible for the results and conclusions presented. Special thanks go to B.H. Jakobsen, G. Asmund, R. S. Sletten and K. LeDrew for comments on the manuscript.

## REFERENCES

- Akindunni, F., R.W. Gillham & R.V. Nicholson 1990. Numerical simulations to investigate moisture-retention characteristics in the design of oxygen-limiting covers for reactive mine tailings. *Can Geotech. J.* 28: 446-451.
- Barnall, D. & D. Slotfeld-Ellington 1983. Pulsed nuclear resonancestudies of doped ice. *J. Phys. Chem.* 87: 4321-4329.

- Black, P.B. & M.J. Hardenberg 1991. Historical perspectives in frost heave research: the early works of S. Taber & G. Beskow. *USA Cold Regions Research and Engineering Laboratory*, Special Report 91-23.
- Boyd, W.L. & J.W. Boyd 1964. The presence of bacteria in permafrost of the Alaskan arctic. *Can. J. Microbiol.* 102: 917-919.
- Brooks, P.D., S.K. Schmidt & M.W. Williams 1997. Winter production of CO<sub>2</sub> and N<sub>2</sub>O from alpine tundra: environmental controls and relationship to inter-system C and N fluxes. *Oecologia*, 110: 403-413.
- Brooks, P.D., M.W. Williams & S.K. Schmidt 1998. Inorganic nitrogen and microbial biomass dynamics before and during spring snowmelt. *Biogeochemistry* 43: 1-15.
- Cameron, E.M. 1977. Geochemical dispersion in mineralized soils of a permafrost environment. *J. Geotechn. Exploration*. 7: 301-326.
- Cameron, E.M. 1979. Effect of graphite on the enhancement of surficial geochemical anomalies originating from the oxidation of sulphides. *J. Geotechn. Exploration*. 12: 35-43.
- Dawson, R.F. & K.A. Morin 1996. Acid mine drainage in permafrost regions: issues, control strategies and research requirements, *Department of Indian and Northern Affairs Canada*, MEND report 1.61.21. CANMET, Natural Resources.
- Elberling, B. 1998. Processes controlling oxygen uptake rates in frozen mine tailings in the Arctic. In: *Ice in Surface Waters* (H.T. Shen, ed), 183-188. A.A. Balkema Rotterdam/Brookfield.
- Elberling, B. 2000. Environmental controls of the seasonal variation in oxygen uptake in sulfidic tailings deposited in a permafrost-affected area. *Water Resour. Res.* (in press).
- Elberling, B. & L.R. Damgaard 2001. Micro-scale measurements of oxygen diffusion and consumption in subaqueous sulfide tailings. *Geochim. Cosmochim. Acta* (in press).
- Elberling, B. & B.R. Langdahl 1998. Natural heavy-metal release by sulphide oxidation in the High Arctic. *Can. Geotech. J.* 35: 895-901.
- Elberling, B. & R.V. Nicholson 1996. Field measurements of oxygen diffusion and sulphide oxidation in mine tailings. *Water Resour. Res.* 326: 1773-1784.
- Elberling, B., R.V. Nicholson & D.V. Darren 1993. Field evaluation of sulphide oxidation rates. *Nordic Hydrol.* 245: 323-338.
- Elberling, B., R.V. Nicholson & J.M. Scharer 1994. A combined kinetic and diffusion model for pyrite oxidation in tailings: a change in control with time. *J. Hydrol.* 157: 47-60.
- Elberling, B. A. Schippers & W. Sand 1999. Bacterial and chemical oxidation of pyritic mine tailings at low temperatures. *J. Cont. Hydrol.* 41: 225-238.
- Evangelou, V.P. 1995. Pyrite oxidation and its control. *CRC Press, Inc.* 293 pp.
- Forster, J. 1887. Ueber einige Eigenschaften leuchtender Bakterien. *Zentr. Bakteriolog. Parasitenk. Infekt. Hyg.* 2:337-340.
- Gilichinsky, D.A., E.A. Vorobyova, L.G. Erokhina, D.G. Fyodorov-Davydov & N.R. Chaikovskaya 1992. Long-term preservation of microbial ecosystems in permafrost. *Adv. Space Res.*, 12:255-263.
- Godwaldt, R.C., K.W. Biggar & D.C. Sego 1999. AMD generation at sub-zero temperatures. In: *Assessment and Remediation of Contaminated sites in Arctic and Cold Climates*, 75-82. ARCSACC'99, Edmonton, May 3-4, 1999.
- Hallet, B. 1978. Solute redistribution in freezing ground. In proceedings of the *Third International Conference on Permafrost*, 85-91. Edmonton, Canada. 1978.
- Jansson, P.E. 1998. Simulation model for soil water and heat conditions: description of the SOIL model. *Commun.* 98:2, Swedish University of Agricultural Science, Department of Soil Science, Uppsala, Sweden.
- Jaynes, D.B., A.S. Rogowski & H.B. Pionke 1984. Acid mine Drainage from reclaimed coal strip mines 1. Model description. *Water Resour. Res.* 20: 233-242.
- Kalin, M. 1987. Ecological engineering for gold and base metal mining operations in the North West Territories, in *Northern Affairs Program*, Department of Indian Affairs and Northern Development, pp. 1-64. Environmental Studies no. 59.
- Kjøller, A. & S. Ødum 1971. Evidence for longevity of seeds and microorganisms in permafrost. *Arctic.* 243: 230-232.

- Konrad, J.M. & A.W. McCammon 1990. Solute partitioning in freezing soils. *Can. Geotech. J.* 67: 726-736.
- Kwong, Y.T.J. 1995. Geochemical, electrochemical and microbial control of sulphide oxidation and their implication for the abatement of acid drainage. In: *International Workshop on Abatement of Geogenic Acidification in Mining Lakes*, Sept. 4-6, 1995, Magdeburg, Germany.
- Kyhn, C. & B. Elberling 2001. Frozen cover actions limiting AMD from mine waste deposited on land in Arctic Canada. *Cold Region Science and Technology* (in press).
- Langdahl, B.R. 1999. Acidophilic microorganisms in a High Arctic gossan environment. PhD. Thesis, *Department of Microbial Ecology, Institute of Biological Sciences, University of Aarhus, Denmark*. 241 pp.
- Langdahl, B.R. & K. Ingvorsen 1997. Temperature characteristics of bacterial iron solubilisation and  $^{14}\text{C}$  assimilation in naturally exposed sulfide ore material at Citronen Fjord, North Greenland (83°N). *FEMS Microbiol. Ecol.* 23:275-283.
- Marion, G.M. 1995. Freeze-thaw processes and soil chemistry. CRREL special report 95-123. US Army Corps of Engineers. *USA Cold Regions Research and Engineering Laboratory*, 1-28.
- Melak, J.M. & J.O. Sickman 1995. Snowmelt induced chemical changes in seven streams in the Sierra Nevada, California. *Biogeochemistry of seasonally snow-covered Catchments* (Proceedings of a Boulder Symposium, 221-234. July 1995. IAHS Publ. 228.
- Meldrum, J.L., H.E. Jamieson & L.D. Dyke 1999. Laboratory determination of sulphide oxidation potential in permafrost using tailings from Rankin Inlet, Nunavut. In: *Mining and the Environment 2*, 119-126. Sudbury, Canada. September 12-16, 1999.
- Mironenko, M.V., S.A. Grant, G.M. Marion & R.E. Farren 1997. FREZCHEM2. A chemical thermodynamic model for electrolyte solutions at subzero temperatures, pp. 1-40, *Cold Regions Research & Engineering Laboratory*, CRREL Report 97-5.
- Morita, R.Y. 1975. Psychrophilic bacteria. *Bacteriol. Rev.* 39: 144-167.
- Mugo, R.K., D. McDonald & G.W. Poling 1999. Subaqueous tailings disposal in freshwater and marine environments - results of predictive geochemical testing using tailings with different compositions. In: *Mining and the Environment 2*, 99-108. Sudbury, Canada, September 12-16, 1999.
- Nicholson, F. H. & H.B. Granberg 1973. Permafrost and snow cover relationships near Schefferville. *Second International conference on Permafrost*. 151-158. Yakutsk, U.S.S.R., 13-28 July 1973.
- Nicholson, R.V., R.W. Gillham & E.J. Reardon 1988. Pyrite oxidation in carbonate-buffered solution: I experimental kinetics. *Geochim. Cosmochim. Acta*. 52: 1077-1085.
- Nordstrom, D.K. & G. Southam 1997. Geomicrobiology of sulfide mineral oxidation. Chapter 11 in *Geomicrobiology*. Mineralogical Society of America. Reviews in Mineralogy. 35: 362-390.
- Pantelis, G. & A.I.M. Ritchie 1992. Macroscopic transport mechanisms as a rate limiting factor in dump leaching of pyritic ores. *Appl. Mat. Model.* 15: 136-143.
- Paktunc, A.D. 1999. Characterization of mine wastes for prediction of acid mine drainage. In: *Environmental impacts of mining activity*. J. M. Azcue (Ed.). Springer, 19-40.
- Price, W.S., H. Ide & Y. Arata 1999. Selfdiffusion of supercooled water to 238 K using PGSE NMR diffusion measurements. *J. Phys. Chem.* 103: 448-450.
- Ramsing, N. & J. Gundersen 1994. Seawater and gases. Tabulated physical parameters, version 1.0. Unisense A/S, Århus, Denmark.
- Rasch, M, B. Elberling, B.H. Jakobsen & B. Hasholt 2000. High-resolution measurements of water discharge, sediment, and solute transport in the river Zackenbergelven, Northeast Greenland. *Arctic, Antarctic, and Alpine Research* 32: 336-345
- Sheeran, D.E. & R.N. Yong 1975. Water and salt redistribution in freezing soils. In *Conference on Soil Water Problems in Cold Regions*, 58-69. Division of Hydrology, AGU, Calgary, Alberta, Canada, May 6-7, 1975.
- Troeh, R.F., J.D. Jabro & D. Kirkham 1982. Gaseous diffusion equations for porous materials. *Geoderma*, 27: 239-253.



ELSEVIER

Cold Regions Science and Technology 32 (2001) 133–142

cold regions  
science  
and technology

www.elsevier.com/locate/coldregions

## Frozen cover actions limiting AMD from mine waste deposited on land in Arctic Canada

Curt Kyhn, Bo Elberling \*

*Institute of Geography, University of Copenhagen, Øster Voldgade 10, DK-1350 Copenhagen, Denmark*

Received 4 August 2000; accepted 10 December 2000

### Abstract

Mining in permafrost-affected areas presents unique characteristics and possibilities that need to be considered in order to investigate alternative actions to minimize the environmental impact of mining. Encapsulating mine waste within the permafrost zone by covering is considered one of the most promising actions to limit acid mine drainage and has been investigated near Nanisivik Mine in northern Canada. Quadrant test pads consisting of approximately 2 m of inactive (non-sulfidic) material have been constructed on top of oxidizing sulfidic mine tailings. A one-dimensional physically based soil water and heat model (WinSoil) has been calibrated and used to simulate observed subsurface temperatures within and below covers. Model input parameters include meteorological data such as air temperatures as well as thermal conductivity of cover material. The model was calibrated against ground temperatures measured in 1998 and validated against ground temperatures measured since 1995. WinSoil simulations were found to match observed ground temperatures reasonably well without calibration and almost perfect matches were obtained by varying the thickness of snow cover by a few centimetres. Observations and simulations reveal that temperatures within mine tailings have been below 0°C since covering 6 years ago. In addition to simulating observed ground temperatures, WinSoil was used to predict ground temperatures in relation to cover thickness and snow cover. The simulations question whether a 2-m cover will hinder sulfide oxidation processes within covered tailings if winter snow increases significantly due to either large-scale application of covers or global climate changes. © 2001 Elsevier Science B.V. All rights reserved.

**Keywords:** Tailings; Low temperature; Frozen ground; Management; Arctic

### 1. Introduction

Acid mine drainage (known as AMD) is a well-known environmental problem resulting from the exposure of mining waste from base metal mines.

Waste materials contain reactive sulfide minerals which oxidize in the presence of oxygen and water. A number of such base metal mines are operating or proposed in regions with permafrost. In these regions, the unique environmental characteristics need to be considered when planning strategies for minimizing AMD. The permafrost environment is generally considered to be a controlling feature itself that allows the mine tailings to freeze or to be kept at near freezing conditions most of the year in order to

\* Corresponding author. Tel.: +45-3532-2520; fax: +45-3532-2501.

E-mail address: be@geogr.ku.dk (B. Elberling).



restrict AMD generation. The low temperatures slow most chemical and biological processes and freezing may restrict the migration of pollutants. However, depending on the thermal properties of the ground material and local weather conditions, an active layer develops each summer, which may promote the transport of oxygen gas and the release and spread of contaminants to the surroundings by acidic drainage to local watershed stream systems and to marine environments. This has been documented from several studies in the Arctic (e.g., McKnight and Bencala, 1990; Godwaldt et al., 1999).

In order to control mine tailing oxidation and acidic mine drainage, the application of permafrost by freezing and encapsulating frozen tailings below engineered covers has been suggested (Dawson and Morin, 1996). Such remediation actions rely on studies indicating that microbial activity is nearly absent at temperatures below 0°C (e.g., Ahonen and Tuovinen, 1992). However, temperatures at 0°C may not eliminate AMD as microbial activity has been shown to take place even in very cold environments (e.g., Gilichinsky and Wagener, 1994). A laboratory study of oxygen uptake within sulfidic tailings collected in Nanisivik reveals that at 0°C, the overall rate of sulfide oxidation may be as high as 20% of full capacity (Elberling, 2001). These findings are consistent with the fact that significant amounts of unfrozen water exists in mine tailings well below 0°C (Nassar et al., 2000; Elberling, 2001) thereby facilitating biogeochemical processes. Thus, prior to a large-scale application of thermal covers, a field evaluation and site specific simulations are required to quantify potential heat and mass transfers within the frozen cover material and mine waste at various temperatures. Several physically based computer models of coupled heat and water flow are available for such simulations and the models have previously been successfully applied to predict ground temperatures (Flerchinger et al., 1990; Peck and O'Neil, 1995). To our knowledge, such models have not been previously used to predict ground temperatures below thermal covers constructed on mine waste deposited in the Arctic.

The objective of this study is to examine thermal covers as an option for minimizing AMD from tailings deposited on land near Nanisivik Mine in northern Canada with special emphasis on cover

composition and thickness, snow cover and future climatic changes in an Arctic environment. The examination was carried out by conducting simulations using a soil heat and water flow model, Win-Soil (Jansson, 1998), which was calibrated and verified based on data from the study area.

## 2. Study area

The Nanisivik Mine is located within the zone of continuous permafrost on the northern part of Baffin Island in the Canadian Archipelago (73°02'N, 84°32'W). The annual precipitation of the area is approximately 125 mm, and the annual mean temperature is -13.5°C (Elberling et al., 2000). In this arid and cold climate, vegetation is almost absent. Daily mean temperatures, net radiation and precipitation (1998–1999) are shown in Fig. 1. Nanisivik Mine is a zinc/lead mine producing about 650 000 tons tailings/year, consisting of approximately 80% pyrite ( $\text{FeS}_2$ ), 20% dolomite ( $\text{CaMg}(\text{CO}_3)_2$ ), and minor contents of galena ( $\text{PbS}$ ) and sphalerite ( $\text{ZnS}$ ). Since the beginning of mining in 1973, the tailings have been pumped uphill from the mill (elevation 250 mas) into West Twin Lake (elevation 371 mas). After filling the lake 6 years ago, a dam was con-

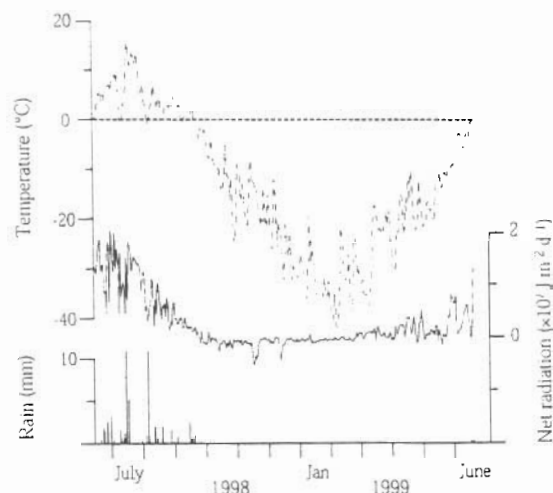


Fig. 1. Daily mean temperatures (dashed line), net radiation (solid line) and precipitation (bars) from June 1998 to June 1999 in Nanisivik, Canada.



and future  
ment. The  
ng simula-  
odel. Win-  
d and veri-

structed. Despite the efforts to maintain tailings under water, a small but increasing amount of tailings are deposited on land directly exposed to the atmosphere.

### 3. Materials and methods

#### 3.1. Test covers and field measurements

Test pads erected by Nanisivik Mine since 1991 consist of various materials, and different construction techniques have been used. Test pad 1 (TP1) was constructed in 1991 and consists of 2 m of shale (Fig. 2) on top of newly deposited tailings, and it covers an area of 30 × 30 m. A string of thermocouples was installed in the centre of the pad at depths of 1, 2, 3 and 5 m. A second test pad (TP2), located next to TP1 and included for comparison, consists of 1.7 m of shale with a layer of sand and gravel (0.3 m) on the top. Both test pads have a thin surface cover of light-coloured rocks, in order to keep down surface temperatures during summers by increasing the solar reflection. The following evaluation is based on these two pads.

Thermocouple temperature readings have been made manually on a monthly basis since 1993 and during periods of intensive field work on a weekly or even daily, basis. In 1998, field work was conducted

in July, August and September and again for 3 weeks from mid-November. Air temperatures, relative humidity, net radiation, wind speed and precipitation (rain, but not snow) have been recorded since 1995 by a weather station at the tailings pond.

#### 3.2. Laboratory measurements

Thermal conductivity ( $k$ ) was measured using conductivity probes (TC 20, Soiltronics), each consisting of a heating element and a thermocouple embedded together in a stainless steel tube. Connected to a power supply, the heating element increases the temperature of its immediate surroundings and itself. After heating, the decreasing temperature in the surroundings was measured during 100 s and used to calculate the thermal conductivity of tailings and cover material at various degrees of water saturation (Shiozawa and Campbell, 1990; Soiltronics, 1992). An average thermal conductivity was calculated based on 24 measurements and used as an input parameter for WinSoil. The water content of samples was determined gravimetrically.

#### 3.3. Modelling concept

In the following, it is assumed that ground temperatures can be analysed in terms of heat conduction theory, as shown by Williams and Smith (1995):

$$Q = -k \frac{dT}{dz} \quad (1)$$

where  $Q$  (J/s m<sup>2</sup>) is the heat flow,  $k$  (W/m K) is the thermal conductivity and  $dT/dz$  is the temperature gradient over the distance  $z$ . A heat balance within a soil layer per unit cross-sectional area and thickness  $z$  can be written as a function of heat flowing into the layer balanced with the heat flowing out and the change of heat content of the soil layer:

$$\frac{\partial T}{\partial t} = \kappa \frac{\partial^2 T}{\partial z^2} \quad (2)$$

where  $\kappa$  is the thermal diffusivity ( $= k/C$ ),  $C$  is the thermal capacity and  $t$  is the time. The soil heat capacity ( $C$ ) equals the sum of heat capacities of soil constituents, including the heat capacity of the solid

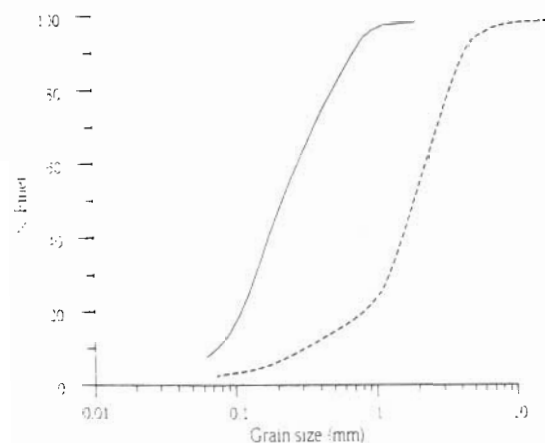


Fig. 2. Grain size distribution of tailings (solid line) and the inert "shale" cover material (dashed line) used in test pads at Nanisivik.

the zone of  
rt of Baffin  
(73°02'N,  
the area is  
mean tem-  
00). In this  
most absent.  
d precipita-  
Nanisivik  
out 650 000  
nately 80%  
O<sub>3</sub>), and  
erite (ZnS).  
the tailings  
(elevation  
371 mas).  
n was con-

Net radiation (solid line) and June 1999 in

soil constituents ( $C_s$ ) and the heat capacity of water ( $C_w$ ):

$$C = (1 - \theta)C_s + \theta C_w \quad (3)$$

where  $\theta$  is the water content. For frozen soil  $C_w$  is replaced by the heat capacity of ice ( $C_i$ ). For partly frozen soil, a weighted fraction for  $C_w$  and  $C_i$  is used.

### 3.4. Modelling setup

WinSoil is a well-documented one-dimensional physically based model for analysing heat and water transport in soil or any given porous media based on the equations of Fourier and Darcy (Jansson, 1998). The thermal conductivity ( $k$ ) is calculated based on two semi-empirical equations for unfrozen and completely frozen soils. The two equations include three ( $a_1$ ,  $a_2$ ,  $a_3$ ) and four ( $b_1$ ,  $b_2$ ,  $b_3$ ,  $b_4$ ) empirical constants, respectively. The empirical equations are for sandy soils adopted from Kersten (1949), but adjusted to accommodate laboratory observations on the volumetric water content ( $\theta$ ) and thermal conductivity (Jansson, 1998):

$$k_{\text{unfrozen}} = \left( a_1 \log \left( \frac{\theta}{\rho_s} \right) + a_2 \right) 10^{a_3 \rho_s} \quad (4)$$

and

$$k_{\text{frozen}} = b_1 10^{b_2 \rho_s} + b_3 \left( \frac{\theta}{\rho_s} \right) 10^{b_4 \rho_s} \quad (5)$$

where  $\rho_s$  is the density of solid matter.

Thermal probe laboratory experiments on unfrozen cover material from Nanisivik were used to fit Eq. (4) utilized by WinSoil (Fig. 3). The three parameters required are ( $a_1$ ,  $a_2$ ,  $a_3$ ): 0.758; 0.003 and 0.088. The thermal capacity of the solid material is set to  $2 \times 10^6 \text{ J/m}^3 \text{ K}^{-1}$  (Jansson, 1998). Fig. 3 shows thermal conductivities for frozen cover materials based on default values ( $b_1$ ,  $b_2$ ,  $b_3$ ,  $b_4$ ): 0.00158; 1.336; 0.00375 and 0.9118. A weighted conductivity ( $k_{\text{wet}}$ ) is used for the partly frozen conditions and the equation is expressed by the mass ratio of frozen water to the total amount of water (Jansson, 1998).

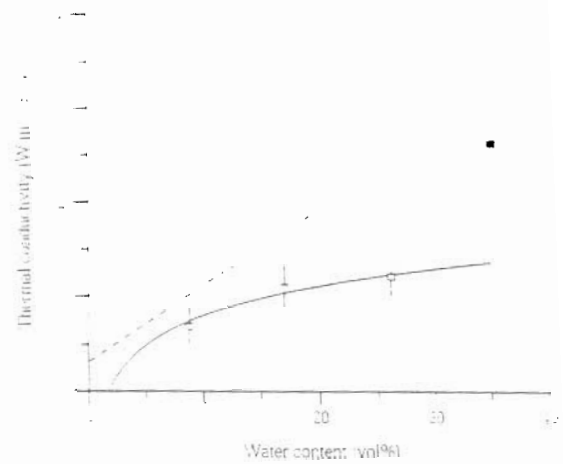


Fig. 3. Observed thermal conductivities vs. water content are shown for unfrozen "shale" material ( $\square$ ) and saturated tailings ( $\blacksquare$ ). The 95% confidence limit of means are shown. A Kersten equation for unfrozen "shale" fitted to observations (solid line) and default values for frozen shale (dashed line) are included.

The surface temperature is calculated based on the air temperature ( $T_a$ ), assuming free interactions between the interface of the atmosphere and the ground. In case of a snow cover, the surface temperature ( $T_{ss}$ ) is adjusted with respect to a steady state heat flow between the soil with a temperature of  $T_1$  and a homogeneous snow pack.

$$T_{ss} = \frac{T_1 + aT_a}{1 + a} \quad (6)$$

The influence of a snow cover ( $\Delta z_{\text{snow}}$ ) on surface temperature is governed by a weighting factor ( $a$ ) which includes thermal conductivities of the upper soil layer ( $k_h$ ) and the snow ( $k_{\text{snow}}$ ) in addition to the thickness of both layers.

$$a = \frac{k_{\text{snow}} \left( \frac{\Delta z_1}{z} \right)}{k_h \Delta z_{\text{snow}}} \quad (7)$$

The thermal conductivity of the snow pack is calculated through an empirical parameter ( $s_k$ ) and the snow density ( $\rho_{\text{snow}}$ ), which is a weighted average of old snow pack and newly fallen snow.

$$k_{\text{snow}} = s_k \rho_{\text{snow}}^2 \quad (8)$$

In the model, the freezing point is utilized to calculate the sensible heat. The freezing point depression ( $r$ ) is expressed by the ratio of the latent heat part ( $E$ ) of the total heat content within the partially frozen soil and the total soil heat content ( $E_t$ ) and the pore size distribution (Jansson, 1998). Finally, the soil temperature ( $T$ ) in specified compartments is calculated as a ratio between sensible heat ( $H$ ) and the heat capacity ( $C_t$ ),

$$T = \frac{H}{C_t} \quad (9)$$

### 3.5. WinSoil calibration

Meteorological variables in WinSoil are provided from the weather station and include daily air temperatures, relative humidity, net radiation, wind speed and precipitation. Some of the meteorological driving variables for specific years were missing due to malfunctioning of the instruments involved (net radiation in 1996–1997 and precipitation in 1997–1998). Instead, the values were carefully estimated according to recordings of similar years. Winter snow has not been included in the model at the calibration state because information during winter is limited and because snow has been observed to blow away from the test pads, leaving only temporary covers of up to a few centimetres of snow throughout the winter. However, in the validation process and in the simulations of future environmental conditions, snow covers are incorporated in the model.

A period from June 15 to December 5, 1998 was selected for calibration as this period was the most intensively studied. A 6-m vertical profile simulating tailings covered with inert material was divided into 10-cm compartments within the upper 3-m and 50-cm compartments below. Initial ground temperatures for each compartment were set according to thermocouple temperature readings and interpolated temperatures.

Based on the grain size distribution (Fig. 2) and an average porosity of 35%, the intermediate range of the water retention curve of cover material and tailings were calculated according to Brooks and Corey (1964). At a water content near the wilting point, a log-linear expression was used and at near-

saturation, a linear expression was used (Jansson, 1998). A physical drainage equation (Hooghoudt, 1940) included in WinSoil, was activated to accommodate the specific drainage conditions within the test pads. Inputs to the drainage equation included the distance from the thermocouple string to the edges of the test pad, the height of the test pad, and the depth to groundwater flow. Evaporation was calculated according to Penman-Monteith (Monteith, 1965). As data on water content in the test pads were not available from the entire observation period, a uniform pressure head was implemented. Because of the very coarse nature of the cover material, the head was set to a 100-cm water column, which approximately equals the wilting point of the material.

## 4. Results and discussion

### 4.1. Ground temperatures in uncovered and covered tailings

Air temperatures in the region vary from a minimum of about  $-40^\circ\text{C}$  in January and February, to a summer temperature maximum of about  $15^\circ\text{C}$  in July. The active layer within uncovered tailings typically evolves down to a maximum of 2 m in August and the tailings are almost completely frozen again by October (Fig. 4). The dimensions of the test pads, i.e. 2 m, were based on active layer characteristics observed prior to construction. Field observations over the period after construction (1993–1999) reveal that the active layer had not extended below the 2 m of cover material.

Thermocouple readings in TP1 (1995–1998) show temperatures at the tailings surface at 2 m of depth from  $-15^\circ\text{C}$  to  $-10^\circ\text{C}$  in February and March. The warmest months are August and September, where temperatures reach  $-2^\circ\text{C}$  to  $-0.5^\circ\text{C}$  at this depth. A maximum temperature at the cover/tailings interface in TP1 of  $-0.2^\circ\text{C}$  was observed in August 1993. Generally, TP2 is slightly colder than TP1, reaching a high of  $-1^\circ\text{C}$  in August 1998 at the cover/tailings interface. On the other hand, TP2 was not as cold in the winter reaching only  $-7.2^\circ\text{C}$  in December 1998. However, due to the low temperature recording frequency (usually once a month) annual maximum and minimum temperatures may be concealed.

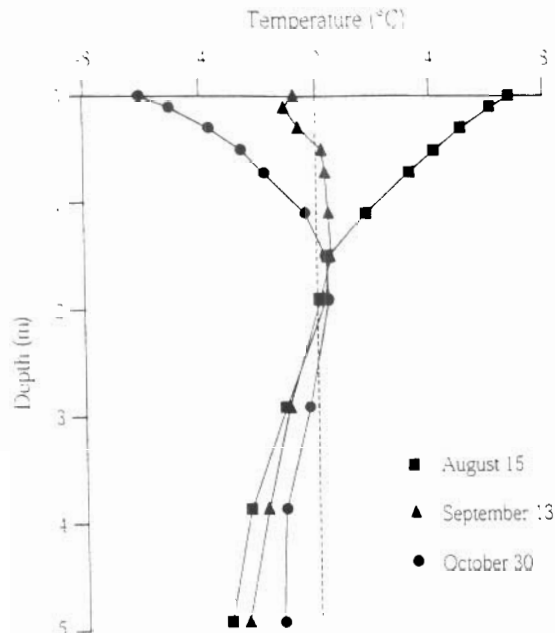


Fig. 4. Ground temperatures within uncovered tailings in 1999.

Calibration of WinSoil without fitting reveals a fair agreement between observed temperatures and simulated temperatures (Fig. 5). The model was subsequently validated on data from the period covering 1995–1998 (Fig. 6). Throughout each year of validation, the model yielded a fair agreement between observed and modelled ground temperatures, except for the winter season of 1997–1998. However, simulating a snow cover of a few centimetres during that winter narrows this difference considerably (Fig. 6(C)). A few centimetres of snow in 1997–1998 is realistic, as the test pads appeared to be white a few times during the winter 1997–1998, according to aerial photographs of the area. The effect of increasing snow accumulation on subsurface mine tailing temperatures below covers is further simulated by WinSoil and discussed in the following.

#### 4.2. Snow accumulation and large-scale cover applications

Test pads used in this study are built as flat mounds, which are almost snow-free during winter; whereas the surroundings are typically covered by in

average 30 cm of snow and up to 150 cm in some places. Therefore, an increasing snow accumulation on thermal covers during winter may result from a large-scale application of thermal covers (e.g., covering an entire tailing impoundment) or as a result of global climate changes. The effects of various snow cover thicknesses on subsurface temperatures have been simulated using WinSoil. Four snow cover scenarios have been simulated, i.e. no snow, 5, 25 and 50 cm of snow. Due to the limited amount of data (dating back to 1995) a representative year (1995–1996) was selected for simulations regarding snow cover as well as tailings cover thickness (Section 4.3). The simulations were allowed to run repeatable for years, however, equilibrium conditions with respect to ground temperatures were obtained in the second year. Simulations with various snow cover thicknesses based on covered tailings similar to TP1 indicate that snow may have a dramatic impact on the temperature regime within covered tailings (Fig. 7). Simulations reveal that a snow cover of only 5 cm has a large and significant damping effect on

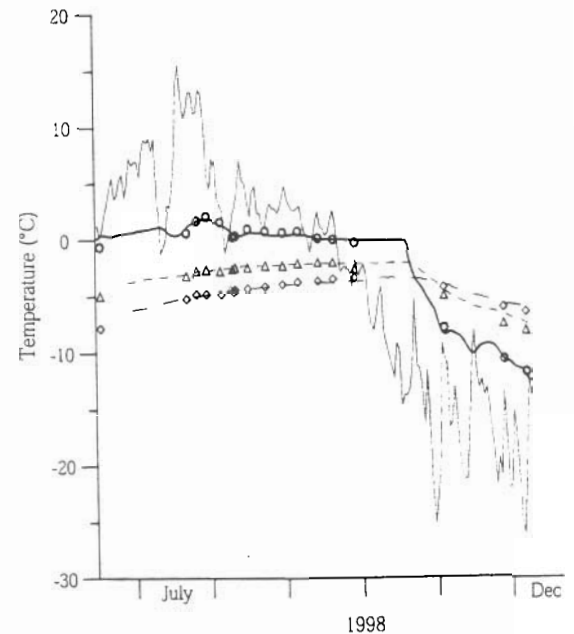


Fig. 5. Ground temperatures in Test pad 1 at depths 1 (O), 2 (Δ) and 3 m (◇) over the calibration period June 15–December 5 1998. Observations are shown as dots and simulated temperatures with lines. Air temperatures used as input are shown as a solid thin line.

cm in some accumulation result from a (e.g., cover is a result of various snow temperatures have snow cover snow, 5, 25 and amount of tentative year ons regarding ickness (Sec- ed to run rem conditions re obtained in is snow cover imilar to TP1 ic impact on tailings (Fig. ver of only 5 ing effect on

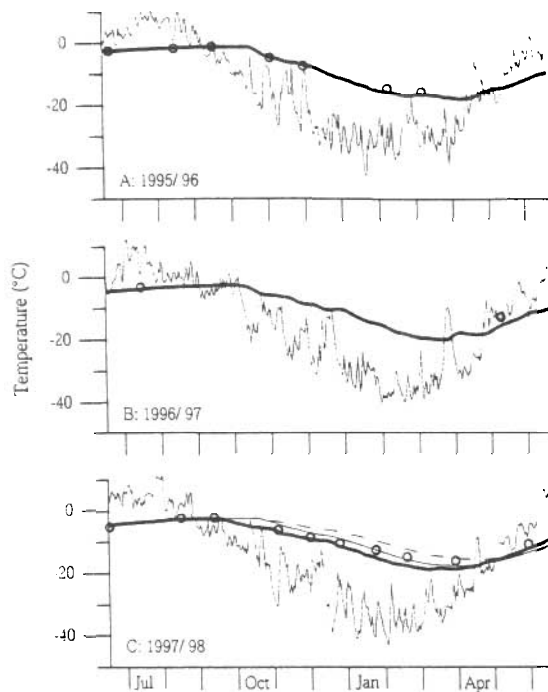


Fig. 6. Temperatures 2 m below cover surface in Test pad 1 (at the tailing/cover interface) in (A) 1995–1996, (B) 1996–1997 and (C) 1997–1998. Simulated temperatures are shown as thick solid lines, observations as open dots, and air temperatures as thin solid lines. For 1997–1998, simulated snow cover thicknesses of 5 cm (dashed line), 2 cm (solid line) and no snow cover (thick solid line) are shown.

temperatures at the cover/tailings interface, whereas snow covers of more than 25 cm have little additional effects. These simulations are consistent with the validation process, revealing the importance of a precise simulation of even a few centimetres of snow (Fig. 6(C)). Flerchinger (1991) also indicated that a snow depth of less than 10 cm significantly affected the total frost depths, based on SHAW model simulations. Attempts to simulate the actual snow cover in Nanisivik in the season of 1997–1998 failed due to lack of information on initial snow fall, snow redistributions during winter and snow melting. Snow redistributions are partly due to strong southeasterly winds during winter, and partly due to an extensive web of snow fences erected by Nanisivik Mine to support snow accumulation in order to prevent wind erosion on the tailings. Although snow fences are not a part of a long-term, large-scale cover strategy in

Nanisivik, the above analysis shows that even a small snow cover is a concern for the overall temperature regime below thermal covers.

Simulations shown in Figs. 6(C) and 7 are based on a stable snow cover throughout the winter time. This is, of course, an important limitation in terms of actual field conditions, where snow is redistributed during winter and thermal characteristics of snow change over time due to melt–freeze events and compression. In addition, the environmental impact of a snow cover on subsurface temperatures are strongly dependent on the time of the first permanent snow cover in relation to the air temperatures and ground cooling prior to a snow cover. The permanent snow cover in simulations was set to October 15, which corresponds to the very marked decline in ground freezing (Fig. 7). If a snow cover was simulated earlier or later, the overall isolation effect of snow would have been different.

#### 4.3. Cover thickness

Simulations of the effects of various thermal cover thicknesses (Fig. 8) indicate that positive ground temperatures at the cover/tailings interface can be

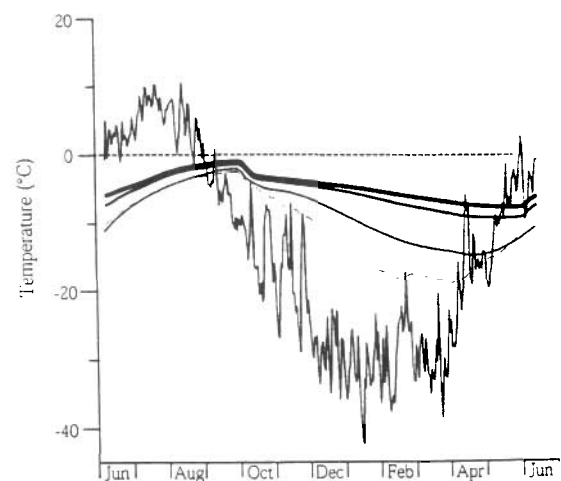


Fig. 7. Predicted ground temperatures at 2 m of depth in Test pad 1 as a result of various snow cover regimes: no snow (dashed line), 5 cm (thin solid line), 25 cm (thick solid line) and 50 cm (very thick solid line) of snow. Meteorological driving variables are based on observations of the period 1995–1996 as representative years. Only the air temperature (solid line) is shown.



paths 1 (○), 2 (△) > 15–December 5  
lated temperatures  
shown as a solid

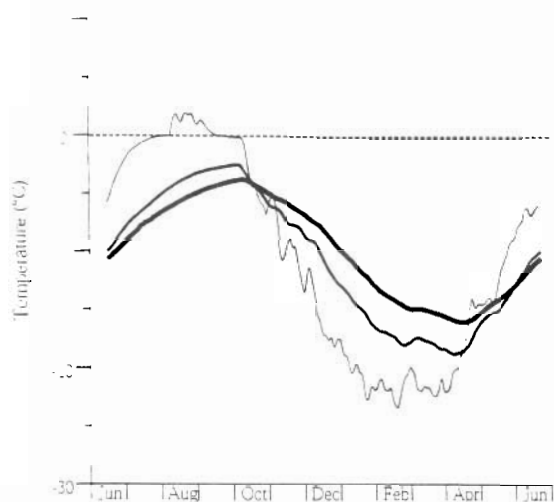


Fig. 8. Predicted ground temperatures at the cover/tailings interface below covers of 1 m (thin line), 2 m (solid line), and 3 m (thick solid line). Simulated cover material represents characteristics observed for material in Test pad 1. Meteorological driving variables are based on 1995–1996 observations, but without any snow.

expected over a month from August to September, if 1 m cover consisting of shale is applied. Consequently, reactive tailings are likely to thaw and may result in AMD generation. Thawing of tailings can be prevented if the cover thickness reaches 2 m. In such case, the maximum temperature below the cover is about  $-3^{\circ}\text{C}$  in September. Increasing the cover thickness to 3 m results in an additional cooling of a few degrees during summer months but up to several degrees during late winter. A snow cover is not included in the thermal cover simulations mentioned above, however, the additional effects of snow can be seen in Fig. 7.

#### 4.4. Low temperature sulfide oxidation and AMD generation

The above discussion has focussed on ground temperatures within cover materials and at the cover/tailings interface, although it is temperatures within the upper part of the tailings that are critical for sulfide oxidation, the production of weathering products and acidic leaching. However, models are not available for simultaneously simulating heat,

mass and chemical transfer in soil exposed to freezing, and at the same time include the effects of temperature and osmotic potentials on liquid water flow/content in porous media (e.g., Nassar et al., 2000). These limitations may not be critical for simulating inert cover material where the pore solution is dominated by rainwater. But in underlying tailings, the pore solution contains large amounts of salts from sulfide oxidation (sulfate and metals) resulting in large amounts of unfrozen water at freezing temperatures. The accurate temperature predictions in covered mine tailings presented in this study (Fig. 5) probably rely on the fact that the thermal covers were constructed on newly deposited tailings prior to release of oxidation products.

The amount of unfrozen water is critical also in relation to other biogeochemical processes than sulfide oxidation, which have recently been confirmed by observations of high levels of microbial (heterotrophic) activity when soil temperatures under a snow cover ranged from  $-5^{\circ}\text{C}$  to  $0^{\circ}\text{C}$  (Brooks et al., 1997). Based on field observations, the authors suggest that subnival heterotrophic activity may be a significant component of the annual C and N cycling in these environments. At the actual study site, Elberling (2001) observed sulfide oxidation at temperatures as low as  $-4^{\circ}\text{C}$ . Thus, an arbitrary "critical temperature" of  $-5^{\circ}\text{C}$  may be a more appropriate criteria for future thermal cover schemes than  $0^{\circ}\text{C}$  in order to hinder sulfide oxidation rates. In that case, the WinSoil simulations suggest that not even a cover of 3 m will ensure that temperatures within tailings remain continuously below such a "critical temperature". Thus, thermal covers alone cannot be expected to be a safe remediation action to control oxidation of reactive tailings. On the other hand, the environmental impact of sulfide oxidation requires a transport of oxidation products into receiving environments. This transport can be very restricted at freezing temperatures as the hydraulic conductivity of porous media decreases orders of magnitudes as water becomes frozen. However, this is an issue beyond the scope of this study as transport properties of frozen tailings and cover materials have not been investigated. An additional factor affecting sulfide oxidation rates is the availability of oxygen within and below thermal covers, which is also strongly affected by frozen water. Therefore, future remedia-



posed to freeze—the effects of on liquid water. Nassar et al., be critical for the pore solution in underlying large amounts of (and metals) released water at free-temperature predicted in this study that the thermal deposited tailings

critical also in processes than sulfide—been confirmed microbial (heterotrophic) under a snow (Brooks et al., the authors suggest activity may be a C and N cycling study site. Elevation at temperature—arbitrary “critical” more appropriate times than 0°C in es. In that case, hat not even a peratures within such a “critical” alone cannot be action to control e other hand, the dation requires a receiving envi-very restricted at ular conductivity of magnitudes as this is an issue nsport properties ds have not been affecting sulfide of oxygen within is also strongly , future remedia-

tion actions should aim to maintain a low availability of oxygen as well as slow reaction rates by a combination of low temperatures and a high water content.

## 5. Conclusions

A field evaluation of thermal covers applied on top of reactive tailings deposited on land near Nanisivik Mine in Arctic Canada shows that the frost table in areas with continuous permafrost can be forced up, thereby maintaining mine tailings at temperatures below 0°C on an annual basis. The WinSoil model was tested and utilized to simulate temperatures within and below covers, indicating that models are available for simulating and predicting the effects of various cover materials on the subsurface temperature regime. The model results illuminate the importance of simulating the snowfall and the resulting snow cover correctly. The study reveals that thermal covers can be an attractive strategy to maintain mine tailings deposited on land at near-zero temperatures throughout the year; however, a 2-m cover may not eliminate acid mine drainage generation due to the difficulties of keeping summer temperatures at the tailing surface below a certain “critical temperature” for inorganic and biological oxidation of sulfide minerals. A future evaluation of large-scale application of inert covers in the Arctic should consider the site-specific winter snowfall and snow cover, as these factors may turn out to be the most important for future scenarios of climatic changes.

## Acknowledgements

Funding for this work was provided by the Danish Environmental Protection Agency, Ministry of Environment and Energy, Denmark, as part of the MIKA-project “Chemical fluxes in frozen soil”. MIKA is now known as DANCEA (Danish Cooperation for Environment in the Arctic). The authors are solely responsible for the results and conclusions presented. We wish to thank Kevin Le Drew, Nanisivik Mine, for assistance provided during the measurement programme. Special thanks to Dr. P.-E. Jansson at the Swedish Royal Institute of Techno-

logy in Stockholm, Dept. of Civil and Environmental Engineering, for valuable discussions regarding WinSoil.

## References

- Ahonen, L., Tuovinen, O.H., 1992. Bacterial oxidation of sulfide minerals in column leaching experiments at suboptimal temperatures. *Appl. Environ. Microbiol.* 58, 600–606.
- Brooks, R.H., Corey, A.T., 1964. Hydraulic properties of porous media. Hydrology Paper, No. 3, Colorado State University, Fort Collins, CO, USA.
- Brooks, P.D., Schmidt, S.K., Williams, M.W., 1997. Winter production of CO<sub>2</sub> and N<sub>2</sub>O from alpine tundra: environmental controls and relationship to inter-system C and N fluxes. *Oecologia* 110, 403–413.
- Dawson, R.F., Morin, K.F., 1996. Acid Mine Drainage in Permafrost Regions: Issues, Control Strategies and Research Requirements. Report for Department of Indian and Northern Affairs, Canada.
- Elberling, B., 2001. Environmental controls of the seasonal variation in oxygen uptake in sulfidic tailings deposited in a permafrost-affected area. *Water Resour. Res.* 37 (1), 99–107.
- Elberling, B., Shippers, A., Sand, W., 2000. Bacterial activity and oxygen uptake in pyritic tailings deposited in the Canadian Arctic. *J. Contam. Hydrol.* 41, 225–238.
- Flerchinger, G.N., 1991. Sensitivity of soil freezing simulated by the SHAW model. *Trans. ASAE* 34, 2381–2389.
- Flerchinger, G.N., Cullum, R.F., Hanson, C.L., Saxton, K.E., 1990. Soil freezing and thawing simulation with the SHAW model. In: Cooley, K.R. (Ed.), *Frozen Soil Impacts on Agricultural, Range and Forest Lands*, March 21–22, Spokane, WA. US Army Corps of Engineers Cold Regions Research and Engineering Laboratory, Hannover, NH, USA, pp. 77–86.
- Gilichinsky, D., Wagener, S., 1994. Microbial life in permafrost. In: Gilichinsky, D. (Ed.), *Viable Microorganisms in Permafrost*. Pushchino Research Center, Pushchino, Russia, pp. 7–20.
- Godwaldt, R.C., Biggar, K.W., Sego, D.C., 1999. AMD generation at sub-zero temperatures. Proceedings of Symposium on Assessment and Remediation of Contaminated sites in Arctic and Cold Climates, Edmonton, Canada, May 3–4, pp. 75–82.
- Hooghoudt, S.B., 1940. Bijdragen tot de kennis van enige natuurkundige grootheden van de grond. *Versl. Landbouwk. Onderz.* 42 (7), 449–541.
- Jansson, P.-E., 1998. Simulation model for soil water and heat conditions. Description of the SOIL model. *Commun.* 98:2, Swedish University of Agricultural Sciences, Department of Soil Sciences, Uppsala, Sweden.
- Kersten, M.S., 1949. Thermal properties of soils. Bulletin no. 28, Institute of Technology, Engineering Experiment Station, University of Minnesota, USA.
- McKnight, D.M., Bencala, K.E., 1990. The chemistry of iron, aluminum, and dissolved organic material in three acidic.

- metal-enriched, mountain streams, as controlled by watershed and in-stream processes. *Water Resour. Res.* 26, 3087–3100.
- Monteith, J.L., 1965. Evaporation and environment. In: Fogg, G.E. (Ed.), *The State and Movement of Water in Living Organisms*, 19th Symp. Soc. Exp. Bio. The Company of Biologists, Cambridge, pp. 205–234.
- Nassar, I.N., Horton, R., Flerchinger, G.N., 2000. Simultaneous heat and mass transfer in soil columns exposed to freezing/thawing conditions. *Soil Sci.* 165 (3), 208–216.
- Peck, L., O'Neil, K., 1995. Heat transfer and frost-thaw penetration in soil surrounding an inclusion of sand. CRREL Report 95-13. US Army Corps of Engineers, Cold Regions Research & Engineering Laboratory, Hannover, NH, USA.
- Shiozawa, S., Campbell, G.S., 1990. Soil thermal conductivity. *Remote Sens. Rev.* 5 (1), 301–310.
- Soiltronics, 1992. The thermal conductivity probe. Model TC20. Burlington, WA, USA.
- Williams, P.J., Smith, M.W., 1995. *The Frozen Earth. Fundamentals of Geocryology*. Cambridge Univ. Press, Cambridge, England.

# Environmental controls of the seasonal variation in oxygen uptake in sulfidic tailings deposited in a permafrost-affected area

Bo Elberling

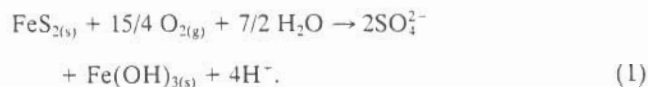
Institute of Geography, University of Copenhagen, Copenhagen, Denmark

**Abstract.** Oxygen consumption, sulfide oxidation, and acid mine drainage (AMD) of pyritic mine tailings were investigated at Nanisivik Mine, which is located in an area with continuous permafrost on Baffin Island in northern Canada. Tailings of varying age and water content have been deposited under alkaline conditions. One area consisting of tailings deposited on land in 1992 was selected for detailed measurements of in situ oxygen uptake rates at the tailing surface in the summers 1998 and 1999 and periodically during autumn and winter in 1998. Measurements included oxygen gas, water content, and temperature in profiles, as well as chemical analyses of pore solution and solids. Additional oxygen consumption rates were measured under controlled temperature conditions on columns filled with partly oxidized tailings. On the basis of temperature dependency of pyrite oxidation observed in the laboratory, an Arrhenius diffusion equation with soil temperature as input was used to simulate the observed temporal variation in oxygen uptake. Field data reveal that the ongoing sulfide oxidation of well-drained tailings primarily takes place in the upper 30 cm and that oxidation has resulted in a depletion of pyrite, carbonates, and metals from this reaction zone. The model provides a reasonable fit to the observed trend in oxygen consumption and documents that oxidation of sulfide minerals in tailings is not reduced to neglectable levels at 0°C. The AMD generation rate has been quantified based on the changes in concentration of oxidation products in the pore water and oxidation rates based on in situ measurements of oxygen consumption. The two rate descriptions provide comparable estimates of seasonal AMD generation and provide detailed information on weather-related controls of AMD generation, i.e., ground temperature, freezing, water content, and snow cover. These environmental controls are crucial for the design of frozen cover schemes in permafrost regions, where the aim is to force the frost table to the top of the tailings, maintaining tailings at subzero temperatures year-round and thereby controlling the AMD generation.

## 1. Introduction

### 1.1. Acid Mine Drainage

Acid mine drainage (known as AMD) is a well-known environmental problem resulting from the exposure of mining waste containing reactive sulfide minerals to oxygen in the presence of water. The oxidation of sulfide minerals and the subsequent acid production contribute to the generation of acidic leachates containing high concentrations of dissolved heavy metals and sulfate. Pyrite ( $\text{FeS}_2$ ) is one of the most common sulfide minerals, and the overall oxidation of pyrite can be described by the following reaction:



The oxidation of pyrite is catalyzed in environments containing iron- and sulfur-oxidizing bacteria. Under acidic conditions, chemolithotrophic bacteria, such as *Thiobacillus ferrooxidans*, are capable of increasing the rate of pyrite oxidation by several orders of magnitude [e.g., Nordstrom, 1982], and, consequently, biological oxidation of pyrite typically accounts for the majority of the observed oxidation. This is not generally

the case for pH values above 4; however, moderately acidophilic sulfur-compound-oxidizing bacteria like *Thiomonas intermedia* have been described in mine tailing environments with pH values between 5 and 7 [Schippers et al., 1996; Elberling et al., 1999].

The sulfide oxidation process is temperature-dependent, and both chemical and biological oxidation rates decrease with decreasing temperatures as described by the Arrhenius equation [Nicholson et al., 1988]:

$$\ln(k_1/k_2) = E_a(T_1 - T_2)/(RT_1T_2), \quad (2)$$

where  $k_1$  and  $k_2$  are reaction rates at temperatures  $T_1$  and  $T_2$ ,  $E_a$  is the activation energy of the reaction, and  $R$  is the gas constant. Values of  $E_a$  reported in the literature for pyrite oxidation vary from 50 to 88 kJ mol<sup>-1</sup> for a variety of experimental conditions [Nicholson et al., 1988]. Although the effects of temperature on sulfide oxidation rates are complex, several studies confirm that the Arrhenius equation is a valid approximation for the chemical and biological reaction rates [Ahonen and Tuovinen, 1992; Dawson and Morin, 1996].

As the oxidation of pyrite proceeds in a vertical profile of tailings, atmospheric oxygen is consumed and an oxygen concentration gradient develops. This gradient is the driving force for the diffusive transport of oxygen through the tailings and is generally accepted as being another limiting factor for the overall AMD generation [Nicholson et al., 1989; Pantelis and Ritchie, 1992]. One-dimensional molecular gas diffusion in soil

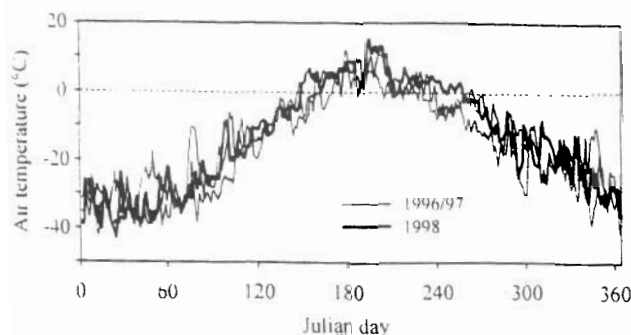


**Figure 1.** Daily mean air temperatures (degrees Celsius) in 1996–1998 in Nanisivik, Baffin Island, Canada. The year 1998 deviates from previous years by a relatively warm period in the end of August.

is proportional to the gas concentration gradient ( $dC/dz$ ), and the effective diffusion coefficient of the soil ( $D_e$ ) as given by Fick's First Law:

$$F = D_e dC/dz. \quad (3)$$

The effective diffusion coefficient of the soil can be calculated as a function of the diffusion in both air and water. Assuming that water-filled and air-filled pathways represent parallel resistance to diffusion, the net diffusion ( $D_e$ ) can be calculated as the weighted sum of the diffusion coefficients in air and water [Colin and Rasmuson, 1988; Elberling and Nicholson, 1996]. Owing to the very reduced diffusivity in water compared to air, both underwater mine tailing disposal and wet barriers are considered among the most natural and economical AMD control technologies for many geographical regions.

## 1.2. AMD Control Technologies in Permafrost-Affected Areas

A number of operating and proposed base metal mines are located in regions with permafrost. The unique environmental characteristics of these regions need to be considered when planning strategies for minimizing AMD. The permafrost environment is generally considered to be a controlling feature itself that allows the mine tailings to freeze or to be kept at near-freezing conditions most of the year in order to restrict AMD generation. The low temperatures slow most chemical and biological processes, and freezing may restrict the migration of pollutants. However, AMD and release of heavy metals from mining is observed in the Arctic [Dawson and Morin, 1996], probably because of the infiltration of water and penetration of atmospheric oxygen initiating an oxidation of tailings within the annual thawing layer. As a result, metals are released and spread to the surroundings by acidic drainage to local watershed stream systems and to marine environments. This has been documented from several studies in the Arctic [e.g., McKnight and Bencala, 1990; Godwaldt et al., 1999].

In order to control mine tailing oxidation and acidic mine drainage the application of permafrost in freezing and encapsulating of frozen tailings below engineered covers has been suggested [Dawson and Morin, 1996]. Such remediation actions rely on studies indicating that microbial activity is nearly absent at temperatures below 3°C [e.g., Ahonen and Tuovinen, 1992]. However, the existence of cold-adapted bacteria has been known for more than 100 years [Foster, 1887], and numerous surveys have shown the presence of viable bacteria in very cold

environments (see Morita [1975] for a review). The presence of psychrophilic (growth at or around 0°C with a maximum temperature for growth below 21°C) thiobacilli have been reported from Arctic mine sites [Kalin, 1987], and a recent review has concluded that AMD generation in cold climates is not negligible [Dawson and Morin, 1996], but there is no reported field data on the impact of temperatures at or below freezing on the overall oxidation rate of sulfidic tailings.

This study aims to quantify the effect of low temperatures and freezing on biological and chemical pyrite oxidation in well-drained tailings deposited in the Arctic. It is hypothesized that the temporal variation in oxygen consumption and the release of oxidation products as a result of ongoing pyrite oxidation will be controlled primarily by temperatures within the near-surface reaction zone.

## 2. Methods

### 2.1. Field Investigations

Nanisivik Mine on Baffin Island in northern Canada (73°02'N, 84°32'W) is located within the High Arctic zone of continuous permafrost. The annual mean temperature (1994–1998) is –15.6°C, and the annual precipitation is approximately 125 mm. Figure 1 shows mean temperatures over 3 years (1996–1998). The dry cold climate discourages development of vegetation, which is completely absent on the tailings. Since 1976, mine tailings have been deposited under water in a tailings impoundment, but tailings have also been deposited on land since 1992. A well-drained test site was selected in the exposed tailings area to evaluate the reactivity of tailings deposited on land in permafrost areas.

The tailings consists of pyrite, dolomite ( $MgCa(CO_3)_2$ ), and residual amounts of sphalerite ( $ZnS$ ) and galena ( $PbS$ ). Weather information is available from a local weather station situated 200 m from the test site and includes temperature, humidity, wind speed, and direction, as well as net radiation and precipitation, all of which have been monitored on an hourly basis since 1994.

In situ oxygen uptake rates were measured as changes in oxygen concentration over time within a gas chamber. The setup consisted of a stainless steel cylinder (18-cm ID and 70-cm long) that was driven into the tailings, leaving the top 0.5–2 cm above the surface. During measurements a cap was placed on top of the cylinder to isolate the tailings profile from the atmosphere. The concentration of oxygen within the gas reservoir between the tailing surface and the cap was measured by an electrochemical oxygen gas sensor (Model GC33-200, G. C. Industrial, Inc., Fremont, California, United States of America) sealed in the cap. The oxygen sensor provides a voltage output, which is linearly related to the absolute concentration of oxygen. The sensor has been intensively investigated for its reliability during variable field conditions, and it provides measurements with an accuracy of 0.1%  $O_2$  for temperatures from –4° to 20°C [Williams, 1993; Elberling and Nicholson, 1996]. The sensor fails to measure oxygen uptake below –4°C because of freezing. Readings from the oxygen sensor were recorded in millivolts each minute for more than 2 hours on a data logger and used to estimate the flux of oxygen across the tailing surface as described by Elberling and Nicholson [1996]. The following equation was used to convert relative changes over time in the  $O_2$  concentration within the gas reservoir to a flux of moles of  $O_2$  per area per time [Nicholson et al., 1989]:



$$F_s = -C_0(kD_e)^{0.5} \quad (4)$$

where  $F_s$  is the flux of oxygen across the tailing surface,  $C_0$  is the initial concentration of oxygen before measurement,  $k$  is the reaction rate constant, and  $D_e$  is the effective diffusion coefficient in the tailings. The parameter  $(kD_e)^{0.5}$  is given by the slope of a plot of the relative change in oxygen concentration within the gas reservoir with time as shown by *Elberling and Nicholson* [1996]. Equation (4) assumes that the oxygen diffusion can be described by Fick's First Law (equation (3)), that the oxygen flux across the surface has reached a steady state prior to measurements, and that sulfide oxidation as a first-order reaction is the only process consuming oxygen. This method of evaluating oxygen uptake in tailings has been referred to as the oxygen consumption method, and it has previously been applied in similar investigations [*Elberling and Nicholson*, 1996; *Meldrum et al.*, 1999]. Laboratory tests of the method reveal that the oxygen consumption within the entire tailings profile is well described by the flux across the surface and that it is consistent with the release of oxidation products [*Elberling et al.*, 1994a].

Measurements were made approximately every third day from July 17 to September 28, 1998, in order to evaluate the temporal trends as the tailings freeze. Additional measurements were made during 3 weeks in November and December 1998 to provide insight into the reactivity when tailings were covered by more than 1.5 m of snow (snow accumulation on tailings due to snow fences) and the daily air temperature was below  $-20^\circ\text{C}$ . The temperature around the oxygen sensor was kept constant and above zero during winter by heating tapes and insulation. Temperature measurements during oxygen consumption measurements revealed that the temperature near the sensor was constant ( $\pm 2^\circ\text{C}$ ).

Pore solutions were collected by Prenart Super Quartz® suction probes installed horizontally at 10-cm intervals to a depth of 80 cm in two unfrozen well-drained tailing profiles. The suction probes, made of PTFE (Teflon), have a pore radius of  $2\ \mu\text{m}$  and a hydraulic conductivity of  $3.31 \times 10^{-7}\ \text{cm s}^{-1}$ . Probes were connected to 250-mL sampling bottles placed on the soil surface using teflon tubes. To ensure a high spatial and temporal resolution of the sampling, small volumes (about 100 mL) were sampled over 24–48 hours with as low a suction as possible (typically 0.15 atm). Conductivity and pH of the recovered water were determined immediately. A subsample of the water was preserved with 10%  $\text{HNO}_3$ . The soil water samples were kept cool and dark until processed in Denmark. Total dissolved concentrations of metals and cations were determined on the acidified samples. Concentrations of Zn, Pb, and Cd were determined using anodic stripping voltammetry, and concentrations of Fe, Mg, Ca, K, and Na were determined by using flame atomic absorption. Concentrations of Cl,  $\text{NO}_3^-$ , and  $\text{SO}_4^{2-}$  were determined on nonpreserved samples using ion chromatography, and the alkalinity was determined by titration of 0.01 M HCl.

Air and ground temperatures were logged at the test site at 2-hour intervals (Tinytag data loggers). Additional ground temperatures (top 15 cm) were measured by thermistors connected to a hand-held thermometer, and the water content was measured by time domain reflectometry (Trase Model 6050X1 equipped with coated waveguides). Waveguides were installed horizontally at approximately 10-cm intervals to a depth of 80 cm in two profiles. Prior to installation, each waveguide was calibrated in the laboratory with tailings from the study area.

Vertical  $\text{O}_2$  concentrations were measured at  $4 \pm 0.5$ -cm-depth intervals by a modified technique described by *Elberling and Nicholson* [1996], where pore gas from a specific depth is withdrawn and measured by the electrochemical oxygen gas sensor. Depth-specific samples representing a 2-cm layer of tailings were collected at 5-cm intervals to a depth of 50 cm. Each sample was analyzed for its total content of Fe, Zn, Pb, and Cd by dissolving approximately 1 g of dry material in aqua regia, after which the metal concentrations were determined by flame atomic absorption ( $\pm 0.01$  ppm). The carbonate content was determined by LECO instrumentation (LECO Corp., St. Joseph, Michigan), the content of percent S (sulfate) by  $\text{BaSO}_4$  precipitation after 20% HCl extraction, and percent S (total) by  $\text{BaSO}_4$  precipitation after fusing tailings with  $\text{Na}_2\text{CO}_3$  and  $\text{Na}_2\text{O}_2$  [*Rasmussen and Willems*, 1981]. Quantitative X-ray powder diffraction analyses were used to verify the presence of other sulfide minerals than pyrite. Volume specific samples were taken at 5-cm-depth intervals and analyzed for porosity, solid bulk density, and grain size distribution as well as water content by the loss in weight after drying at  $110^\circ\text{C}$ .

## 2.2. Laboratory Experiments

Additional samples of partly oxidized tailings were collected for laboratory experiments. Samples were stored in sterile plastic containers and kept dark at  $2$ – $4^\circ\text{C}$ . Tailings with a water content of approximately 8–10% were subsequently mixed to produce a homogenous bulk sample with an average pyrite content of  $60 \pm 2\%$  and pH values of 5–6. Half of the bulk sample was sterilized by adding chloroform as described by *Schippers et al.* [1995]. Subsamples of approximately 400 g were packed in cylinders with only one end of the cylinder exposed to the atmosphere. The oxygen consumption was measured with the same technique as used in the field. Measurements were made on five replicates of both sterilized (chemical oxidation) and nonsterilized samples (chemical and biological oxidation). Measurements were made in 11 steps from  $15^\circ\text{C}$  to  $-4^\circ\text{C}$  in a freezer at constant temperatures ( $\pm 0.2^\circ\text{C}$ ). Tailings used for the laboratory experiment were analyzed as described in section 2.1 for tailing samples collected in the field. The frozen and unfrozen water contents were measured from  $15^\circ\text{C}$  to  $-10^\circ\text{C}$  in PVC cylinders (10-cm ID and 25-cm long) by time domain reflectometry (TDR) as described by *Egbert et al.* [1995]. Samples for TDR measurements represented samples from 20 and 80 cm collected in August 1998. Subsequently, the chemical composition of the water collected in situ from these depths at this time has been used to model the unfrozen water content versus temperature by the FREZCHEM program [*Mironenko et al.*, 1997]. FREZCHEM includes the coefficients for the Pitzer equations in a model for the solute redistribution during freezing.

The activation energy for pyrite oxidation was determined by measuring the heat output resulting from oxidation of tailing samples using a thermal-activity monitor (type 2277, Thermometric, Sweden, or C3-Analysentechnik, Germany) as previously described by *Elberling et al.* [1999]. Calorimetric measurements were made at  $5^\circ\text{C}$ ,  $10^\circ\text{C}$ ,  $17^\circ\text{C}$ ,  $24^\circ\text{C}$ , and  $30^\circ\text{C}$ .

## 3. Results

### 3.1. Tailing Characteristics

A drop in the oxygen gas concentration from atmospheric content (20.9%) to below the detection limit (0.1%) was observed at all well-drained sites within the top 30 cm (Figure 2).

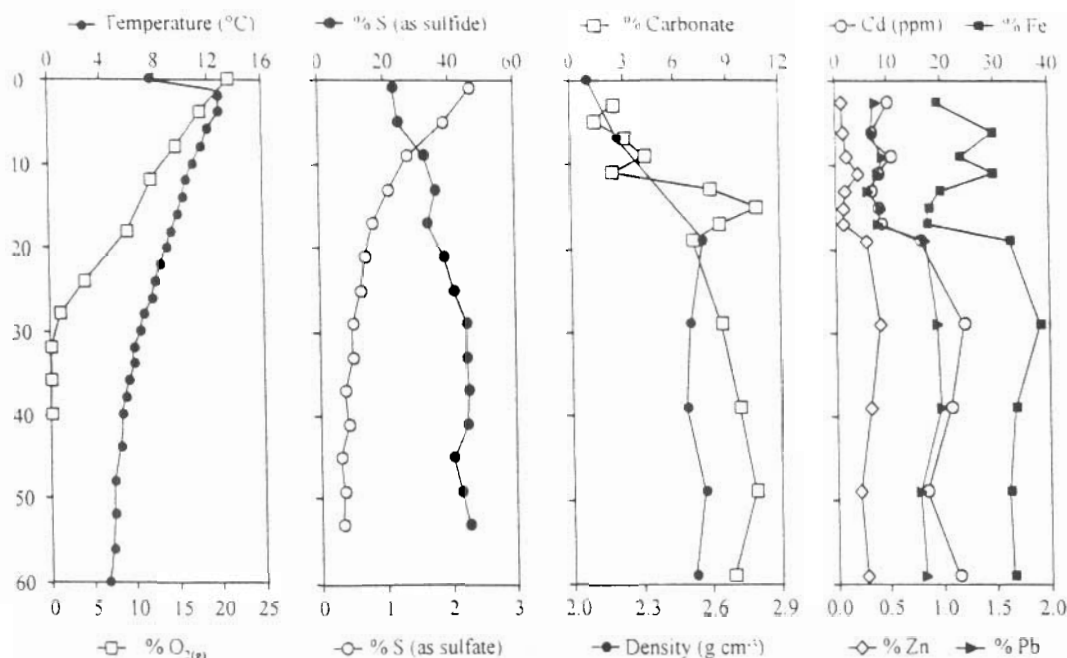


**Figure 2.** Temperature, bulk density, and concentrations of oxygen gas, sulfide, sulfate, carbonate minerals, iron, zinc, lead, and cadmium in a tailing profile, as measured in mid-August 1998. The profile is characterized by an upper oxidized zone with oxygen and partly depleted in metals and a lower reduced zone without oxygen and with a higher content of metals.

The depth of oxygen depletion was consistent with a drastic change in color from red/yellow to grey. Soil temperatures in mid-August were approximately 13°C near the surface, 4–6°C at 60 cm depth, and 0°C at the frost table. The frost table moved from a depth of approximately 1 m in mid-July to 1.5 m in mid-August to almost 2 m by the end of October 1998.

Tailings from the study area consist of well-sorted, fine sand with a pyrite content between 40 and 75% in the partly oxidized upper 30 cm and between 75 and 85% within the reduced zone (Figure 2). Quantitative X-ray analyses indicate that the remaining part of the oxidized zone consists of primarily dolomite, small amounts of gypsum, and traces of quartz. The remaining part of the reduced zone consists only of dolomite. For all samples (except for the top 2 cm), less than 1% by weight of the tailing consists of amorphous phases like Fe hydroxides.

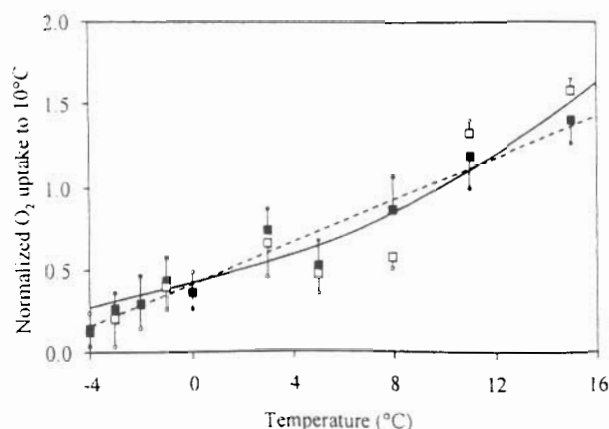
Water saturation varied typically from 8 to 10% within the oxidized zone and up to 100% near the frost table. After major rainfalls the water content in the oxidized zone increased up to 45% but decreased again to its original value ( $\pm 2\%$ ) within 24 hours.

Figure 2 shows the content of metals in the same profile, indicating that the upper partly oxidized zone contained on average  $9 \pm 3$  ppm Cd,  $0.1 \pm 0.07\%$  Pb,  $0.4 \pm 0.1\%$  Zn, and  $24 \pm 6\%$  Fe and that the average metal concentrations below this zone were  $20 \pm 3$  ppm Cd,  $0.3 \pm 0.08\%$  Pb,  $0.9 \pm 0.04\%$  Zn, and  $34 \pm 3\%$  Fe. The latter concentrations are higher than the average concentrations in fresh tailings deposited in Nanisivik but within the range of concentrations reported in production records from the time of mining (Nanisivik Mine).

### 3.2. Temperature-Dependent Oxidation

Calorimetric measurements ( $n = 100$ ) of the heat development from tailings in the temperature range 5°C to 30°C

reveal that the activation energy is  $50.5 \pm 0.8$  kJ mol<sup>-1</sup> based on an Arrhenius plot ( $r^2 = 0.987$ ). Independent oxygen uptake rate measurements were made in the laboratory at 10 temperatures around 0°C where the calorimetric equipment failed to provide reliable results. Oxygen uptake (mol O<sub>2</sub> m<sup>-2</sup> d<sup>-1</sup>) resulting from biological and chemical pyrite oxidation is normalized to 10°C (Figure 3). A linear increase in the oxygen uptake with increasing temperature is observed ( $r^2 = 0.98$ ). Consistency in oxygen uptake rates with the Arrhenius plot can



**Figure 3.** Laboratory oxygen consumption rates normalized to 10°C as a function of temperature. Open squares represent chemical rates measured on sterilized tailings. Solid squares represent biological rates calculated as the difference between measurements of sterilized and nonsterilized tailings. Bars represent the standard deviation for chemical and biological rates, respectively. The linear regression line for both chemical and biological rates is shown as a dashed line, whereas the Arrhenius equation is shown as a solid line.



be observed in the temperature range above 0°C. Below 0°C an increasing disagreement is noted, and the linear correlation provides the best fit. Comparisons of absolute oxygen consumption rates for sterilized and nonsterilized samples reveal that the chemical oxidation without microbial catalyzation accounts for approximately 70–75% of the overall oxygen consumption observed (data not shown). As the relative dependency of biological and chemical oxidation rates on temperature is similar, the influence of temperature on overall sulfide oxidation rates can be evaluated regardless of the degree of biological oxidation. In this study, temperatures of the reaction zone within the tailings varied between –3°C and 13°C, and the linear fit is used to model the sensitivity of both chemical and biological rates as a function of temperature.

### 3.3. Temporal Trends in Oxygen Uptake and Release of Heavy Metals

Over a period from July 18 to September 28, 1998, rates of oxygen consumption and air and soil temperatures as well as precipitation were measured almost every third day (Figure 4). Oxygen uptake rates in 6-year-old well-drained tailings were of the order of 0.2–0.5 mol of O<sub>2</sub> m<sup>-2</sup> d<sup>-1</sup> which are of the same magnitude as rates observed in temperate climates [Elberling and Nicholson, 1996]. Measurements were initiated during a period with air temperatures between 15° and 20°C. During the following period of 2 months, air temperatures dropped to below 0°C and even as low as –10°C on cold nights. Soil temperatures within the reaction zone (0–30 cm) show a similar temporal trend but with a smaller amplitude.

The observed change in oxygen uptake over time was modeled using daily average soil temperatures at 10, 20, and 30 cm. The temperatures were used to model the temporal variation in the reaction constant  $k$  and in the diffusion coefficient and thus the expected variation in oxygen uptake over time. The model fit shown in Figure 4 is normalized based on the average oxygen uptake and temperature observed during the first 8 days. Figure 4 demonstrates that significant changes in oxygen uptake can be modeled taking only the soil temperature into account. However, the model failed to predict the oxygen uptake during the first days following a major precipitation event on Julian day 216 (11 mm in less than 10 hours) where water saturation within the reaction zone reached 45%. A site covered with plates to prevent infiltration of rainwater but allowing free oxygen diffusion made it possible to differentiate between the effects of temperature and increasing water content on the overall oxygen uptake. Simulations show that the model could predict the effect of temperature but not the effect of reduced diffusion of oxygen due to a high water content. On the basis of rough estimates of the effective diffusion coefficient versus water saturation (as previously shown by Elberling and Nicholson [1996]) an increase from 10% to 40% water saturation can explain the additional restriction of oxygen uptake observed compared to model predictions. One of the basic assumptions of the oxygen consumption method is that steady state conditions prevail, which is not valid during and after major precipitation events. However, measurements of the water content within the top 30 cm of the tailings revealed that the site was so well drained that no significant changes in water content could be observed after 24 hours (data not shown). The results suggest that the temporal trend in the rate of oxygen consumption within well-drained tailings is controlled to a large extent by soil temperature. The presented model fit of the daily variation in oxygen uptake is based on

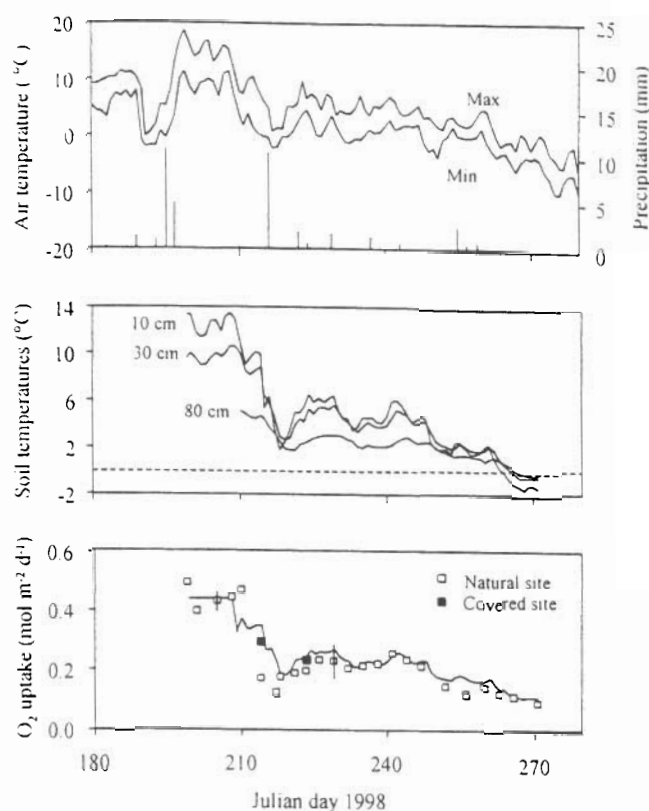


**Figure 4.** Air and soil temperatures (curves), precipitation (bars), and in situ oxygen consumption rates at a natural site (open squares) and a covered site (solid squares) within well-drained tailings measured in 1998. Bars through squares represent the standard deviation of replicates ( $n = 6$ ). The simulated oxygen consumption is shown as a solid line.

one daily average temperature. A more correct fit can be made by using temperatures from several depths. However, simulations made using temperatures from four depths within the top 80 cm provided fits to measured uptake rates that did not vary significantly from the result shown (Figure 4).

Over a 3-week period in November and December 1998, oxygen consumption rates at the same sites were  $0.12 \pm 0.02$  mol of O<sub>2</sub> m<sup>-2</sup> d<sup>-1</sup>. Measurements were taken after removing between 1 and 1.5 m of snow to get to the sites. Soil temperatures within the top 20 cm were found to vary among the sites but were within the range of –1° to –3°C. The winter measurements of oxygen consumption were approximately one fourth of rates observed in the summer, which is consistent with the expected decrease in the kinetics (equation (2)). Measurements were continued in May 1999, revealing that oxygen consumption was not measurable in mid-May when soil temperatures were below –8°C at depths of 10–15 cm, but an oxygen uptake was detected as the soil temperatures increased to –4°C.

## 4. Discussion and Conclusions

### 4.1. Oxygen Uptake and Release of Weathering Products

Temporal changes in concentration of oxidation products from sulfide oxidation and decreasing pH in extracted pore water are shown in Figure 5. Changes are primarily observed in pore water collected 20–30 cm below surface, which is in

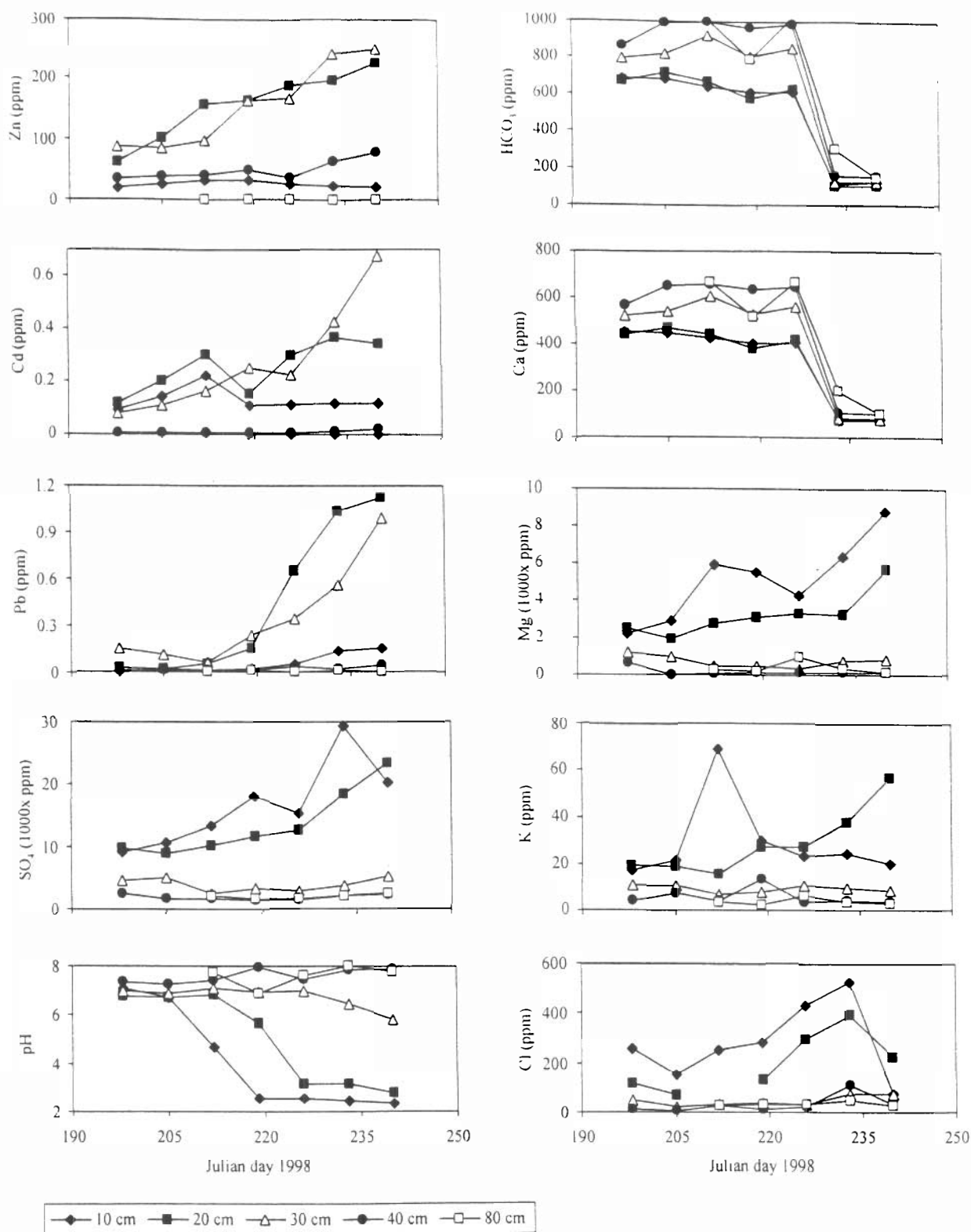


Figure 5. Temporal trends in concentrations of metals, selected cations and anions, and pH in pore water collected at five depths within the unsaturated zone of a well-drained tailing profile.

agreement with the depth of the reaction zone where oxygen is consumed. The acid production is accompanied by increased magnesium concentrations as result of dolomite ( $\text{Mg-Ca}(\text{CO}_3)_2$ ) dissolution, while the smaller increase in calcium concentration is probably due to gypsum ( $\text{CaSO}_4 \cdot 2\text{H}_2\text{O}$ ) precipitation. During a period of 20 days (Julian days 220–240),

water movement within the tailing profile was limited (almost no precipitation). Increasing concentrations of sulfate in the pore solution during that time period were therefore assumed to be a result of pyrite oxidation and evaporation and precipitation of secondary sulfate minerals. The concentration of sulfate has been corrected for evaporation by assuming that

changes in chloride concentrations are due to evaporation. The precipitation of gypsum can be roughly estimated by using the depletion of calcium as compared to magnesium. Thus the final corrected increase in sulfate corresponds to the oxidation of sulfide minerals which can be compared with observed  $O_2$  uptake rates. Over the 20-day period the  $O_2$  consumption rate was fairly constant, with an average of  $0.22 \pm 0.005 \text{ mol m}^{-2} \text{ d}^{-1}$ . Over the same time,  $0.1 \text{ mol of SO}_4 \text{ m}^{-2} \text{ d}^{-1}$  (corrected for evaporation and precipitation) were released. This rate production of sulfate requires the consumption of  $0.19 \text{ mol of } O_2 \text{ m}^{-2} \text{ d}^{-1}$  and indicates that the two ways of evaluating oxidation rates in situ provide results within the same range.

There are several issues related to these estimates which require further attention. The stoichiometry of the oxidation process is given by a simple equation (1) assuming that nitrate and other oxidizing agents can be neglected and that only pyrite oxidation contributes to oxygen uptake. These assumptions are based on observations of low nitrate concentrations ( $<10 \text{ ppm}$ ), precipitation of ochre in the reaction zone, and the fact that organic matter has not been detected in the tailings ( $<0.5 \text{ ppm}$ ). A second issue concerns the assumption of diffusion as the primary transport mechanism for oxygen in tailings. Although several mechanisms of gas transport can be distinguished in porous media like tailings, for example, Knudsen diffusion, multicomponent molecular diffusion, and advective flow [Thorstenson and Pollock, 1989], ordinary gaseous diffusion is considered to be the most important mechanism for tailing systems consisting of fine sand and for systems where oxygen is depleted within the uppermost  $0.5 \text{ m}$  [Pantelis and Ritchie, 1992; Elberling et al., 1994b; Elberling and Nicholson, 1996]. It is unclear to what extent the oxygen uptake may result in a pressure gradient acting as a driving force for a gas transport. In carbonate-buffered tailings,  $CO_2$  production within the reaction zone will reduce such pressure gradients. In this study, pressure ports were installed within the upper  $0.5 \text{ m}$  at the field site, but no pressure gradients were detected ( $<0.01 \text{ mbar}$ ). As the depth-dependent oxygen uptake was not measured in this study, it is not possible to directly evaluate the importance of this additional transport mechanism. However, it is assumed to be neglectable as the rate of oxygen consumption based on changes in pore water concentrations is less than the corresponding in situ oxygen uptake rate.

The annual oxygen uptake has been estimated based on weekly averaged observations of air and soil temperatures over 1 year and is compared to observed rates of oxygen uptake (Figure 6). Of the average annual estimated  $O_2$  uptake of  $38 \text{ mol m}^{-2}$ , 40% is consumed during the long period with sub-zero ground temperatures. This annual rate description can be compared to historical weathering rates based on the depletion of pyrite since deposition. Assuming oxidation from the top of a homogeneous tailing profile during 6 years, a mass balance based on the solid chemistry (Figure 2) is made. Assuming that the average pyrite content of 82%, the porosity of 43%, and the bulk density of  $2.45 \text{ g cm}^{-3}$  observed below the reaction zone (below  $30 \text{ cm}$ ) represent initial conditions prior to oxidation, the depletion of pyrite per area can be calculated as a depth-integrated loss based on 5-cm intervals. On the basis of solid geochemistry an average of  $260 \text{ mol of FeS}_2 \text{ m}^{-2}$  have been oxidized per year, which is equivalent to  $980 \text{ mol of oxygen m}^{-2} \text{ yr}^{-1}$ . This estimate is much higher than the annual rate description based on the extrapolation of short-term observations of oxygen uptake. These conflicting estimates are discussed in the following.

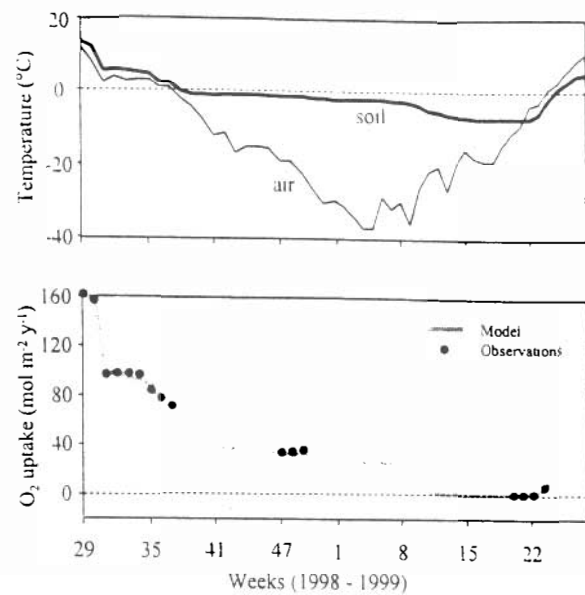
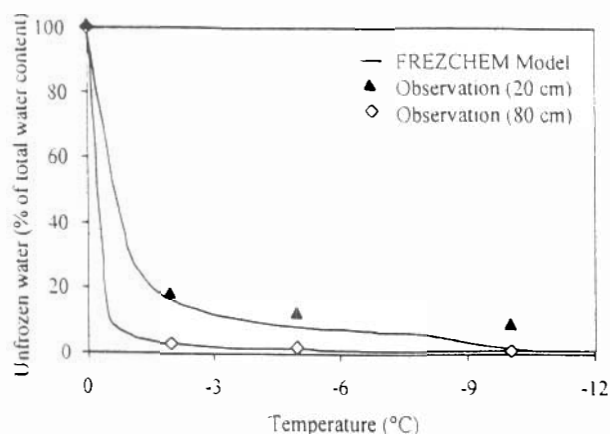


Figure 6. Annual variation in temperature and observed oxygen uptake. Simulations are based on weekly estimates.

The average rate description over 6 years based on the solid geochemistry of the tailing profile assumes that the solid geochemistry below the reaction zone represents the original composition within the reaction zone. As indicated in section 3.1, this part of the tailing profile has a higher content of heavy metals and pyrite than average tailings deposited in Nanisivik, and it may therefore not be representative of the initial conditions within the reaction zone. The pyrite content in tailings produced over the last 20 years, which is known from daily production records (Nanisivik Mine), reveals an average pyrite content in fresh tailings of 72% with a standard deviation of 10% and minimum values as low as 55%. Assuming an original pyrite content within the reaction zone of 72%, the solid mass balance indicate that  $470 \text{ mol of } O_2 \text{ m}^{-2} \text{ yr}^{-1}$  are required in order to correspond to the current distribution of pyrite. The original pyrite content must equal approximately 60% in order to match an annual  $O_2$  uptake of  $38 \text{ mol m}^{-2}$  since deposition. This discussion shows that comparisons of historical weathering rates over several years and extrapolated seasonal  $O_2$  uptake measurements are not straightforward, as extrapolation of in situ oxygen uptake rates beyond the observation period may not be safe and as average estimates of long-term oxidation rates based on solid geochemistry may not represent current oxidation rates. This agrees with long-term observations of sulfide oxidation [e.g., Nicholson et al., 1988] indicating that the oxidation rate varies over time, with higher oxidation rates during initial atmospheric exposure due to the presence of a fresh surface area of pyrite particles. Over time, coating and other surface processes as well as increasing  $O_2$  diffusion distances result in decreasing oxidation rates. Such temporal changes in the actual oxidation rate of the tailings may partly explain the inconsistency in the long-term and short-term oxidation rates presented above.

#### 4.2. Sulfide Oxidation Controlled by Freezing

Freezing of tailings is considered an effective way to slow both the reaction kinetics and the oxygen diffusion in cold regions [Dawson and Morin, 1996]. Thus covering reactive tail-



**Figure 7.** Unfrozen water content (percent of total water content) in mine tailings collected August 7, 1998, from the upper oxidized zone (20 cm) and lower reduced zone (80 cm). Observations are compared to FREZCHEM simulations.

ings with an inert layer to ensure that the permafrost moves into the tailings has been suggested as a control strategy for Arctic tailing systems [Dawson and Morin, 1996]. The theoretical considerations and the independent measurements of oxygen uptake rates at near-zero temperatures presented here indicate that a drop in temperature from 15°C to -3°C will limit the overall oxidation of alkaline sulfidic tailings because of slower reaction kinetics but only by a factor of approximately 3–4. This is independent of the degree of biological oxidation. This conclusion can be combined with the conclusion from laboratory measurements of diffusion coefficients of frozen tailings from Nanisivik at varying degrees of water content [Elberling, 1998]. That study reveals that freezing of tailings with a degree of water saturation below 30% (or a water content below 10%) has no significant effect on diffusion of oxygen. Thus freezing of well-drained tailings as found within the test area in Nanisivik only results in slower reaction kinetics, a process that seems to be predictable down to at least -3°C. Prediction of reaction kinetics below this temperature requires further laboratory studies of bacterial adaptation to freezing temperatures as well as quantification of the range of activation energies as the overall chemical processes may be completely different. Prediction of the effects of freezing on reaction kinetics and diffusion coefficients also requires further insight into the relationships between the increasing ion concentration due to the ion exclusion of the ice phase, the depression of the freezing point of the solution, and the unfrozen water content. The model FREZCHEM [Mironenko *et al.*, 1997] has been applied to verify the amount of unfrozen water in the laboratory freezer experiments (Figure 7). The significant amount of unfrozen water, particularly within the reaction zone, suggests that liquid water is available within the temperature regime studied in this paper.

The above conclusions are important in relation to the application of snow fences, which at the present study site are used to build up a snow cover on the tailing surface during winter to prevent wind erosion and redistribution of tailings during storms. The results indicate that deeper and earlier snow cover as a result of snow fences may result in high sub-nival oxidation of tailings since the snow insulates the tailings from the very low winter air temperatures, thereby reducing winter heat loss. The actual uptake of oxygen below the snow

cover in Nanisivik has not been measured as the snow cover was removed prior to measurements. Consequently, the impact of the snow cover as a diffusion barrier for oxygen has not been evaluated. However, the mass balance of the annual pyrite oxidation suggests that a significant amount of the total oxidation takes place during a period with ground freezing. These conclusions are consistent with recent observations of high levels of bacterial (heterotrophic) activity under seasonal snow cover in alpine tundra [Brooks *et al.*, 1997, 1998]. Brooks *et al.* [1997] measured fluxes of CO<sub>2</sub> and N<sub>2</sub>O as well as an active microbial biomass when soil temperatures under a snow cover ranged from -5°C to 0°C. On the basis of these observations the authors suggest that sub-nival heterotrophic activity may be a significant component of the annual C and N cycling in these environments.

From the above discussion it can be concluded that the effects of soil temperatures on tailing oxidation rates and release of weathering products in the Arctic are only partly understood. It can also be concluded that a temperature of 0°C is not an important temperature for controlling the reactivity of well-drained tailings as decreasing reaction rates around 0°C are more likely to be continuous than abrupt.

#### 4.3. Alternative Control Strategies

AMD generation may be reduced by environmental factors other than temperature, for instance, by the exclusion of oxygen, maintenance of high pH values, and bacterial control of the oxidation rate. The exclusion of O<sub>2</sub> is probably the most effective long-term AMD control technique, and it is well known from other regions. Water cover is a natural option for limiting O<sub>2</sub> availability in tailings and includes both underwater disposal and wet barriers. The effectiveness of water cover is based on the fact that diffusion of oxygen in water is approximately 10,000 times slower than in air [Elberling and Nicholson, 1996]. As a single remediation action, tailing storage under water is consequently expected to provide the optimal reduction in sulfide oxidation among several control strategies. In the Arctic, freezing of water-covered tailings during winter may further limit the oxidation process as well as the subsequent transport of pollutants. A water cover will also prevent wind erosion in the winter, and snow fences will therefore not be necessary.

**Acknowledgments.** Funding for this study was provided by the Danish Environmental Protection Agency, Ministry of Environment and Energy, Denmark, as part of the MIKA project "Chemical fluxes in frozen soil." MIKA is now known as Dancea, Danish Cooperation for Environment in the Arctic. The project is supported by National Environmental Research Institute, Institute of Geography (University of Copenhagen), and Nanisivik Mine. Special thanks go to Curt Kyhn and Per Misser, who participated in the fieldwork, R. V. Nicholson and coworkers for helping with the setup for controlling temperatures during winter measurements, G. Asmund and T. Andersen for doing the chemical analyses, T. Rohwerder for doing the calorimetric measurements, and K. LeDrew at Nanisivik Mine for access to data and the field site in Nanisivik. I am indebted to E. P. Weeks, L. Dyke, B. H. Jakobsen, D. Postma, and R. Sletten for many helpful comments on the manuscript.

#### References

- Ahonen, L., and O. H. Tuovinen, Bacterial oxidation of sulfide minerals in column leaching experiments at suboptimal temperatures. *Appl. Environ. Microbiol.*, 58, 600–606, 1992.
- Brooks, P. D., S. K. Schmidt, and M. W. Williams, Winter production of CO<sub>2</sub> and N<sub>2</sub>O from alpine tundra: Environmental controls and



- relationship to inter-system C and N fluxes, *Oecologia*, 110, 403–413, 1997.
- Brooks, P. D., M. W. Williams, and S. K. Schmidt, Inorganic nitrogen and microbial biomass dynamics before and during spring snowmelt, *Biogeochemistry*, 43, 1–15, 1998.
- Colin, M., and A. Rasmuson, A comparison of gas diffusivity models for unsaturated porous media, *Soil Sci. Soc. Am. J.*, 53, 1559–1565, 1988.
- Dawson, R. F., and K. A. Morin, Acid mine drainage in permafrost regions: Issues, control strategies and research requirements, *MEND Proj. 1.61.2*, 68 pp., Dep. of Indian and North. Aff. Canada, Ottawa, Ont., Canada, 1996.
- Egbert, J., A. Spaans, and J. M. Baker, Examining the use of time domain reflectometry for measuring liquid water content in frozen soil, *Water Resour. Res.*, 31, 2917–2925, 1995.
- Elberling, B., Processes controlling oxygen uptake rates in frozen mine tailings in the Arctic, in *Ice in Surface Waters*, edited by H. T. Shen, pp. 183–188, A. A. Balkema, Brookfield, Vt., 1998.
- Elberling, B., and R. V. Nicholson, Field determination of sulphide oxidation rates in mine tailings, *Water Resour. Res.*, 32, 1773–1784, 1996.
- Elberling, B., R. V. Nicholson, E. J. Reardon, and P. Tibble, Evaluation of sulphide oxidation rates—A laboratory study comparing oxygen fluxes and rates of oxidation product release, *Can. Geotech. J.*, 31, 375–383, 1994a.
- Elberling, B., R. V. Nicholson, and J. M. Scharer, A combined kinetic and diffusion model for pyrite oxidation in tailings: A change in controls with time, *J. Hydrol.*, 157, 47–60, 1994b.
- Elberling, B., A. Schippers, and W. Sand, Bacterial and chemical oxidation of pyritic mine tailings at low temperatures, *J. Contam. Hydrol.*, 41(3–4), 225–238, 1999.
- Foster, J., Über einige Eigenschaften leuchtender Bakterien, *Zent. Bakteriell. Parasitenk. Infec. Hyg.*, 2, 337–340, 1887.
- Godwaldt, R. C., K. W. Biggar, and D. C. Sego, AMD generation at sub-zero temperatures, paper presented at Symposium on Assessment and Remediation of Contaminated Sites in Arctic and Cold Climates, Public Works and Govt. Serv. Can., Edmonton, Alberta, Canada, May 3–4, 1999.
- Kalin, M., Ecological engineering for gold and base metal mining operations in the North West Territories, in *Northern Affairs Program*, *Environ. Stud.* 59, pp. 1–64, Dep. of Indian Aff. and North. Dev., Ottawa, Ont., Canada, 1987.
- McKnight, D. M., and K. E. Bencala, The chemistry of iron, aluminum, and dissolved organic material in three acidic, metal-enriched, mountain streams, as controlled by watershed and in-stream processes, *Water Resour. Res.*, 26, 3087–3100, 1990.
- Meldrum, J. L., H. E. Jamieson, and L. D. Dyke, Laboratory determination of sulphide oxidation potential in permafrost using tailings from Rankin Inlet, Nunavut, in *Mining and the Environment II*, edited by D. Goldsack, et al., pp. 119–126, CANMET, Ottawa, Ont., Canada, 1999.
- Mironenko, M. V., S. A. Grant, G. M. Marion, and R. E. Farren, FREZCHEM2: A chemical thermodynamic model for electrolyte solutions at subzero temperatures, *CRREL Rep. 97-5*, pp. 1–40, Cold Reg. Res. Eng. Lab., Hanover, N. H., 1997.
- Morita, R. Y., Psychrophilic bacteria, *Bacteriol. Rev.*, 39, 144–167, 1975.
- Nicholson, R. V., R. W. Gillham, and E. J. Reardon, Pyrite oxidation in carbonate-buffered solution. 1. Experimental kinetics, *Geochim. Cosmochim. Acta*, 52, 1077–1085, 1988.
- Nicholson, R. V., R. W. Gillham, J. A. Cherry, and E. J. Reardon, Reduction of acid generation in mine tailings through the use of moisture-retaining cover layers as oxygen barriers, *Can. Geotech. J.*, 26, 1–8, 1989.
- Nordstrom, D. K., Aqueous pyrite oxidation and the subsequent formation of secondary minerals, in *Acid Sulphate Weathering*, edited by L. R. Hossner, J. A. Kittrick, and D. S. Fanning, pp. 37–56, Soil Sci. Soc. of Am., Madison, Wis., 1982.
- Pantelis, G., and A. I. M. Ritchie, Macroscopic transport mechanisms as a rate limiting factor in dump leaching of pyritic ores, *Appl. Math. Model.* 15, 136–143, 1992.
- Rasmussen, K., and M. Willems, Pyrite oxidation and leaching in excavated lignited soil, *Acta Agric. Scand.*, 31, 107–115, 1981.
- Schippers, A., R. Hallmann, S. Wentzien, and W. Sand, Microbial diversity in Uranium mine waste heaps, *Appl. Environ. Microbiol.*, 53, 2930–2935, 1995.
- Schippers, A., H. von Rège, and W. Sand, Impact of microbial diversity and sulfur chemistry on safeguarding sulfidic mine waste, *Miner. Eng.*, 9, 1069–1079, 1996.
- Thorstenon, D. C., and D. W. Pollock, Gas transport in unsaturated zones: Multicomponent systems and the adequacy of Fick's laws, *Water Resour. Res.*, 25, 477–507, 1989.
- Williams, G. D., Flux estimates from oxygen concentration measurements in surface reservoirs, M.Sc. thesis, 179 pp., Univ. of Waterloo, Waterloo, Ont., Canada, 1993.

B. Elberling, Institute of Geography, University of Copenhagen, Øster Voldgade 10, DK-1350 Copenhagen K., Denmark. (be@geogr.ku.dk)

(Received January 26, 2000; revised August 21, 2000; accepted August 28, 2000.)





## Bacterial and chemical oxidation of pyritic mine tailings at low temperatures

Bo Elberling<sup>a,\*</sup>, Axel Schippers<sup>b</sup>, Wolfgang Sand<sup>b</sup>

<sup>a</sup> Institute of Geography, University of Copenhagen, Øster Voldgade 10, DK-1350 Copenhagen K., Denmark

<sup>b</sup> Institut für Allgemeine Botanik, Abteilung Mikrobiologie, Universität Hamburg, D-22609 Hamburg, Germany

Received 8 February 1999; received in revised form 26 August 1999; accepted 17 September 1999

### Abstract

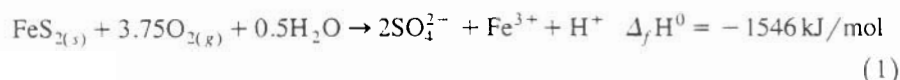
Microbial and chemical sulfide oxidation activity and oxygen consumption was investigated in the active layer of pyritic mine tailings at Nanisivik Mine, located in a permafrost area on Baffin Island in northern Canada. Samples of tailings were collected up to a depth of 60 cm in mid-August 1998 at 4 sites, for which the metabolic activity of sulfur- and iron-oxidizing leaching bacteria besides the chemical pyrite oxidation activity were measured on 39 tailings samples and 7 samples from a natural pyritic site by calorimetry. The tailings of varying age and water content were deposited under alkaline conditions. In situ oxygen uptake rates were measured at the tailings surface every third day, prior to sampling. In addition, cell counts of iron(II), sulfur, and thiosulfate oxidizing, lithotrophic bacteria and chemoorganotrophic microorganisms were determined quantitatively by the most-probable-number technique or by agar-plating. Results show consistent pyrite oxidation rates based on in situ oxygen uptake rates, and laboratory heat output measurements. Litho- and organotrophic bacteria were found in the tailings. Calorimetric measurements revealed that the present bacterial activity is responsible for approximately one third of the ongoing oxidation. Although leaching bacteria have previously been found in the Arctic, this study is the first to prove the significance of bacterial activity in the overall pollution resulting from tailings deposited in the Arctic. © 2000 Elsevier Science B.V. All rights reserved.

**Keywords:** Pyrite oxidation; Oxygen; Microbial activity; High Arctic

\* Corresponding author. Tel.: +45-35322520; fax: +45-35322501; e-mail: be@geogr.ku.dk

## 1. Introduction

The cold climate in permafrost areas is generally thought to offer several opportunities for a disposal of sulfide mine tailings. Low temperature laboratory tests show that oxygen consumption and acid generation in tailings is significantly slower at temperatures approaching freezing but not necessarily reduced to negligible levels on a year round basis (Dawson and Morin, 1996). This is a result of the annual thawing of the active layer up to several metres depth depending on the local ground conditions and the weather. Within this thawing zone infiltration of water and atmospheric oxygen gas will take place and initiate an oxidation of reactive mine tailings. Pyrite ( $\text{FeS}_2$ ) is the dominant sulfide mineral at the present field site and oxidizes, when exposed to oxygen in the presence of water. The oxidation reaction produces acid and is followed by a release of sulfate and metals (acid rock drainage). The oxidation of pyrite and the concurrent acid generation are complex processes that involve a number of reactants and products under various conditions (Lowson, 1982; Nordstrom, 1982; Rohwerder et al., 1998; among others). The complete oxidation of the iron and sulfur moieties of pyrite in an alkaline environment can be written as:



Fe(III) ions may act as an additional oxidizing agent which will oxidize pyrite about ten times faster than oxygen (Nordstrom, 1982). Since the solubility of Fe(III) ions increases as a third order function with decreasing pH, sulfide mineral oxidation by Fe(III) ions is particularly important at low pH. However, the overall rate of oxidation will decrease rapidly, unless Fe(III) ions is replenished by oxidation of Fe(II) ions. Below pH 4 the rate of inorganic Fe(II) ion oxidation is considerably slower than sulfide oxidation by Fe(III) ions (Singer and Stumm, 1970). Under highly acidic conditions the chemolithotrophic bacteria *Thiobacillus ferrooxidans* and *Leptospirillum ferrooxidans* are capable of catalysing the Fe(II) ion oxidation (Sand et al., 1992; Johnson, 1995; Schrenk et al., 1998). The bacterial Fe(II) ion oxidation has been found to increase the rate of sulfide oxidation by several orders of magnitude over the purely chemical oxidation rate (Nordstrom, 1982). Consequently, tailings are often mixed with carbonate minerals before deposition, in order to ensure an alkaline environment and thereby limit the importance of biologically catalysed oxidation. However, under alkaline conditions moderately acidophilic sulfur/-compound oxidizing bacteria like *Thiomonas intermedia* produce sulfuric acid by oxidation of thiosulfate and polythionates, which are a result of chemical pyrite oxidation (Schippers et al., 1996b).

### 1.1. Sulfide oxidation at low temperatures

Low temperatures may directly and indirectly impose constraints on the overall reaction rate of pyrite oxidation. The direct influence can be described by the Arrhenius equation (Nicholson et al., 1988):

$$\ln(k_1/k_2) = E_a/2.3(T_1 - T_2)/RT_1T_2 \quad (2)$$

where  $k_1$  and  $k_2$  are reaction rates at temperatures  $T_1$  and  $T_2$ ,  $E_a$  is the activation energy of the reaction and  $R$  is the gas constant. Values of  $E_a$  for pyrite reported in the

literature vary from 39 to 88 kJ/mol for a variety of experimental conditions (Nicholson et al., 1988). Although the effects of temperature on sulfide oxidation rates can be complex, particularly under field conditions, several studies confirm that the relatively simple relationship given by Eq. (2) is a valid approximation for the chemical and the microbial reaction rate (Ahonen and Tuovinen, 1992; Dawson and Morin, 1996). Dawson and Morin (1996) reviewed reaction rates related to *T. ferrooxidans* and concluded that the reaction rate generally decreases from maximum rates around 30°C to rates, which are orders of magnitude lower in case of near freezing temperatures. However, in reality bacteria have been found to adapt to very low temperatures. Kalin (1987) reported the presence of psychrophilic (growth at or round 0°C with a maximum temperature for growth < 21°C) thiobacilli at the Nanisivik field site and Langdahl and Ingvorsen (1997) observed maximum microbial pyrite oxidation rates at approximately 20–25°C and 30% of the maximum rate at 0°C. Although the occurrence of sulfide-oxidizing bacteria in the high Arctic has been reported, the actual activity and importance of microbes for sulfide oxidation have not received much attention. Moderately acidophilic or neutrophilic thiobacilli (pH optima of 5–8) have been found in ore samples with neutral pH-values at temperate latitudes (Johnson, 1995; Schippers et al., 1995, 1996b), but despite the relevance for decision making with respect to control strategies for limiting pollution from mine tailings in the Arctic, information on the activity of neutrophilic thiobacilli in the Arctic is not available. This study aims to quantify the importance of bacterial and chemical sulfide oxidation and to evaluate the temporal trends in oxygen uptake within uncovered tailings deposited in a permafrost-affected area in the High Arctic.

## 2. Materials and methods

### 2.1. The study area

Nanisivik Mine on Baffin Island (NWT) in northern Canada (73°02'N, 84°32'W) is located within the High Arctic zone of continuous permafrost. The annual mean temperature is minus 15.6°C and precipitation is approx 125 mm annually. The arid cold climate discourages development of vegetation and on the tailings vegetation is completely absent. Mine tailings have been deposited under water in a tailings impoundment since 1976. However, tailings are presently partly deposited "on land" and consequently some of the tailings are exposed to atmospheric oxygen gas. The tailings nowadays consist of 75–95% pyrite with the remainder made up of dolomite and residual amounts of sphalerite (ZnS) and galena (PbS). Typical analyses of tailings by weight are 35–40% Fe, 0.3% Zn, and 0.1% Pb. Weather information is available from a local weather station situated 200 m from the test site and includes temperature, humidity, wind speed and direction, as well as net radiation and precipitation monitored on a hourly basis year round.

### 2.2. Oxygen and temperature measurements

Vertical oxygen concentrations were measured at  $4 \pm 0.5$  cm depth intervals by a modified technique described by Elberling and Nicholson (1996). Pore gas from a

specific depth was withdrawn by connecting a stainless steel tube to a Mityvac Vacuum Pump® (PrisTech, USA). The oxygen concentration was measured by connecting the stainless steel tube directly to an electrochemical oxygen gas sensor (Model GC33-200, G.C. Industrial, Fremont, CA, USA). The oxygen sensor provides a voltage output, which is linearly related to the absolute concentration of oxygen. The sensor has been intensively investigated for its reliability during variable field conditions and was found to provide measurements within an accuracy of 0.1% O<sub>2</sub> (Williams, 1993; Elberling and Nicholson, 1996). The total gas volume of the sampling equipment was less than 30 ml.

In situ oxygen uptake rates were measured as changes in oxygen concentration over time within a gas chamber, open only to the tailings surface. The set-up consisted of stainless steel cylinders (18 cm ID) of 70 cm lengths, which were driven into the tailings, leaving the top 0.5–2 cm of the cylinders above the surface. During measurements a cap was placed on top of the cylinder to close the tailings profile within the cylinder from the atmosphere. The concentration of oxygen within the gas reservoir between the tailings surface and the cap was measured by the electrochemical oxygen gas sensor sealed into the cap. Readings from the oxygen sensor in mV were recorded each minute over 2 h on a logger and used to estimate the flux of oxygen across the tailings surface, as described previously (Elberling and Nicholson, 1996). The following equation was used to convert relative changes in oxygen concentration within the gas reservoir over time to a flux of moles of oxygen per area per time:

$$F_s = C_0(kD_e)^{0.5} \quad (3)$$

where  $F_s$  is the flux of oxygen across the tailing surface and  $C_0$  is the initial concentration of oxygen before measurement. The parameter  $(kD_e)^{0.5}$  is given by the slope of a plot of the relative change in oxygen concentration within the gas reservoir with time as previously shown (Elberling and Nicholson, 1996; Elberling et al., 1994a).

Air and sub-surface temperatures were logged at the test sites at 2 h intervals (Tinytag Gemini Data Loggers, UK). Soil temperatures (top 20 cm) and water content were measured by portable instruments.

### 2.3. Water and tailings samples

Pore solution was extracted by PHRENART® suction probes installed 10, 20, 30, 40 and 80 cm below the surface. Solutions were collected after 24–48 h of extraction and repeated on a weekly basis. Water samples were acidified (10% HCl) and kept cool (5°C) and dark until analysed. Total concentrations of Zn, Cd and Pb were determined by using Atomic Absorption Spectrometer (AAS) and SO<sub>4</sub> was determined on non-pre-served samples by using ion chromatography (IC). Conductivity and pH were measured on site.

Prior to departure from the field area (between 14–18 August 1998), 39 depth specific samples of tailings were collected of 5 cm intervals. Each sample represented a 2 cm layer. Sampling was made in the oxidized zone (approximately top 30 cm at dry sites) and at least 30 cm below. Sampling was made under sterile conditions using cups of 100 cm<sup>3</sup>. Sampling cups were only half filled with tailings from the oxidized zone in order to allow oxidation, whereas cups with reduced tailings were filled and stored in

gas-tight plastic bags flushed with nitrogen gas to avoid oxidation. Samples were kept dark and between 4–6°C, until processed in the lab within a week. The pyrite content was determined by quantitative X-ray powder diffraction analysis. The content of pyrite was determined from diffraction intensity in samples before and after addition of 30% by weight of pure pyrite from the area (Zunic, 1996). For further chemical analysis 2 g of each sample was added to 20 ml of a 0.9% NaCl-solution in 100 ml flasks. For extraction of soluble compounds the flasks were shaken on a rotary shaker for 2 h at 28°C. After centrifugation for 10 min (Heraeus, 9000 rpm), sulfate and nitrate were determined by ion chromatography (Dionex, model DX 500), and thiosulfate and polythionates were determined by high-pressure-liquid chromatography with diode array detection (HPLC/DAD, Kontron, Germany), as previously described (Schippers et al., 1996a). Ingold electrodes were used for pH measurements. Elemental sulfur was extracted with ethanol from the samples, and also quantified by HPLC/DAD (Schippers et al., 1996a). The grain size distribution and porosity of the samples were determined of every third sample with depth. For comparison of the tailings material with naturally exposed sulfide material, 7 samples were taken from the gossan surface of naturally weathered ore material.

#### 2.4. *Calorimetric measurements*

For determination of microbial and chemical pyrite oxidation rates, the heat output of the ore-samples was measured using a thermal-activity-monitor (type 2277, Thermometric, Sweden, or C3-Analysentechnik, Germany) equipped with ampoule cylinders (4 ml twin, type 2277-201, and 20 ml twin, type 2230). Glass ampoules containing 4 g or 15 g of ore in air were inserted in the measuring cylinders and, after thermal equilibration, the heat output resulting from microbial degradation of pyrite was recorded, as previously described (Sand et al., 1993; Schröter and Sand, 1993). Heat output, only caused by chemical oxidation, was measured after exterminating the microorganisms by chloroform addition to the samples. After 2 h the chloroform was removed by vacuum evaporation and heat output was measured again. Measurements were made at 6°C, 10°C, and 20°C.

#### 2.5. *Enumeration of microorganisms*

Strongly acidophilic, lithotrophic iron(II) ion and sulfur oxidizing bacteria (pH 1.8 and 4.5), and moderately acidophilic, lithotrophic thiosulfate oxidizing bacteria (pH 6.8) were enumerated by a three-tube most-probable-number (MPN) technique. Acidophilic (pH 2) and neutrophilic (pH 7) chemoorganotrophic microorganisms (COT) were counted by plating on agar. Tubes were incubated in the dark at 20°C on a shaker (100 rpm) for 6 weeks. Agar plates were incubated in the dark at 20°C for 4 weeks. Media and enumeration procedures have previously been described (Schippers et al., 1995).

#### 2.6. *Estimated oxygen uptake from measured heat output*

Values of heat output at 10°C from samples, representing an entire soil profile, have been corrected for the actual temperature measured during sampling by using the linear



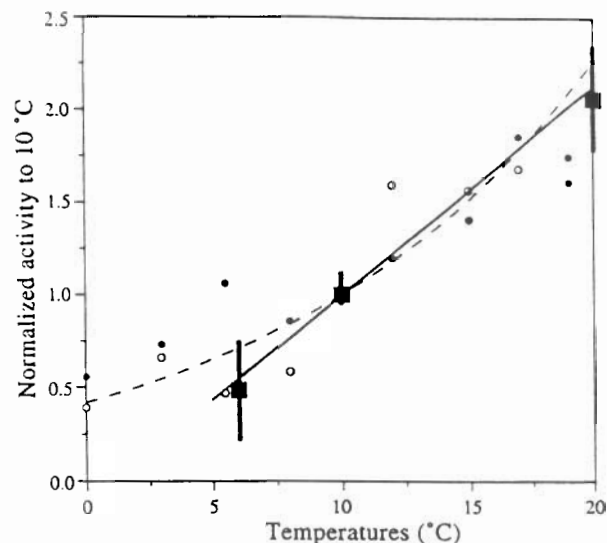


Fig. 1. Normalized activity of pyrite oxidation vs. temperature. Solid squares (■) represent calorimetric measurements of samples from Nanisivik Mine and the straight line a linear fit for temperatures between 6°C and 20°C ( $r^2 = 99\%$  — maximum and minimum measured values are indicated with bars). Normalized pyrite oxidation activity based on dissolved iron production data from Langdahl and Ingvorsen (1997) are included for comparison. Open circles (○) represent chemical rates and solid circles (●) microbial rates. The Arrhenius plot based on the activation energy observed by Langdahl and Ingvorsen (1997) is shown as a dashed line.

relationship shown in Fig. 1. The total heat output within the profile has then been estimated as the depth-integrated heat output and further converted to a rate of pyrite oxidation, by using a reaction energy values for pyrite oxidation of 1546 kJ/mol, given for biological pyrite oxidation by calorimetry (Rohwerder et al., 1998). The final conversion to total oxygen consumption within the profile per surface area takes into account the depth dependent density of the tailings (2.9–3.1 g/cm<sup>3</sup>), the porosity (35%), the water content (5–12%), as well as the stoichiometric conversion of pyrite oxidation by oxygen (given by Eq. (1)). The calculated total oxygen uptake in moles per m<sup>2</sup> per day can then be compared to the in situ measurements of oxygen uptake.

### 3. Results

#### 3.1. Tailings reactivity

Tailings from the study area consisted of well-sorted and fine sand with a pyrite content between 15–40% in the upper, partly oxidized zone, and up to 80% within the reduced zone. The permafrost boundary moved from a depth of approximately 1 m in mid July to 1.5 m in mid August. Three characteristic sites have been evaluated: well-drained 6 years old tailings, nearly water-saturated 6 years old tailings, and well-drained 1/2 year old tailings. The characteristics of the solid chemistry of the sites

are summarized in Table 1. The tailings are well-buffered and the oxidation proceeds at neutral pH values between 7.4 and 7.7. Sulfate is the dominant oxidation product, and typically accounts for more than 98% of the dissolved sulfur species. Intermediary sulfur compounds including thiosulfate, polythionates, and elemental sulfur are found at all depths in all profiles. Tetrathionate ( $\text{S}_4\text{O}_6^{2-}$ ) is the dominant species of the intermediary species between sulfide and sulfate, and concentrations of tetrathionate correlate linearly with depth with the concentrations of sulfate ( $r^2 = 88\%$ ), pentathionates ( $r^2 = 98\%$ ), and trithionate ( $r^2 = 92\%$ ). A steady decrease in concentration with increasing depth were observed for sulfate, tetrathionate, pentathionate, and for trithionate only for the 1/2 year old site. In contrast, trithionate increases with depth at the other sites. The highest concentration of elemental sulfur was observed at the interface between the oxidized and reduced zone at a depth of 20–40 cm (data not shown).

Pore solution collected at depths of 40 cm and below had pH-values between 6.8 and 7.9 and fairly consistent total concentrations during the summer period (in ppm  $\pm$  SD): Zn:  $35 \pm 15$ ; Pb:  $0.05 \pm 0.02$ , Cd:  $0.004 \pm 0.002$ , and  $\text{SO}_4$ :  $1970 \pm 370$ . Concentrations and pH within the upper 30 cm at well-drained sites, however, varied significantly over time. After precipitation events, total concentrations in this reactive zone were similar to those at depths of 40 cm and below, but during a 4-week dry period, pH dropped as low as 2.3 and total concentrations in the pore solution increased to the following maximum concentrations (in ppm): Zn: 250; Pb: 1.1, Cd: 0.6, and  $\text{SO}_4$ : 29,340. These changes in total concentrations (data not shown) are a result of both the release of weathering products from sulfide oxidation, ion up-concentration due to evaporation, and interactions between the solid phase and the pore solution. Therefore, the concentrations of metals in pore solution are not discussed further in relation to the actual sulfide oxidation and oxygen uptake observed in this study.

### 3.2. Temperature dependent activity

The total heat output values (activity) in  $\mu\text{W g}^{-1}$  for 5 samples at three temperatures are shown in Fig. 1. A linear correlation exists between activity and temperature is

Table 1  
Characteristics of tailing and chemistry of suspension (average  $\pm$  SD)

Sites	1 and 2 <sup>a</sup>	3	4
Years since deposition	6	6	0.5
Water Content	well-drained	wet	well-drained
pH	$7.4 \pm 0.2$	$7.7 \pm 0.2$	$7.4 \pm 0.4$
Sulfate	$2668 \pm 1100$	$2001 \pm 1799$	$1493 \pm 772$
Thiosulfate	$1.3 \pm 0.8$	$3.2 \pm 3.1$	$3.8 \pm 2.3$
Elemental sulfur	$58 \pm 52$	$25 \pm 23$	$95 \pm 108$
Trithionate	$9 \pm 5$	$3 \pm 3$	$98.2 \pm 63$
Tetrathionate	$173 \pm 69$	$52 \pm 41$	$738 \pm 386$
Pentathionate	$34 \pm 12$	$9 \pm 1$	$110 \pm 70$
Nitrate	$8.1 \pm 6.2$	$7.3 \pm 2.1$	$25.2 \pm 28.6$

<sup>a</sup>Site 1 and 2 are replicates.

observed ( $r^2 = 99\%$ ). For comparison, normalized chemical and microbial pyrite oxidation activity data based on dissolved iron production at different temperatures for ore material from Citronen Fjord, North Greenland (Langdahl and Ingvorsen, 1997), are shown. Based on the activation energy and the maximum pyrite oxidation rate observed by Langdahl and Ingvorsen (1997) an Arrhenius plot according to Eq. (2) has been calculated. A consistency in the activity of the Nanisivik-samples with the Arrhenius plot in the temperature range between 5°C and 20°C can be noted. However, as the temperature approaches zero, an increasing disagreement is observed. In this study, temperatures of the reactive zone varied between 4°C and 13°C and, therefore, the linear fit is used to convert measured activities at 10°C to actual activity by taking the temperature into account.

### 3.3. Depth dependent activity

A drop in the oxygen gas concentration from atmospheric content (20.9%) to below detection limit (0.1%) was observed at all sites. At well-drained sites the oxygen penetration was approximately 30 cm (Fig. 2A), but at wet sites oxygen gas was not detected below the top 2 cm. These observations were consistent with a drastic change in colour from red/yellow to grey at the border of oxygen depletion. Temperatures were approximately 13°C near the surface, 4–6°C at 60 cm depth, and reached 0°C at the permafrost level. Fig. 2B shows calorimetric data from well-drained, 6 years old tailings and data from a replicate profile of less than 2 m away. Based on the average measured activity at atmospheric oxygen concentrations, corrected for temperature (see Fig. 1), the actual activity ( $\mu\text{W g}^{-1}$ ) is shown as a thick, solid curve. Heat output of the same samples after chloroform treatment revealed that chemical oxidation (without the influence of bacteria) accounted for 50–100% of the total activity with an average of 65%. The variations in this percentage could not be related to either depth or pH. Table 2 summarizes the reactivity of the four sites. Values of oxygen uptake from the surface prior to sampling are found to be consistent with heat output. There is no significant variation in the reactivity due to the age of the two well-drained sites. Here the water content was approximately 10%, whereas at the wet site the water content is approximately 30% reaching saturation at a depth of 20 cm. At the wet site the actual rate of oxygen consumption is reduced by a factor of 100, compared to the well-drained sites.

### 3.4. Microorganisms

In some of the samples from the oxidized upper zone of the well-drained and the near-saturated, 6 years old well-buffered tailings, from an unbuffered sampling site, and from naturally exposed sulfide ore material rod-shaped, strongly acidophilic, lithotrophic iron(II) ion (*Thiobacillus ferrooxidans*) and sulfur oxidizing bacteria (*T. thiooxidans*), moderately acidophilic, lithotrophic, thiosulfate oxidizing bacteria (*Thiomonas intermedia*), as well as chemoorganotrophic microorganisms (COT) were detected in some cases up to a depth of 25 cm. Cell counts of strongly acidophilic, lithotrophic bacteria amounted to a maximum of  $10^4$  cells  $\text{g}^{-1}$  sample. Cell counts of moderately acidophilic, lithotrophic, and of organotrophic microorganisms amounted to maximally  $10^6$  cells  $\text{g}^{-1}$  sample. Lithotrophic bacteria were detected in about two thirds of the samples from the

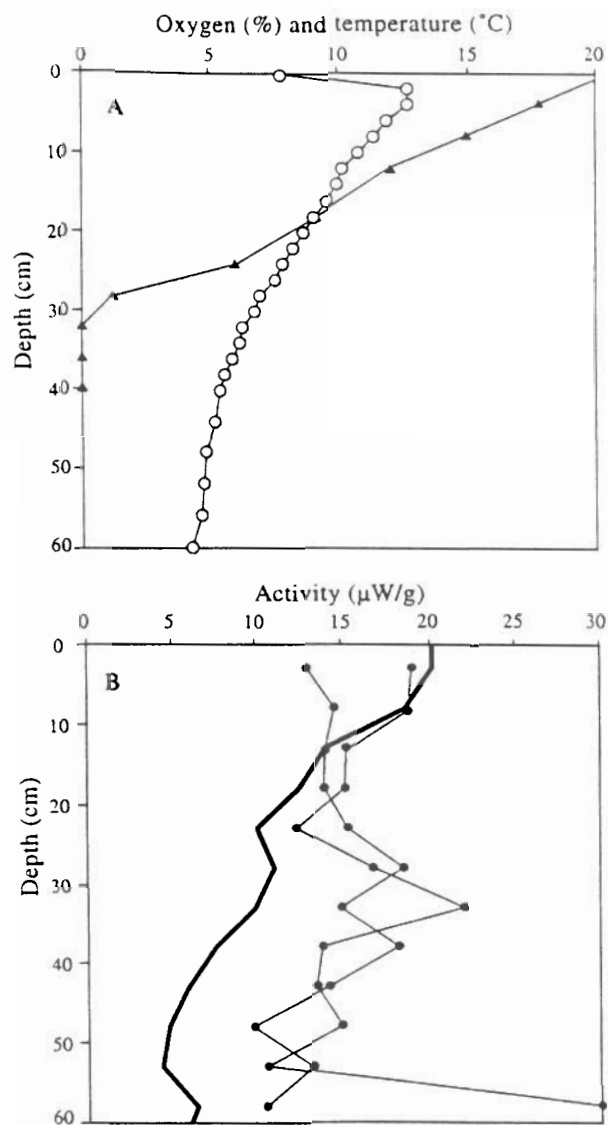


Fig. 2. Depth dependent related data for well-drained tailings deposited 6 years ago. A: oxygen gas concentration ( $\blacktriangle$ ) and temperature ( $\circ$ ) prior to sampling, B: measured heat output at  $10^{\circ}\text{C}$  ( $\bullet$ ), and total heat output (—) corrected according to on-site temperatures using the linear relationship shown in Fig. 1.

oxidized zone of the well-buffered tailings. Litho- and organotrophic microorganisms were found in all samples from the unbuffered tailings and from the natural sampling site. However, microorganism were not detectable in samples from the reduced zone below 30 cm of the well-buffered tailings as well as from the 1/2 year old tailings, in the latter case irrespective of the zone.

Table 2

Characteristics of tailings reactivity (average  $\pm$  SD)

Sites	1 and 2	3	4
Oxygen uptake <sup>a</sup> (moles m <sup>-2</sup> day <sup>-1</sup> )	0.40 $\pm$ 0.06	0.0055 $\pm$ 0.008	0.39 $\pm$ 0.05
Heat output converted to O <sub>2</sub> uptake (moles m <sup>-2</sup> day <sup>-1</sup> )	0.43 $\pm$ 0.03	0.0027	0.38
Chemical oxidation (percent of total oxidation)	70 $\pm$ 14	63 $\pm$ 29	68 $\pm$ 9

<sup>a</sup>SD-values for in situ oxygen uptake values represent the sensitivity of the slope estimate.

### 3.5. Temporal trends in activity

Measurements of air temperatures, soil temperatures, and precipitation from mid July to mid August 1998 are shown in Fig. 3. In addition, data from oxygen uptake measurements of the well-drained sites are included. Soil temperatures at a depth of 20 cm have been used to simulate the expected relative variation in oxygen uptake over time due to only the soil temperature. For that purpose the linear relationship between activity and temperature (Fig. 1) has been used. The model fit shown in Fig. 3 is normalized, based on the average oxygen uptake and temperature observed during the

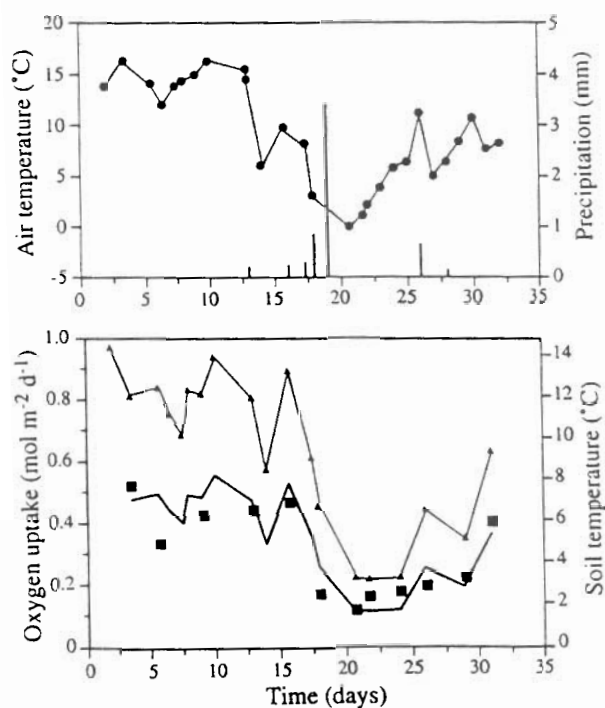


Fig. 3. Temporal trends in air temperatures (●), soil temperatures (▲), precipitation (solid bars), and oxygen uptake rates (■) measured from the 15th of July to 18th of August 1998. The site consists of well-drained tailings deposited 6 years ago. Simulated oxygen uptake is shown as a thick solid line.



first 10 days. Fig. 3 demonstrates that significant changes in oxygen uptake can be modelled, taking only the top soil temperature into account. This is despite of a pronounced precipitation event after 19 days. Measurements of the top tailings revealed that the site was so well-drained that no significant changes in water content before and after the rain event could be observed after 12 h (data not shown). The results indicate that the oxygen uptake rate (pyrite oxidation rate) is determined by the soil temperature of well-drained tailings sites. Due to the general very low oxygen uptake rate at the wet site, the oxygen uptake measurements failed to provide similar detailed information on temporal trends at that site.

#### 4. Discussion and conclusions

Two different methods were applied to determine oxidation activities in pyritic mine tailings: oxygen uptake rates measured in situ and microcalorimetric pyrite oxidation activity measurements at in situ temperatures in the laboratory. An earlier laboratory study (Rohwerder et al., 1998) has shown that the calorimetrically determined reaction energy value for chemical and bacterial pyrite oxidation agrees with the theoretical value according to Eq. (1). Thus, the amount of oxygen consumed can be determined by calorimetric measurements. Results from laboratory measurements of calorimetric pyrite oxidation activity agreed well with the in situ oxygen uptake observed in the field. However, some deviation may be a result of that the calorimetric pyrite oxidation activity was measured at atmospheric oxygen concentrations and therefore may not represent in situ conditions for samples throughout the profiles. Bacteria activity is not sensitive to variations in oxygen concentrations at moderate and high concentrations. Only at very low oxygen concentrations a decrease of the pyrite oxidation rate has been observed (Bailey and Hansford, 1993). Therefore, only calorimetric measurements on samples from the reduced zone, where oxygen is almost absent, may lead to biased results in form of higher activities. However, this oxygen contamination was limited by careful oxygen exclusion during sample handling in the field and transport to the laboratory. Consequently, the oxygen contamination was limited to the slow diffusion of oxygen in water during laboratory measurements, as samples from the reduced zone were almost saturated with water. The contamination has therefore been evaluated to be negligible.

##### 4.1. Control of oxidation rates

This study is in agreement with the general concept that diffusion of oxygen gas is the controlling parameter for the overall oxidation (Pantelis and Ritchie, 1991; Elberling et al., 1994b; Evangelou, 1995; among others). We observed variations in oxygen uptake rates by a factor of 100, which can be described by the variable water content, and therefore directly by the effective diffusion coefficient of the tailings. But we also observe that other parameters, such as the temperature, may directly influence the oxygen uptake over time by a factor of 2 or more.

The model fit presented here uses only the temperature in one depth to model temporal trends in oxygen uptake. Although the model fits data the model may not

necessarily account for all environmental factors controlling the observed changes in oxygen uptake. A more correct fit can be made by taking the temperature at several depths into consideration. This was done for temperatures at four depths within the top 80 cm. However, the resulting model fit did not vary significantly from the result shown in Fig. 3. For estimating trends on a time scale of months or years, a more detailed description of soil temperatures is required to improve the interpretation.

The pH-value is another parameter, which may become important. At the well-buffered site pH is high and the influence of bacteria remains limited, as compared to an acidic environment. Calorimetric data revealed that microbial pyrite oxidation accounts for about one third of the total activity. Since pyrite oxidizing iron(II) ion and sulfur/-compound oxidizing bacteria have not been detected in all samples from the well-buffered sites, a yet unknown bioleaching bacteria may exist, which is not detectable with our media. Heat output measurements were also made for samples from a non-buffered spill of tailings, which beside of tailings also consists of fine rock fragments. Here, leaching bacteria were regularly detected. The pH-value of one sample was 2.9 and the heat output was found to be 100% biologically controlled. The absolute value of reactivity cannot be compared to the other values reported here, as the samples consist of an unsorted and much coarser material than the tailings. But the observation is important in relation to the expected pH with time in relation to the acidifying and neutralizing potential of the tailings. Based on the chemical composition of the tailings, the acid production exceeds the neutralization potential by at least a factor of 10. This indicates that over time the microbial oxidation rates most likely will become more and more important for the overall oxidation rate.

#### 4.2. Frozen tailings

It has been suggested that freezing of the tailings will prohibit both oxygen diffusion and biological reaction, and thereby control the acid production and heavy metal release. Consequently, covering reactive tailings with an inert cover, to ensure that the permafrost grows up into the tailings, has been suggested as an appropriate remediation scheme for Arctic tailings systems (Dawson and Morin, 1996). However, recent laboratory diffusion coefficient measurements of tailings from the study area suggest that freezing of fairly well-drained tailings with a degree of water saturation below 30% has no significant effect on the effective diffusion coefficient (Elberling, 1998). In addition, those laboratory observations only apply to systems, where the tailings solution actually freezes around 0°C. This will not be the case for most tailings solutions, as the high ion content will lower the freezing temperature (Dawson and Morin, 1996). The availability of water at minus degrees is important for microbial activity. Although our heat output measurements between 6°C and 20°C suggest a rate close to zero at freezing temperatures, this is not a valid assumption. Both, the theoretical equation and independent measurements near 0°C (Langdahl and Ingvorsen, 1997), suggest significant activity near 0°C. From above it can be concluded that a temperature decline will gradually limit the overall reactivity in mine tailings, but also that temperatures just below 0°C are no guarantee for neglectable rates of pyrite oxidation in well-drained pyritic tailings.

## Acknowledgements

This study is part of the MIKA-project "Chemical fluxes in frozen soil" funded by the Environmental Department, Ministry of Environment and Energy (Denmark). The project is supported by National Environmental Research Institute, Institute of Geography (University of Copenhagen) and Nanisivik Mine. Many thanks to T.B. Zunic for help with the X-ray measurements and to K. LeDrew and J. Goyman, Nanisivik Mine for help, access to data, and hospitality. A.S. was funded by contract No. 1490954 to W.S. from the German BMBF via Umweltbundesamt. Also thanks to anonymous reviewers for many helpful comments on the manuscript.

## References

- Ahonen, L., Tuovinen, O.H., 1992. Bacterial oxidation of sulfide minerals in column leaching experiments at suboptimal temperatures. *Appl. Environ. Microbiol.* 58, 600–606.
- Bailey, A.D., Hansford, G.S., 1993. Factors affecting bio-oxidation of sulfide minerals at high concentrations of solids: a review. *Biotechnol. Bioeng.* 42, 1164–1174.
- Dawson, R.F., Morin, K.A., 1996. Acid mine drainage in permafrost regions: issues, control strategies and research requirements. MEND Project 1.61.2. Departments of Indian and Northern Affairs Canada, Ottawa, Ontario, 68 pp.
- Elberling, B., 1998. Processes controlling oxygen uptake rates in frozen mine tailings in the arctic. In: Shen, H.T. (Ed.), *Ice in surface waters. Proceedings of the 14th International Conference on Ice*, July, 28–30, A.A. Balkema, Rotterdam, New York, USA, pp. 183–188.
- Elberling, B., Nicholson, R.V., 1996. Field determination of sulphide oxidation rates in mine tailings. *Water Resour. Res.* 32 (6), 1773–1784.
- Elberling, B., Nicholson, R.V., Reardon, E.J., Tibble, P., 1994a. Evaluation of sulphide oxidation rates — a laboratory study comparing oxygen fluxes and rates of oxidation product release. *Can. Geotech. J.* 31, 375–383.
- Elberling, B., Nicholson, R.V., Scharer, J.M., 1994b. A combined kinetic and diffusion model for pyrite oxidation in tailings: a change in controls with time. *J. Hydrol.* 157, 47–60.
- Evangelou, V.P.B., 1995. Pyrite oxidation and its control. CRC Press, Boca Raton, FL, USA, 182 pp.
- Johnson, D.B., 1995. The role of 'iron bacteria' in the biodegradation of minerals. *Biodeterioration Abstracts* 9, 1–7.
- Kalin, M., 1987. Ecological engineering for gold and base metal mining operation in the North West Territories. Northern Affairs Program, Department of Indian Affairs and Northern Development, Environmental Studies no. 59, pp. 1–64.
- Langdahl, B.R., Ingvorsen, K., 1997. Temperature characteristics of iron solubilisation and  $^{14}\text{C}$  assimilation in natural exposed ore material at Citronen Fjord, North Greenland (83°N). *FEMS Microbiol. Ecol.* 23, 275–283.
- Lowson, R.T., 1982. Aqueous oxidation of pyrite by molecular oxygen. *Chem. Rev.* 82, 461–497.
- Nicholson, R.V., Gillham, R.W., Reardon, E.J., 1988. Pyrite oxidation in carbonate-buffered solution: I. Experimental kinetics. *Geochim. Cosmochim. Acta* 52, 1077–1085.
- Nordstrom, D.K., 1982. Aqueous pyrite oxidation and the subsequently formation of secondary minerals. In: Hossner, L.R., Kittrick, J.A., Fanning, D.F. (Eds.), *Acid Sulphate Weathering*. Soil Science of Society of America Press, Madison, WI, pp. 37–56.
- Pantelis, G., Ritchie, A.I.M., 1991. Macroscopic transport mechanisms as a rate limiting factor in dump leaching of pyritic ores. *Appl. Math. Model.* 15, 136–143.
- Rohwerder, T., Schippers, A., Sand, W., 1998. Determination of reaction energy values for biological pyrite oxidation by calorimetry. *Thermochimica Acta* 309, 79–85.

- Sand, W., Rohde, K., Sobotke, B., Zenneck, C., 1992. Evaluation of *Leptospirillum ferrooxidans* for leaching. *Appl. Environ. Microbiol.* 58, 85–92.
- Sand, W., Hallmann, R., Rohde, K., Sobotke, B., Wentzien, S., 1993. Controlled microbiological in-situ stope leaching of a sulphidic ore. *Appl. Microbiol. Biotechnol.* 40, 421–426.
- Schippers, A., Hallmann, R., Wentzien, S., Sand, W., 1995. Microbial diversity in uranium mine waste heaps. *Appl. Environ. Microbiol.* 53, 2930–2935.
- Schippers, A., Jozsa, P.G., Sand, W., 1996a. Sulfur chemistry in bacterial leaching of pyrite. *Appl. Environ. Microbiol.* 62, 3424–3431.
- Schippers, A., von Rège, H., Sand, W., 1996b. Impact of microbial diversity and sulfur chemistry on safeguarding sulfidic mine waste. *Minerals Engineering* 9, 1069–1079.
- Schrenk, M.O., Edwards, K.J., Goodman, R.M., Hamers, R.J., Banfield, J.F., 1998. Distribution of *Thiobacillus ferrooxidans* and *Leptospirillum ferrooxidans* for generation of acid mine drainage. *Science* 279, 1519–1522.
- Schröter, A.W., Sand, W., 1993. Estimations on the degradability of ores and bacterial leaching activity using short-time microcalorimetric tests. *FEMS Microbiol. Rev.* 11, 79–86.
- Singer, P.C., Stumm, W., 1970. Acid mine drainage: the rate determining step. *Science* 167, 1121–1123.
- Williams, G.D., 1993. Flux estimates from oxygen concentration measurements in surface reservoirs. M.Sc. Thesis, University of Waterloo, Waterloo, Ontario, Canada, 179 pp.
- Zunic, T.B., 1996. Addition method in the quantitative analysis: dependence of error on the quantity of additive. *Material Science Forum* 288, 43–48.



## Microscale measurements of oxygen diffusion and consumption in subaqueous sulfide tailings

BO ELBERLING<sup>1,\*</sup> and LARS RIIS DAMGAARD<sup>2</sup>

<sup>1</sup>Institute of Geography, University of Copenhagen, Øster Voldgade 10 DK-1350 Copenhagen K, Denmark

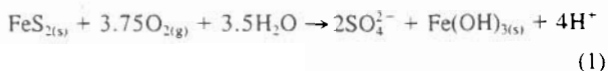
<sup>2</sup>Unisense Aps, Science Park Aarhus, Gustav Wieds Vej 10, DK-8000 Aarhus C, Denmark

(Received October 10, 2000; accepted in revised form January 23, 2001)

**Abstract**—The disposal of sulfide mine tailings in an environmentally sound, yet cost-effective, manner is an issue facing most metal mines. Subaqueous tailing disposal is considered an attractive option for disposal that limits oxygen (O<sub>2</sub>) availability within sulfide mine tailings and controlling sulfide oxidation and the resultant acid mine drainage (AMD). Assuming that O<sub>2</sub> profiles represent steady-state conditions, we aim to evaluate the depth-dependent and temperature-dependent rates of O<sub>2</sub> consumption in saturated mine tailings. Measurements include microscale O<sub>2</sub> gradients and diffusivity profiles within columns representing undisturbed mine tailing profiles from an impoundment near Nanisivik Mine in northern Canada. Measurements were made across the diffusive boundary layer (DBL) above the tailing-water interface as well as in the tailings below. Laboratory measurements of O<sub>2</sub> profiles are compared to in situ profiles. From the laboratory results it is possible to evaluate the O<sub>2</sub> flux across the DBL and the depth-integrated O<sub>2</sub> uptake. The results are compared with the average sulfate production rate over 3 months. O<sub>2</sub> uptake in saturated tailings is discussed in relation to O<sub>2</sub> uptake measured in columns after free drainage. The methods applied provide consistent O<sub>2</sub> consumption rates as well as reliable predictions for controlling AMD by keeping tailings under water. Copyright © 2001 Elsevier Science Ltd

### 1. INTRODUCTION

One of the most significant challenges facing base metal mines is the disposal of mine tailings in an environmentally sound, yet cost-effective manner. Mine tailings comprise the finely ground waste that remain after mineral extraction from ores. Sulfide tailings pose, in particular, a well-known environmental risk due to the potential generation of acid mine drainage (AMD) through tailings oxidation (e.g., Dubrovsky et al., 1984; Nicholson et al., 1988; Nicholson et al., 1990; Blowes and Jambor, 1990). Pyrite (FeS<sub>2</sub>) is by far the most common sulfide mineral giving rise to AMD. The oxidation of pyrite is a complex biogeochemical process involving several redox reactions, hydrolysis and complex ion formation, solubility control as well as microbial catalysis. Important aspects of this process are not clearly understood. However, when the reaction solution is alkaline, and if complete oxidation of the iron and sulfur components of pyrite occur, the overall resulting reaction is (Nicholson et al., 1988):



In an alkaline carbonate solution, the hydrogen ion is quickly neutralized, and the major net products of oxidation are sulfate and ferric hydroxide precipitation. However, in many cases, initially neutral environments become acidic, resulting in the potential migration of heavy metals that often are associated with the sulfide formations.

To control the generation of AMD, management of sulfide waste material has customarily involved the deposition of tail-

ings into impoundments (known as subaqueous tailing disposal) that are constructed to maintain mine tailings fully saturated, thereby minimizing O<sub>2</sub> diffusion into the tailing materials. Despite the potential control of AMD by underwater disposal, few investigations have focused on the actual reduction in the amount of O<sub>2</sub> consumed by sulfide oxidation in saturated mine tailings. Laboratory tests on the release of reaction products from pyritic rock and mine tailings underwater (Aubé et al., 1995; Mugo et al., 1999), indicate that storage of reactive pyritic material underwater is effective in attenuating long-term fluxes of contaminants to the overlying water column as well as concentrations of weathering products in drainage water. Aubé et al. (1995) concluded that although water cover may not completely prevent oxidation, it must be considered the most promising control technology yet known to the industry. Evaluating the effectiveness of water covers in field settings on the basis of geochemical analysis of water samples alone is difficult. This is due to the influence of a complex geochemistry controlling the actual concentration of weathering products rather than the actual rate of sulfide oxidation (Blowes and Jambor, 1990). Thus, predictions of sulfide oxidation rates for various water regimens have to a large extent been based on model predictions (e.g., Narasimhan et al., 1986; Elberling et al., 1994b; Wunderly et al., 1996).

Direct measurement of the O<sub>2</sub> consumption rates provides an alternative and instantaneous measure of the actual AMD generation, which has been applied for well-drained tailings. In Elberling and Nicholson (1996), the O<sub>2</sub> decrease was measured in situ over time in closed chambers placed on the tailing surface and related to the O<sub>2</sub> flux across the surface (O<sub>2</sub> consumption method). The O<sub>2</sub> uptake observed by Elberling and Nicholson (1996) corresponded to the in situ sulfate production in flushed tailing profiles. The O<sub>2</sub> consumption method

\*Author to whom correspondence should be addressed (be@geogr.ku.dk).



was applied along a transect from well-drained mine tailings toward a ponded area within a tailing impoundment. Results revealed that the increasing water content toward a pond reduced the near-surface effective diffusion as well as the  $O_2$  uptake by approximately a factor of 100. However, the low  $O_2$  consumption observed near the pond was on the same order of magnitude as the detection limit for the instrumentation used. Thus, it was concluded that the chambers were not suitable for evaluating  $O_2$  uptake in saturated or near-saturated tailings.

Microscale measurements of  $O_2$  concentration gradients and subsequent calculations of  $O_2$  fluxes may be an alternative method for evaluating the actual  $O_2$  consumption within water-covered tailings. This kind of measurement has been widely used to evaluate  $O_2$  uptake in lake, fiord, and marine sediments (e.g., Revsbech et al., 1986; Rasmussen and Jørgensen, 1992) and is generally accepted as a reliable and direct measure of chemical processes involving  $O_2$  consumption. To our knowledge, no direct measurements on AMD generation or  $O_2$  consumption in water-covered tailings have yet been reported.

In the present study, we aim to evaluate the  $O_2$  consumption rates as a measure for AMD generation rates in sulfide tailings of various ages and depositional environments. The evaluation is based on  $O_2$  concentration gradients measured in the diffusive boundary layer of water-covered tailings as well as measured diffusivity and  $O_2$  concentrations within the upper part of tailings. Oxidation measurements based on sulfate released from replicate columns packed with prewashed tailings is included and represents a direct measure of pyrite oxidation. Oxygen consumption rates are also evaluated in columns, filled with tailings drained to field capacity, by a closed chamber technique to provide insight into the environmental effects of keeping tailings saturated. Finally, we aim to evaluate the  $O_2$  uptake in saturated tailings over the temperature range 0 to 20°C, because increasing  $O_2$  solubility in cold water has been suggested to be a concern when covering tailings with water in cold regions (Dawson and Morin, 1996; Godwaldt et al., 1999).

## 2. DIFFUSION AND REACTION CONCEPTS

The availability of  $O_2$  in subaqueous tailings relies on the transport of atmospheric  $O_2$  dissolved in water by solute movement and molecular diffusion (e.g., Berg et al., 1998). In marine sediments, bioturbation (i.e., the diffusion-like transport caused by fauna activity) will influence the overall transport of  $O_2$  (Aller, 1980). However, in sulfide tailings, macro fauna activity has not been observed, probably because of extremely high concentrations of heavy metals and low pH. Although the  $O_2$  dynamics in tailings is a three-dimensional problem, it is generally accepted that it is possible to apply one-dimensional models for porous media similar to tailings (e.g., Pantelis and Ritchie, 1992; Iversen and Jørgensen, 1993). By assuming steady-state conditions and neglecting the effect of pore water movement due to groundwater flow and wave actions, oxygen transport can be described by Fick's First Law:

$$J = -\phi_s D_s \frac{dC(x)}{dx} \quad (2)$$

where  $J$  is the diffusional flux,  $C$  is the concentration at depth  $x$ ,  $\phi_s$  is the porosity, and  $D_s$  is the molecular diffusion coefficient. Eqn. 2 describes the dominant transport of dissolved

materials such as  $O_2$  within the diffusion boundary layer (DBL), a thin film of water (often <2 mm) over saturated sediments as lake and marine sediments (Gundersen and Jørgensen, 1990). Within this layer, the water velocity is so low that molecular diffusion becomes the dominant form of transport. The DBL constitutes an important diffusion barrier to many dissolved species and has been found to affect the exchange of  $O_2$ , nutrients, and metal ions in several natural environments (e.g., Gundersen and Jørgensen, 1990; Hofman et al., 1991; Ploug et al., 1999). A steady-state  $O_2$  gradient across the DBL in a tailing environment is only a result of  $O_2$  uptake below the DBL and therefore easily identified by its linear decrease in  $O_2$  concentration (Fig. 1).

Within tailings, both diffusion and chemical reactions will determine the  $O_2$  gradient, and a flux calculation in this region consequently requires additional high-resolution measurements of the sediment diffusion coefficient and porosity as described by Fick's Second Law. Assuming steady-state conditions, this law can be written as (Berg et al., 1998):

$$\frac{\delta C^2}{\delta^2 x} = \frac{R}{\phi_s D_s} \quad (3)$$

where  $R$  is the net rate of consumption (or production if  $R$  is negative) per unit volume of tailings. If  $\phi_s$ ,  $D_s$ , and  $R$  are constant with depth, the concentration gradient is given by a parable, which is seen as the curvature of the  $O_2$  concentration profile below the tailing surface (Fig. 1). Measured  $O_2$  concentrations in tailings can be used to approximate  $d^2C/dx^2$  in Eqn. 3 and known values of  $\phi_s$  and  $D_s$  to calculate the value of  $R$  for every measured interior point within the tailing profile. However, as discussed by Berg et al. (1998), this will in most cases lead to strongly oscillating values of  $R$  with depth (in the following referred to as the consumption profile) that would be difficult to interpret. However, the problem can be solved if analytical fitting functions are replaced with a numerical solution to Eqn. 3 as shown by Berg et al. (1998). Measuring the combined parameter  $\phi_s D_s$ , hereafter called the apparent diffusivity ( $D^*$ ), and the concentration of  $O_2$  in the tailing profiles will, therefore, allow an estimation of the consumption profile. The integrated consumption within the entire profile equals the flux across the DBL. Consequently, microscale  $O_2$  measurements within the DBL and within tailing below DBL provide two independent rate descriptions of the  $O_2$  consumption rate.

## 3. SAMPLING AND METHODOLOGY

### 3.1. Study Area and Sampling

Columns with tailings were sampled at the tailing impoundment near Nanisivik Mine on Baffin Island (NWT) in northern Canada (73°02'N, 84°32'W). The site is located within the High Arctic zone of continuous permafrost with an annual mean temperature below -15°C (1994–1998). Since 1976, mine tailings have been deposited underwater in a tailings impoundment. However, during the last few years, tailings have also been deposited on land. Two test areas have been selected for this study, with the first site representing well-drained mine tailings that have been directly exposed to atmospheric  $O_2$  since 1992 and tailings of the same age deposited underwater. The second site represents almost fresh tailings produced and deposited underwater within 1 yr. The geochemical characteristics of the sites have previously been described (Elberling, 2000). Mine tailings exposed to atmospheric  $O_2$  for several years consist of well-sorted, fine sand with a pyrite content between 40 and 75% in the partly oxidized upper 30 cm

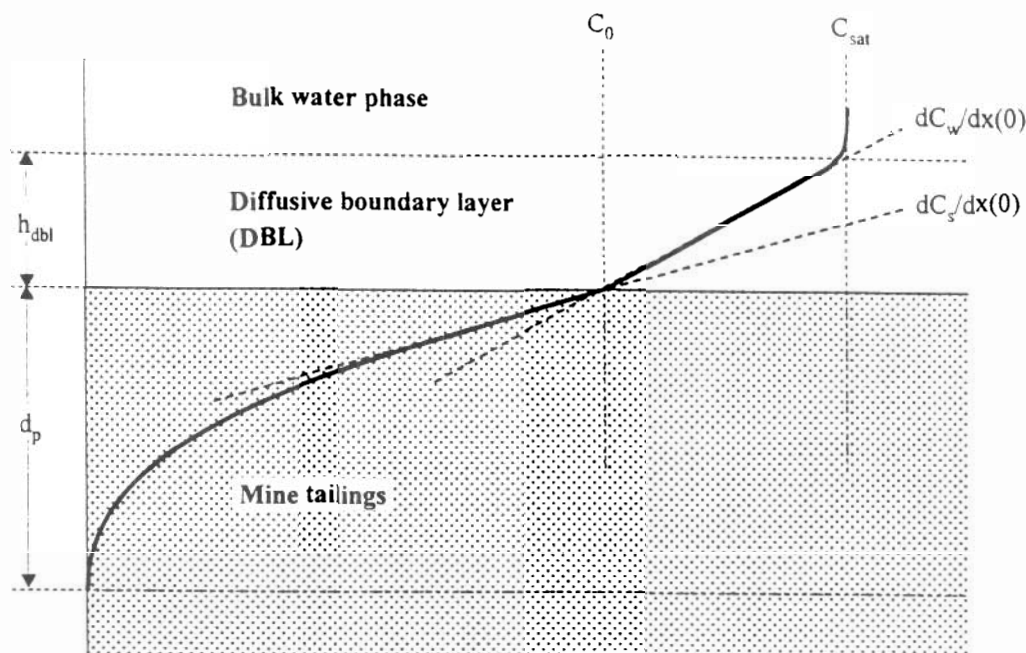


Fig. 1. Schematic presentation of the  $O_2$  concentration profile through a system consisting of mine tailings covered with atmospherically saturated water, where  $h_{dbl}$  is the height of diffusive boundary layer,  $d_p$  is the  $O_2$  penetration depth,  $C_0$  is the  $O_2$  concentration at the tailing surface,  $C_{sat}$  is the  $O_2$  concentration in saturated water phase,  $dC_w/dx(0)$  is the  $O_2$  concentration gradient in the diffusive boundary layer at the tailing surface, and  $dC_s/dx(0)$  is the  $O_2$  concentration gradient in the tailings at the surface.

and between 75 and 85% within the reduced zone. Mine tailing profiles, which have not been exposed to the atmosphere, consist of 70 to 85% pyrite. Organic matter is not present in the tailings ( $<0.02$  ppm). X-ray analysis indicates that the remaining part of the oxidized zone consists primarily of dolomite and traces of gypsum and quartz. The presence of carbonate mixed with tailings is responsible for only slightly acidic conditions. Biologic pyrite oxidation accounts for up to 30% of the overall oxidation (Elberling et al., 2000).

Tailings from the test area were sampled in 1998 by slowly pushing a Plexiglas cylinder (120 mm ID) down to a depth of 50 cm and subsequently removing it by excavating the site. Columns were kept frozen during transportation and until experiments were initiated.

### 3.2. Column Preparation

Measurements were performed on columns filled with undisturbed tailing in a temperature controlled room ( $\pm 0.5^\circ$ ). To maintain field conditions, distilled water was added on a regular basis to offset evaporation. Watering on floating styrofoam ensured a minimum disturbance of the tailing surface. A stream of air on the water surface was maintained to ensure mixing in the water. Some columns were drained to field capacity (described as well-drained conditions) by controlling an artificial groundwater level through a porous plate in the bottom of the columns.

Additional columns were packed with homogenized, washed, and saturated unoxidized mine tailings and kept at constant temperatures close to  $2^\circ$ ,  $10^\circ$ ,  $16^\circ$ , and  $20^\circ\text{C}$  over 3 months. Subsequently, the columns were flushed with water, and the effluent was collected for determining sulfate production. To verify the importance of the DBL, various thicknesses of DBL were simulated by covering columns with up to 10 cm 1% Bacto-agar (Difco Laboratories, Detroit, MI). Agar was placed on top of tailings in columns as a liquid (at  $40^\circ\text{C}$ ) and allowed to cool down to  $20^\circ\text{C}$ . The columns were left at  $20^\circ\text{C}$  for up to 17 d to achieve steady state before measurements. The oxygen diffusion coefficient in agar was assumed to be 90% of the diffusion coefficient in pure water (Nakayama and Jackson, 1963).

### 3.3. Microsensors

$O_2$  concentrations were measured in water, and saturated tailings with a miniaturized Clark-type  $O_2$  microsensor (OX10, Unisense, Science Park, DK-8000 Aarhus, Denmark) were equipped with an internal reference and a guard cathode (Revsbech, 1989). The output current was measured by a picoampere meter (PA2000, Unisense) that simultaneously kept the cathode polarized against the internal reference. The sensors had a tip diameter of  $18\text{ }\mu\text{m}$ , a stirring sensitivity of  $<1\%$ , and a 90% response time of 2 to 3 s. The linearity of the sensor response was confirmed by recording the output current in pA in water sparged with  $N_2$ , air, and pure  $O_2$ . The sensor was calibrated at the experimental temperature by using the output current in the overlying water and in strongly reduced water (alkaline 0.1 M sodium ascorbate solution). Calibration before and after profiling revealed that instrument drift over a few hours was insignificant. Profiling measurements with oxygen sensors were made at 100- $\mu\text{m}$  depth intervals controlled manually by a micromanipulator. The reference depth for vertical positioning was determined by approaching the tailing surface with the sensor tip in small steps and moving the sensor horizontally after each step. The highest position at which the sensor was able to make surface particles move was defined as the surface. Subsequently, the reference depth was confirmed by a change in the slope of the  $O_2$  gradient at the tailing surface. The observation of the change in slope was the only method of identification of the surface position during in situ measurements, because the visual detection was not possible because of the light conditions.

Microscale diffusivity sensors (Unisense) with a diameter of 200 to 400  $\mu\text{m}$  were applied to measure apparent diffusivity of the medium surrounding the sensor tip by measuring concentrations of a tracer gas from an internal gas reservoir within the sensor tip (Revsbech et al., 1998). The internal gas reservoir was flushed by 1 to 4% acetylene ( $C_2H_2$ ) mixed with  $N_2$ . Acetylene was used as the tracer gas to avoid interference with the  $O_2$  consumption or  $CO_2$  production within the mine tailings. Acetylene has previously been used as an inert tracer in similar diffusivity sensors (Santegoeds et al., 1999).

A mathematical model describing the sensor signal as a function of

diffusivity is presented by Revsbech et al. (1998) showing that a calibration curve can be constructed from measurements in two media with known diffusivity. In this study, stagnant water and 40 to 60  $\mu\text{m}$  unsorted glass beads in water were used as standards for calibration. The apparent diffusivity of the glass beads was previously measured in diffusion chambers as  $0.57 \times 10^{-5} \text{ cm}^2 \text{ s}^{-1}$  (Revsbech et al., 1998). Diffusivity sensors have been designed to have a diameter of at least twice the average grain size to avoid the influence of single grains at the sensor tip. Profiling with diffusion sensors was conducted at 500- $\mu\text{m}$  intervals, a value insufficient for direct comparison with the measured  $\text{O}_2$  concentration profiles. Therefore, measurements of apparent diffusivity ( $D^*$ ) were converted to the same spatial resolution as  $\text{O}_2$  measurements by fitting the following equation:

$$D^* = D^*_\infty + (D^*_0 - D^*_\infty)e^{-ax} \quad (4)$$

where  $D^*$  is the depth-dependent apparent diffusivity,  $D^*_\infty$  is a constant apparent diffusivity at depth,  $D^*_0$  is the apparent diffusivity at the tailing/water interface,  $a$  is a constant, and  $x$  is the depth. This fit equation was previously used in a similar manner to fit porosity (Iversen and Jørgensen, 1993).

For calculating final  $\text{O}_2$  concentrations, fluxes, and  $\text{O}_2$  diffusion coefficients, table values for  $\text{O}_2$  solubility and diffusion in water under different salinities and temperatures have been used. A table (Ramsing and Gundersen, 1994) based on an absolute diffusivity of oxygen in distilled water at  $10^\circ\text{C}$  of  $1.57 \times 10^{-5} \text{ cm}^2 \text{ s}^{-1}$  (Broeker and Peng, 1974) has been used consistently. The table presents calculated diffusion coefficients at various temperatures and salinities using formulas presented by Li and Gregory (1974). The  $\text{O}_2$  solubility is based on formulas presented by Garcia and Gordon (1992).

### 3.4. Oxygen Chamber Measurements

The  $\text{O}_2$  consumption in columns with well-drained tailings could not be evaluated by microsensors, and therefore, an  $\text{O}_2$  consumption method was applied as previously described by Elberling and Nicholson (1996). A cap was placed on top of the column to close the tailing profile from the atmosphere over a period of  $\approx 1$  h, whereas the concentration of  $\text{O}_2$  within the gas reservoir between the tailing surface and the cap was measured by an electrochemical oxygen gas sensor (Model GC33-200, G.C. Industrial Inc., Fremont, CA) sealed in the cap. The oxygen sensor provides a voltage output, which is linearly related to the absolute concentration of  $\text{O}_2$  with an accuracy of 0.1%  $\text{O}_2$  (Elberling and Nicholson, 1996). Readings from the oxygen sensor in mV were recorded each minute on a logger and used to estimate the flux of  $\text{O}_2$  across the tailing surface. The following equation was used to convert relative changes in  $\text{O}_2$  concentration within the gas reservoir over time to a flux of moles of  $\text{O}_2$  per area per time (Nicholson et al., 1989):

$$F_s = -C_0 \times (kD^*)^{0.5} \quad (5)$$

where  $F_s$  is the flux of  $\text{O}_2$  across the tailing surface,  $C_0$  is the initial concentration of  $\text{O}_2$  before measurement, and  $k$  is the reaction rate constant. The parameter  $(kD^*)^{0.5}$  is given by the slope of a plot of the relative change in  $\text{O}_2$  concentration within the gas reservoir with time as shown in Elberling and Nicholson (1996). Eqn. 5 assumes that  $\text{O}_2$  diffusion can be described by Fick's First Law, that the  $\text{O}_2$  flux across the surface has reached a steady state before measurements, and that sulfide oxidation as a first-order reaction is the only process consuming  $\text{O}_2$ . The method was previously applied in similar investigations (Elberling and Nicholson, 1996; Meldrum et al., 1999). Laboratory tests reveal that the  $\text{O}_2$  flux across the surface represents the  $\text{O}_2$  consumption within the entire tailing profile and the release of oxidation products (Elberling et al., 1994a).

Measurements on the four columns were repeated every second day, revealing that a steady-state oxygen consumption was reached after 6 days after initial drainage.

### 3.5. In Situ Measurements

Additional microscale profiles with oxygen sensors were made in situ within the test area in Nanisivik over 10 d in August 2000. Profiling was controlled manually by mounting the micromanipulator on a

separate wooden rack standing on the bottom of  $\approx 10$  cm water-covered mine tailings. Measurements were performed at 100- $\mu\text{m}$  depth intervals and under shading and with wave breakers to ensure stable conditions for the rack.

### 3.6. Oxygen Diffusion-Consumption Model

The numerical model PROFIL (Berg et al., 1998) was used to analyze measured  $\text{O}_2$  concentration profiles and apparent diffusivity. PROFIL calculates the rate of net consumption as a function of depth, assuming that the concentration-depth profiles represent steady states. The procedure involves finding a series of least square fits to the measured concentration profile, followed by comparisons of these fits through statistical F-testing. This approach leads to an objective selection of the simplest consumption profile that reproduces the measured concentration profiles. The model has been tested successfully against analytical solutions describing the transport and consumption of  $\text{O}_2$  in tailing pore water (Berg et al., 1998). Based on the calculated consumption profiles, the integrated  $\text{O}_2$  consumption was estimated and compared with the  $\text{O}_2$  flux across the DBL and to the sulfate production.

### 3.7. Sensitivity Modeling

To predict the influence of temperature and stagnant water cover on the oxygen flux into reactive tailings, a simple one-dimensional steady-state model was developed. The model assumes a well-stirred water phase above a DBL of well-defined thickness and that the diffusion coefficient and reaction rate of the tailing are constant within the entire oxygen penetration depth.

Double integration of Eqn. 3 shows that the concentration profile under this assumption is parabolic (Nielsen et al., 1990), and because both the slope and the concentration must equal zero at the oxygen penetration depth  $d_p$ , i.e.,

$$C(d_p) = \frac{dC(d_p)}{dx} = 0, \quad (6)$$

the concentration as a function of depth,  $x$ , can be described by

$$C_i(x) = \frac{R}{2\phi D_i} x^2 - \frac{Rd_p}{\phi D_i} x + \frac{Rd_p^2}{2\phi D_i} \quad (7)$$

Furthermore, there must be mass conservation across the tailing surface:

$$J_s = J_{dbl} \Rightarrow -\phi_i D_i \frac{dC_i(0)}{dx} = -\phi_{dbl} \frac{C_0 - C_{sat}}{h_{dbl}} \quad (8)$$

where  $J_s$  and  $J_{dbl}$  are the oxygen fluxes at the tailing surface calculated in the tailings and in the DBL, respectively, and  $h_{dbl}$  is the height of the

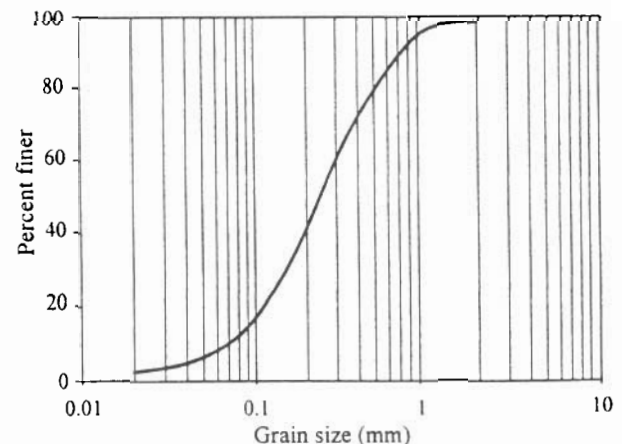


Fig. 2. The grain size distribution in tailings from the study site.

DBL (Fig. 1). By combining Eqn. 6 to 8, the oxygen flux across the tailing surface can be calculated:

$$J_s = J_{DBL} = \frac{(\phi_s D_s R)^2}{\sqrt{(\phi_{DBL} D_{DBL})^2 h_{DBL}^2 + 2\phi_s D_s R C_{sat} - \frac{\phi_s D_s R}{\phi_{DBL} D_{DBL}} h_{DBL}}} \quad (9)$$

#### 4. RESULTS AND DISCUSSION

##### 4.1. Tailings Diffusivity

The range in grain size distribution for tailings at the field site reveals that tailings consist of 60% fine sand between 0.1 and 0.4 mm (Fig. 2). The material is fairly well sorted with <5% finer than 0.03 mm. The apparent diffusivity of saturated tailing material was  $\approx 0.38\text{--}0.42 \times 10^{-5} \text{ cm}^2 \text{ s}^{-1}$ . Figure 3 illustrates the measured apparent diffusivities as a function of depth. Near the tailing surface the apparent diffusivity gradually decreases with depth, primarily due to compaction; however, the diffusivity approaches almost constant values at a depth of 1 to 2 mm. Significant changes within this upper 2 mm can be observed in tailings of various ages. In older and partly oxidized tailings, the zone is less compacted, giving rise to higher apparent diffusion coefficients (Fig. 3). This can be explained by mineral precipitation processes following oxidation in partly oxidized tailings but may also solely be a result of disturbance of the column after removal from the field.

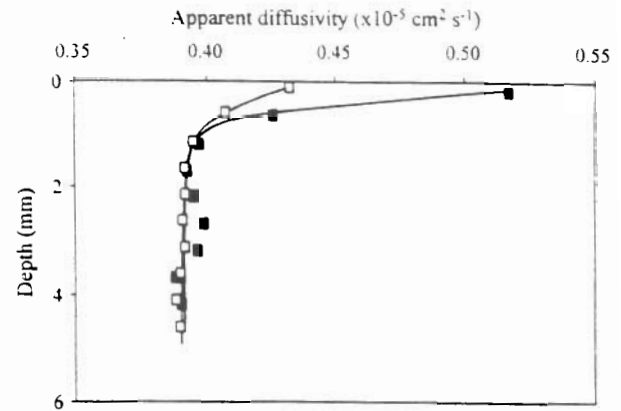


Fig. 3. Apparent diffusion profiles in saturated fresh tailings ( $\square$ ) and in older partly oxidized tailings ( $\blacksquare$ ). The solid lines represent Eqn. 4 fitted to observations.

##### 4.2. Oxygen Diffusion and Consumption

The  $\text{O}_2$  concentration gradient across the water phase and upper part of an undisturbed 6-year-old tailing profile is shown in Figure 4. Constant  $\text{O}_2$  concentrations above the diffusive

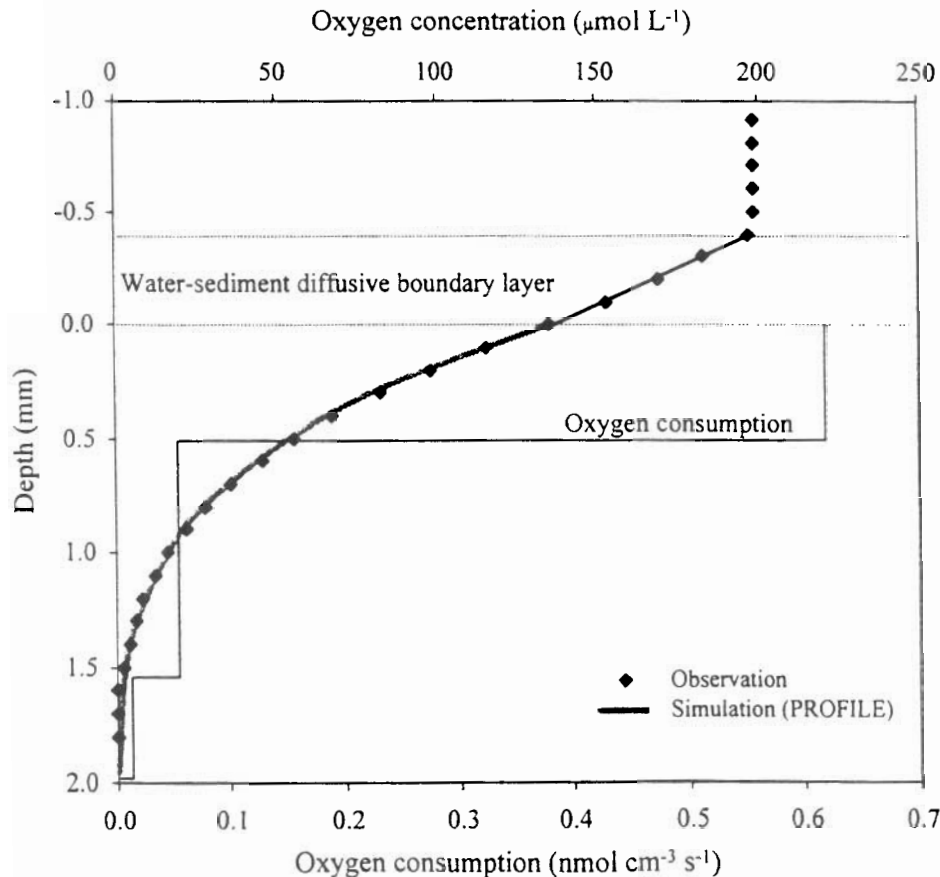


Fig. 4. Steady-state microprofile of  $\text{O}_2$  in saturated tailings. Symbols are measured concentrations of oxygen. The linear line across DBL represents the gradient for evaluating the DBL flux, whereas the gray line below the DBL is the calculated gradient based on PROFIL giving rise to the consumption profile shown as boxes.

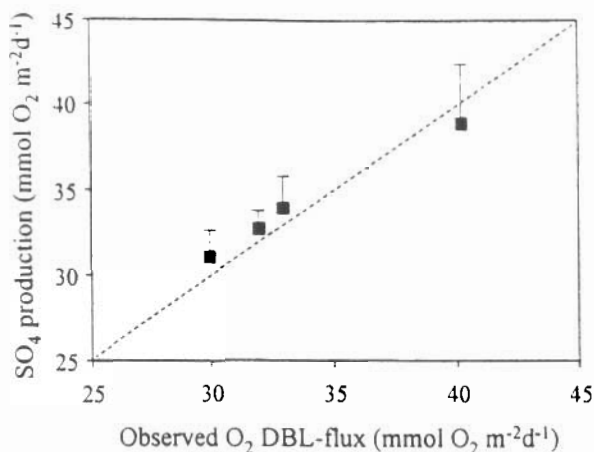


Fig. 5. Sulfate production rates (converted to O<sub>2</sub> consumption rates using Eqn. 1) are shown as a function of the estimated O<sub>2</sub> flux across the DBL in terms of mmol O<sub>2</sub> m<sup>-2</sup> d<sup>-1</sup>. The dashed line represents the 1:1 relationship.

boundary layer (DBL) confirm that this reservoir is well mixed. Across the DBL the O<sub>2</sub> concentration decreases linearly, corresponding to an O<sub>2</sub> flux of  $35 \pm 4$  mmol m<sup>-2</sup> d<sup>-1</sup> across the DBL. The thickness of the DBL is to some extent controlled by the experimental setup including the column dimensions and the water circulation. However, the observed DBL thickness is consistent with observations in natural systems (Gundersen and Jørgensen, 1990). Below the DBL in the tailings, oxygen is consumed and depleted at a depth of 1.7 mm. For the actual profile shown (Fig. 4), the depth-integrated O<sub>2</sub> consumption profiles equals 34 mmol m<sup>-2</sup> d<sup>-1</sup> without changing the default settings of the model. For most experiments, an agreement within 2% was observed between the O<sub>2</sub> flux across the DBL and the modeled O<sub>2</sub> consumption. But disagreements up to 12% were noted. However, a perfect match could be obtained in all cases by allowing the slope within the DBL to vary within the 90% confidence interval of the linear regression. Consumption profiles of various in situ columns with saturated tailings were fairly consistent and predict that >80% of the total O<sub>2</sub> consumption takes place within the upper 0.5 mm zone of partly oxidized tailings. In fresh tailings, 92% of total consumption occurs in this zone.

To correlate oxygen consumption with pyrite oxidation (AMD generation), the sulfate production rates observed in prewashed columns over 3 months were converted to O<sub>2</sub> consumption rates based on Eqn. 1 and compared with observed O<sub>2</sub> consumption (Fig. 5). Consistency in the two rate descriptions reveals that fluxes across DBL not only represent the total O<sub>2</sub> consumption in tailings below the DBL but also the production of weathering products resulting from O<sub>2</sub> consumption.

#### 4.3. Oxygen Concentration Gradient Measured In Situ

Results from field work in Nanisivik reveal that repeated O<sub>2</sub> profiling within water-covered tailings provide consistent microscale oxygen gradients across DBL. Figure 6 shows an example of normalized oxygen concentrations measured in situ near the tailing/water interface. The tailing surface is identified

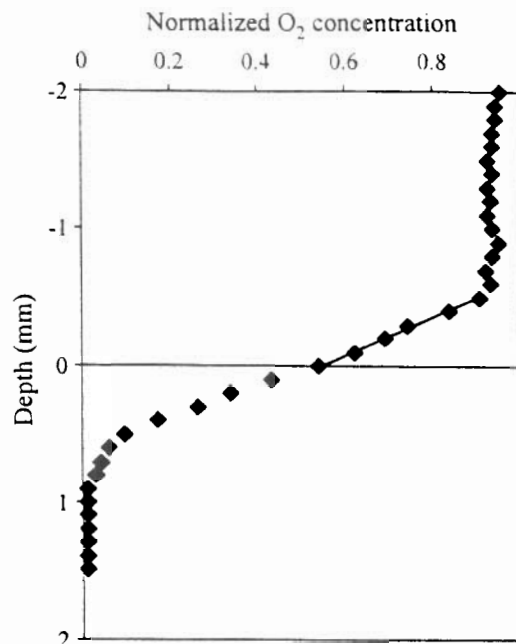


Fig. 6. In situ microprofile of O<sub>2</sub> within 10-cm water-covered tailings deposited near Nanisivik in Canada.

visually as the change in the slope of the O<sub>2</sub> gradient. Six O<sub>2</sub> gradients measured over 4 h and within an area of  $\approx 5$  cm<sup>2</sup> show consistent linear gradients ( $R^2 > 0.99$ ) across the DBL. Taking the temperature (14°C) and water salinity (0.3%) into account, the average flux over this time period was estimated to be  $35 \pm 4$  mmol O<sub>2</sub> m<sup>-2</sup> d<sup>-1</sup>, indicating that laboratory microscale profiles are representative for the field conditions. In addition, the depth of oxygen depletion observed in the field and laboratory experiments was almost the same. The variations in fluxes observed in the field based on repeated O<sub>2</sub> profiles are surprising compared with the expected influence of heterogeneous conditions within the profile, weather patterns, and other environmental factors. Variations in the thickness of DBL were observed to be on the order of 50% without giving rise to similar changes in the O<sub>2</sub> slope across the DBL. Short-term changes in DBL thickness was primarily due to wind and waves, resulting in a spontaneous reduction of the thickness of DBL. When stable O<sub>2</sub> fluxes are observed over hours, it may be due to that an average DBL-thickness, and not short-term variations in DBL thickness, control the overall consumption of oxygen.

#### 4.4. Strategic Disposal Options

Average O<sub>2</sub> consumption rates obtained from undisturbed columns are summarized in Table 1. Slightly higher rates in saturated fresh tailings compared with older partly oxidized tailings probably reflect that fresh tailings consist of more reactive sulfide particles and that protective coatings on older and partly oxidized particles may slow the oxidation as described by Nicholson et al. (1990). These observations contradict the fact that the lowest pH values are observed in old tailings, which are expected to increase biologic oxidation. The



Table 1. Laboratory results at 20°C for measured and calculated oxygen consumption rate  $\pm$  SD (mmol O<sub>2</sub> m<sup>-2</sup> d<sup>-1</sup>) in tailing columns from Nanisivik.

Field condition	Saturated—fresh tailings		Well-drained—old tailings	
Laboratory treatment	—	Drained	—	Saturated
pH	8.5 $\pm$ 0.5	8.2 $\pm$ 0.6	4.5 $\pm$ 1.2*	6.2 $\pm$ 0.5
Observed O <sub>2</sub> flux (DBL measurements)	40 $\pm$ 6	nd	nd	35 $\pm$ 4
Calculated O <sub>2</sub> flux (using PROFIL)	39 $\pm$ 2	nd	nd	34
O <sub>2</sub> uptake in well-drained tailings (chamber measurements)	nd	2860 $\pm$ 2	1217 $\pm$ 123	nd

\* Measured in the field on extracted water by suction probes. nd = not determined.

difference in rate becomes even more clear within well-drained columns in which fresh tailings oxidize more than twice as fast as older tailings.

Comparisons of well-drained and water-saturated columns confirm that underwater disposal of fresh tailings may decrease the overall oxygen consumption by up to a factor of 70 (or a factor of 35 for partly oxidized tailings) compared with a well-drained disposal scenario. This general control of AMD generation by maintaining tailings underwater is well known but not previously quantified under cold extreme field condition.

The high Arctic represents an extreme environment in which low temperatures, permafrost, and snow covers most of the year may retard oxidation. With respect to subaqueous disposal strategies, the increasing solubility of oxygen in water in cold water has been a concern (Dawson and Morin, 1996). However, low temperatures also affect the diffusion of oxygen, and the combined effect will govern the transport rate in diffusion-controlled systems (Fig. 7A). Columns placed at five temperatures show that the overall O<sub>2</sub> consumption rate decreases  $\approx$ 30% from 20 to 2°C (Fig. 7B). The sensitivity model was used to simulate this change with temperature and to quantify the extent to which temperature-dependent O<sub>2</sub> transport can explain the observations. Despite the fact that the analytical equation assumes that the reaction rate is independent of depth and temperature, Figure 7B indicates that the analytical model provides a reasonable sensitivity fit to observations. Although the analytical model is a conservative and very simple expression of the O<sub>2</sub> consumption, the overall consistency between the observations and the simulation suggest that diffusion rather than reaction kinetics controls the overall O<sub>2</sub> consumption. Consequently, it is obvious to try to further limit the potential diffusion.

One way to limit the oxygen availability at the tailing surface is to increase the thickness of the DBL. The results of applying layers of various thickness of agar on top of tailings are shown in Figure 8. Again, observations are fairly consistent with the model assuming a depth-independent reaction rate in the tailings. As an alternative to using Eqn. 9 to model the flux, it is useful to note that it can be rewritten as

$$J_s = J_{dbl} = \sqrt{\left(\frac{\phi_s D_s R}{\phi_{dbl} D_{dbl}} h_{dbl} + \frac{\phi_{dbl} D_{dbl}}{h_{dbl}} C_{sat}\right)^2 - \left(\frac{\phi_{dbl} D_{dbl}}{h_{dbl}} C_{sat}\right)^2} - \frac{\phi_s D_s R}{\phi_{dbl} D_{dbl}} h_{dbl} \quad (10)$$

which approaches

$$J_s = J_{dbl} = \phi_{dbl} D_{dbl} \frac{C_{sat}}{h_{dbl}} \quad (11)$$

for increasing  $h_{dbl}$ . Eqn. 11 signifies that for a sufficiently large  $h_{dbl}$  the specific reaction rate becomes insignificant as a limiting factor in the oxygen consumption compared with the diffusional barrier through the diffusive boundary layer and that the flux becomes inversely proportional to  $h_{dbl}$  (Fig. 8). To estimate for what values of  $h_{dbl}$  in Eqn. 11 is a sufficiently good approximation, we can combine Eqn. 9 and 11 to show that Eqn. 11 overestimates the exact value (Eqn. 9) by a factor less than or equal to  $k$  if

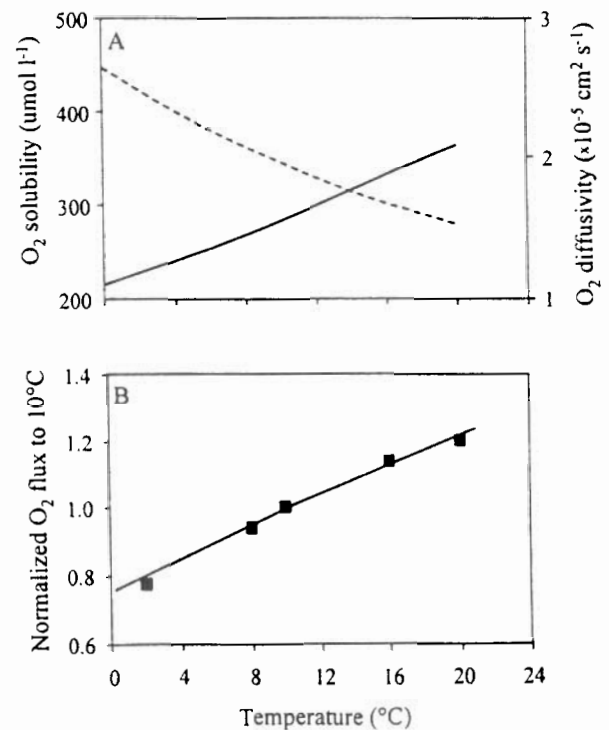


Fig. 7. A: Tabulated oxygen diffusion coefficients (solid line) and oxygen solubility (dashed line) in tailing effluent (salinity  $\approx$  3‰) in the temperature range 0 to 20°C (from Ramsing and Gundersen, 1994). B: Normalized observed and simulated O<sub>2</sub> fluxes across DBL as a function of temperature.

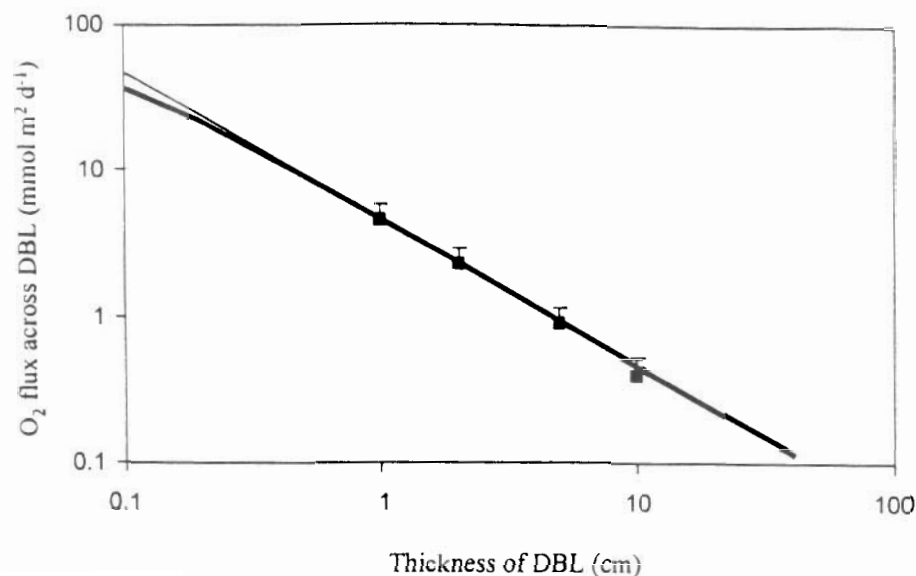


Fig. 8. Observed and simulated  $O_2$  fluxes in  $\text{mmol } O_2 \text{ m}^{-2} \text{ d}^{-1}$  across DBL as a function of DBL thickness (cm). The thick line represents the conservative estimate of  $O_2$  flux (Eqn. 10) and the thin line an approximation (Eqn. 11), which is valid for DBL thicknesses above 6 mm.

$$h_{dbl} \geq \sqrt{\frac{\phi_{dbl}^2 D_{dbl}^2 C_{sat}}{2 \phi_s D_s R(k^2 - k)}} \quad (12)$$

By using this formula with the measured values for  $\phi_s D_s$ , and the reaction rates derived from the measured concentration profile in Figure 6 along with table values for oxygen solubility and  $D_{dbl}$  in water (Ramsing and Gundersen, 1994) at ambient temperature, Eqn. 11 approximates the real flux with an error <5% when  $h_{dbl}$  is >6 mm.

By using Eqn. 9, it can be estimated that increasing  $h_{dbl}$  from  $\approx 0.5$  (as measured in saturated tailings) to 6 mm decreases the oxygen flux by a factor 3.7. Further increases in  $h_{dbl}$  will result in an approximately inversely proportional decrease in oxygen flux. A diffusive boundary layer of more than a few millimeters can only be created in practice by stabilizing the water physically, for instance by covering the tailings with water-saturated shale. The pore water between the shale particles will be stabilized because of friction, and furthermore, the shale will provide a  $\phi_{dbl} < 1$  and a  $D_{dbl}$  less than that of water. The combined effect by covering mine tailings with a water-saturated layer of shale with a height of 60 cm as opposed to well-drained conditions will thus be a reduction in the oxygen flux by a factor of >20,000.

## 5. CONCLUSIONS

Microscale profiles of oxygen concentration and diffusion in saturated tailings are found to provide consistent estimates of the overall oxygen consumption in saturated sulfide tailings. Rates observed can be interpreted as a measure of sulfide oxidation rates and AMD generation rates. Comparisons of saturated and well-drained tailings show that saturation as a remediation action for controlling AMD may reduce  $O_2$  diffusion and consumption by a factor of 70. In saturated tailings, low temperatures (near  $0^\circ\text{C}$ ) will further decrease the overall

$O_2$  consumption as the decreasing diffusivity with temperature is more important than the increasing  $O_2$  dissolution at low temperatures. Thus, saturation of tailings can be recommended also in cold regions, where other actions such as freezing is often considered. The experiments and model simulations show that the thickness of the DBL is very important for controlling AMD, and only a few centimeters of saturated inert sediment covers on top of saturated tailings will further reduce the AMD generation additionally by a factor of 10 to 1000.

**Acknowledgments**—This study was funded by the Danish Environmental Protection Agency, Ministry of Environment and Energy, Denmark, as part of a DANCEA (Danish Cooperation for Environment in the Arctic). The authors are solely responsible for the results and conclusions presented. Special thanks to L.B. Pedersen for constructing the micro-sensors and P. Berg for valuable discussions regarding the model PROFIL.

*Associate editor:* B. E. Taylor

## REFERENCES

- Aller C. A. (1980) Quantifying solute distribution in the bioturbated zone of marine sediments by defining an average microenvironment. *Geochim. Cosmochim. Acta* **44**, 1955–1965.
- Aubé B. C., St-Arnaud L. C., Payant S. C., and Yanful E. K. (1995) Laboratory evaluation of the effectiveness of water covers for preventing acid generation from pyritic rock. In *Sudbury 95, Conference on Mining and the Environment*, 495–504. Sudbury, Ontario, May 28–June 1, 1995.
- Berg P., Risgaard-Petersen N., and Rysgaard S. (1998) Interpretation of measured concentration profiles in sediment pore water. *Limnol. Oceanogr.* **43**, 1500–1510.
- Blowes D. W. and Jambor J. L. (1990) The pore-water geochemistry and the mineralogy of the vadose zone of sulfide tailings. Waite Amulet Quebec, Canada. *Appl. Geochem.* **5**, 327–346.
- Broecker W. S. and Peng T. H. (1974) Gas exchange rates between air and sea. *Tellus* **26**, 21–35.
- Dawson R. F. and Morin K. A. (1996) Acid mine drainage in perma-

- frost regions: Issues, control strategies and research requirements. MIEND Project 1.61.2. Department of Indian and Northern Affairs Canada, Ottawa, Canada. 68 pp.
- Dubrovsky N. M., Morin K. M. M., Cherry J. A., and Smuth D. J. A. (1984) Uranium tailings acidification and subsurface contaminant migration in a sand aquifer. *Water Pollut. Res. J. Can.* **19**, 55–89.
- Elberling B. (2001) Environmental controls of the seasonal variation in oxygen uptake in sulfide tailings deposited in a permafrost-affected area. *Water Resour. Res.* **37**, 99–107.
- Elberling B., Nicholson R. V., Reardon E. J., and Tibble P. (1994a) Evaluation of sulphide oxidation rates—A laboratory study comparing oxygen fluxes and rates of oxidation product release. *Can. Geotech. J.* **31**, 375–383.
- Elberling B., Nicholson R. V., and Scharer J. M. (1994b) A combined kinetic and diffusion model for pyrite oxidation in tailings: A change in control with time. *J. Hydrol.* **157**, 47–60.
- Elberling B. and Nicholson R. V. (1996) Field measurements of oxygen diffusion and sulphide oxidation in mine tailings. *Water Resour. Res.* **32**, 1773–1784.
- Elberling B., Schippers A., and Sand W. (2000) Bacterial and chemical oxidation of tailings at low temperatures. *J. Cont. Hydrol.* **41**, 225–238.
- Garcia H. and Gordon L. I. (1992) Oxygen solubility in seawater: Better fitting equations. *Limnol. Oceanogr.* **42**, 1029–1042.
- Godwaldt R. C., Biggar K. W., and Sego D. C. (1999) AMD generation at sub-zero temperatures. In *Proceedings of Symposium on Assessment and Remediation of Contaminated sites in Arctic and Cold Climates*, pp. 75–82. Edmonton, Canada, 3–4 May, 1999.
- Gundersen J. K. and Jørgensen B. B. (1990) Microstructure of diffusive boundary layers and the oxygen uptake of the sea floor. *Nature* **345**, 604–607.
- Hofman P. A. G., de Jong S. A., Wagenvoort E. J., and Sandee A. J. J. (1991) Apparent sediment diffusion coefficients for oxygen and oxygen consumption rates measured with microelectrodes and bell jars: Applications to oxygen budgets in estuarine intertidal sediments (Oosterchelde, SW Netherlands). *Mar. Ecol. Prog. Ser.* **69**, 261–272.
- Iversen N. and Jørgensen B. B. (1993) Diffusion coefficients of sulfate and methane in marine sediments: Influence of porosity. *Geochim. Cosmochim. Acta* **57**, 571–578.
- Li Y. and Gregory S. (1974) Diffusion of ions in sea water and in deep-sea sediments. *Geochim. Cosmochim. Acta* **38**, 703–714.
- Meldrum J. L., Jamieson H. E., and Dyke L. D. (1999) Laboratory determination of sulphide oxidation potential in permafrost using tailings from Rankin Inlet, Nunavut. In *Mining and the Environment II* (eds. D. Goldack, N. Belzile, P. Yearwood, and G. Hall), pp. 119–126. Sudbury, Ontario, Canada.
- Mugo R. K., McDonald D., and Poling G. W. (1999) Subaqueous tailings disposal in freshwater and marine environments—Results of predictive geochemical testing using tailings with different compositions. In *Mining and the Environment*, pp. 99–108, Sudbury, Ontario, Canada.
- Nakayama F. S. and Jackson R. D. (1963) Diffusion of tritiated water ( $\text{H}^3\text{H}^{16}\text{O}$ ) in agar gel and water. *J. Physical Chem.* **67**, 932–933.
- Narasimhan T. N., White A. F., and Tokunaga T. (1986) Groundwater contamination from an inactive uranium mine tailings pile. 2. Application of a dynamic mixing model. *Water Resour. Res.* **22**, 1820–1834.
- Nicholson R. V., Gillham R. W. and Reardon E. J. (1988) Pyrite oxidation in carbonate-buffered solution. 1. Experimental kinetics. *Geochim. Cosmochim. Acta* **52**, 1077–1085.
- Nicholson R. V., Gillham R. W., Cherry J. A., and Reardon E. J. (1989) Reduction of acid generation in mine tailings through the use of moisture-retaining cover layers as oxygen barriers. *Can. Geotech. J.* **26**, 1–8.
- Nicholson R. V., Gillham R. W., and Reardon E. J. (1990) Pyrite oxidation in carbonate-buffered solution. 1. Rate control by oxide coatings. *Geochim. Cosmochim. Acta* **54**, 395–402.
- Nielsen L. P., Christensen P. B., Revsbeck N. P., and Sørensen J. (1990) Denitrification and oxygen respiration in biofilms studied with a microsensor for nitrous oxide and oxygen. *Microb. Ecol.* **19**, 63–72.
- Pantelis G. and Ritchie A. I. M. (1992) Macroscopic transport mechanisms as a rate limiting factor in dump leaching of pyritic ores. *Appl. Mat. Model* **15**, 136–143.
- Ploug H., Støtte W., and Jørgensen B. B. (1999) Diffusive boundary layers of the colony-forming plankton alga *Phaeocystis* sp.—Implications for nutrient uptake and cellular growth. *Limnol. Oceanogr.* **44**, 1959–1967.
- Ramsing N. and Gundersen J. (1994) Seawater and gases—Tabulated physical parameters of interest to people working with microsenors in marine systems. Version 2.0. Unisense Internal Report, 16 pp.
- Rasmussen H. and Jørgensen B. B. (1992) Microelectrode studies of seasonal oxygen uptake in a coastal sediment: Role of molecular diffusion. *Mar. Ecol. Prog. Ser.* **81**, 289–303.
- Revsbeck N. P. (1989) An oxygen microelectrode with a guard cathode. *Limnol. Oceanogr.* **34**, 474–478.
- Revsbeck N. P., Madsen B., and Jørgensen B. B. (1986) Oxygen production and consumption in sediments determined at high spatial resolution by computer simulation of oxygen microelectrodes data. *Limnol. Oceanogr.* **31**, 293–304.
- Revsbeck N. P., Nielsen L. P., and Ramsing N. B. (1998) A novel microsensor for determination of apparent diffusivity in sediments. *Limnol. Oceanogr.* **43**, 986–992.
- Santegoeds C. M., Damgaard L. R., Hesselink G., Zopfi J., Lens P., Muyzer G., and De Beer D. (1999) Distribution of sulfate-reducing and methanogenic bacteria in anaerobic aggregates determined by microsensor and molecular analysis. *Appl. Environ. Microbiol.* **65**, 4618–4629.
- Wunderly M. D., Blowes D. W., Frind E. O., and Ptacek C. J. (1996) Sulfide mineral oxidation and subsequently reactive transport of oxidation products in mine tailings impoundments: a numerical model. *Water Resour. Res.* **32**, 3173–3187.